Drug Abuse Takes a Toll:

Toll-Like Receptor 4 Signaling is Required for the

Rewarding and Reinforcing Effects of

Opioids, Cocaine, and Methamphetamine

by

Alexis Linsey Northcutt

B.A., University of Colorado, 2006

M.A., University of Colorado, 2011

***

A thesis submitted to the

Faculty of the Graduate School of the

University of Colorado in partial fulfillment

of the requirement for the degree of

Doctor of Philosophy

Department of Psychology and Neuroscience

2014

This thesis entitled:

Drug Abuse Takes a Toll: Toll-Like Receptor 4 Signaling is Required for the Rewarding and Reinforcing Effects of Opioids, Cocaine, and Methamphetamine

written by Alexis Linsey Northcutt

has been approved for the Department of Psychology and Neuroscience

_____
Dr. Linda Watkins, Distinguished Professor

_____
Dr. Steven Maier

_____
Dr. Mark Hutchinson

_____
Dr. Ryan Bachtell

_____
Dr. Michael Stallings

_____
Dr. Benjamin Greenwood

Date_____

The final copy of this thesis has been examined by the signatories, and we
Find that both the content and the form meet acceptable presentation standards
Of scholarly work in the above mentioned discipline.

Northcutt, Alexis Linsey (Ph.D., Psychology and Neuroscience)

Drug abuse takes a toll: Toll-Like Receptor 4 signaling is required for the rewarding and reinforcing effects of opioids, cocaine, and methamphetamine

Thesis directed by Distinguished Professor Linda R. Watkins

Abstract

Drug abuse and addiction is a globally pervasive issue, and has detrimental effects on society in terms of financial burden and undermining the health, well-being, and productivity of the addicted individual as well as their friends and family. Although commonly abused drugs originate from differing classes, such as opioids and psychostimulants, they share a common effect of influencing the mesolimbic dopamine pathway to produce an increase of dopamine within the nucleus accumbens. This increased dopaminergic signaling is thought to underlie the euphoric and reinforcing effects of drugs that prompt repeated drug taking, and can lead to the development of addiction. Understandably, research for the past several decades has focused on neuronal targets for drug actions. Opioids are known to disinhibit ventral tegmental area control over dopaminergic projections to the nucleus accumbens, whereas psychostimulants increase dopamine concentrations through disruption of dopamine transport directly within the nucleus accumbens. Medication development targeting these mechanisms has resulted in very limited success in opioids, and there is no approved pharmacotherapy for psychostimulant abuse.

However, in recent decades the role of glial cells in the brain, including microglia and astrocytes, has garnered much attention, as it has become clear they serve a far more expansive role than simply operating as "supporting cells". It is now known that glial cells express receptors and, when activated, release proinflammatory molecules that can influence neuronal signaling. One such family of receptors is the highly conserved, innate immune Toll-Like Receptors (TLRs), including the prototypical TLR4, responsible for detecting invading pathogens. As a pattern-recognition receptor, TLR4 can also detect and respond to a wide-range of molecules including endogenous danger signals and xenobiotic or "foreign" substances.

Here we demonstrate that opioids, cocaine, and methamphetamine activate TLR4. Further, drug-induced TLR4 signaling is necessary to disrupt mesolimbic functioning and influence reward/reinforcement, leading to our newly proposed xenobiotic hypothesis. We also continue to characterize the (+)-isomers of naloxone/naltrexone, recently identified as selective TLR4 antagonists, ideal for use to study drug-induced TLR4 actions as well as potential candidates for pharmaceutical development to aid in the treatment of addiction.

Dedication

*

To my big brother:

Christopher,
to everyone who watched us grow up together
I was the teacher, the mentor, the "big" sister.
But I know a secret:
The truth is that
you taught me

You taught me how to live with exuberance
how to laugh and how to play
how to give really good hugs
and dance with abandon.
You taught me how to embrace a teachers heart
while always remaining an eager student.
You taught me how to do what everyone says can't be done
through hard work and perseverance,
and to do so with a humble yet genuine demeanor.

Your joyful spirit is in every rolled down window
where loud music shakes the speakers while cruising
under sun drenched blue skies.
Your persistence and determination echo in dusty hoofprints,
each soft horse's nicker resonates of your laugh
and in my soul I know that you are always riding with me.

*

And to my beloved horse, Hannah Handi-Pac
Not everyone is lucky enough to have a horse for a soul mate.
Sometimes it feels like my heart is out walking around on four hooves.

*

Acknowledgements

*

I could not have asked for a better advisor: Thank you Linda, for the times you pushed me, and the times you reassured me; thank you for the trust and confidence you have always placed in me. Thank you for the opportunity to work under your mentorship, to be able to look to you as I work to mold myself into an excellent scientist and an enthusiastic teacher.

Friend Amanda, there aren't words to express what your friendship has meant to me. I must be the luckiest person in the world to have shared this graduate school journey with you and to have the opportunity to continue to grow as a scientist (and Friend!) with you. Know you always have a place in my heart- whether we are walking to get coffee after a frustrating or exciting day in the lab, discussing football (Go Broncos!) or if we end up in separate parts of the world.

Tara, I am so grateful you were my office mate and now my dear friend. I will always treasure late nights writing in our office together with Stella Luna and Mr. Charlie. Your friendship has meant the world to me and I am eager to see where we both take our journeys—and I know that no matter what, we will be there for each other, along with our furry friends.

To the rest of the Maier-Wakins lab, all the post-docs, graduate students, and techs: you have truly been family these past years. I am so grateful for the interactions, friendships, and relationships that I have built with each and every one of you and count myself lucky to work with such excellent scientists.

To the Chocolate Juiceboxes!!! Sometimes science is rewarding and exciting, sometimes it's just flat out hard and frustrating; thank goodness for Thursday night softball! I hope you all know how much that time has meant to me!! I'm so grateful for the friendships formed in the dugouts that carried over into the hallways of Muenzinger Psychology.

To all my amazing undergraduate assistants/scientists-in-training over the years: believe me when I say that I know how lucky I have been to have such excellent, motivated students sharing the workload and long days, early mornings, and late nights in the lab. I hope you know I considered it a privilege to work with you.

Sister! Your support in my years as a graduate student has meant the world to me. I love you and I am proud of you. I hope you know that I value our relationship: as fellow scientists (aka: nerds), sisters, and friends.

And Mom, I know my science-world doesn't always make sense to you. It is when you and I are in the barn or the arena together, that we are connected and understand each other's hearts, and that is a bond that I deeply treasure.

Table of Contents

***

Tables

***

Chapter 3

Figures

***

Chapter 1

Preface

Humankind has a long-standing tradition of both recreational and medicinal drug use leading to abuse and addiction. For example, there are descriptions of both the analgesic or pain-relieving, effects of opium (from which morphine is derived) paired with their potentially dangerous side-effects, dating back to Egyptian, Greek, and Roman societies. Scientific reports began to emerge in the late 1800s speculating on the potentially addictive and damaging effects of cocaine use [1]. Depictions of recreational drug use are commonplace in art across cultures ranging from ancient to contemporary. Conflict, violence, and even wars, have persistently erupted over issues with drug trafficking.

Unfortunately substance abuse and addiction remain serious contemporary issues, having widespread detrimental effects involving not only drug-using individuals, but for society as a whole. Estimates of the total overall costs of illicit drug abuse in the United States (including healthcare, loss of productivity and, and crime-related costs) exceed $190 billion annually [2]. In 2009, drug use prompted 2.1 million emergency room visits while an estimated 7.8 million Americans were in need of treatment for illicit drug abuse. As alarming as these numbers are, they do not fully capture the widespread destructive effects on public health, such as family disintegration, loss of employment, failure in school, domestic violence, and child abuse that often arise as a consequence of drug addiction [3].

Addiction is a chronic brain disease that is characterized by compulsive drug seeking and use, and includes repeated relapses to drug-use or an inability to stop drug-use, despite harmful

consequences to the addicted individual and to those around him or her. Although the initial decision to take drugs is voluntary for most people, with repeated use brain changes occur that undermine impulse control and decision-making [4, 5]. This limited capacity for executive functioning severely interferes with the ability of the individual to resist urges or cravings for drug use, regardless of their desire to recover from drug addiction or the knowledge that continued drug-use will have or already has had devastating effects in their life [6].

Addiction is often understood as a cycle (Fig. 1) It begins with the voluntary choice to use one or more drugs, which is rewarding and/or reinforcing, often leading the individual to use again. The individual may then choose to use drugs recreationally, but with continued exposure drug use increases or becomes habitual. This habitual use leads to physical and psychological dependence, meaning that the individual requires the drug to feel "normal" or to prevent the unpleasant symptoms of withdrawal. In this stage, many drug users find themselves going to extraordinary lengths to acquire drugs, and the perceived need for the drug outweighs their values, making normal social, occupational, or educational (etc.) functioning nearly impossible. At any point in this phase, drug addicts may attempt to quit, and find themselves repeatedly relapsing to drug use [7].

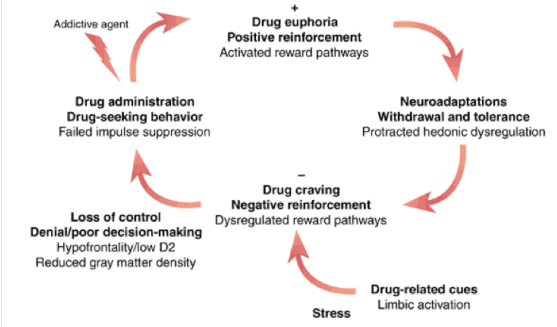

Figure 1: *The cycle of drug use.*
Although the initial decision to take drugs is voluntary for most people, with repeated use changes in brain pathways occur that lead to the development of tolerance, withdrawal symptoms in the absence of the drug, and over time can lead to brain alterations that undermine impulse control and executive functioning making it difficult to stop drug use. *Image credit: Dr. Bachtell, 2010*

Each part of the cycle of drug use and addiction has corresponding neurobiological correlations or explanations. While there has been a substantial increase in the understanding of

how drugs affect the brain and central nervous system, there are still many processes and mechanisms related to all stages of drug use that remain unknown or are still not well understood.

The first stage of drug use, when an individual or organism is in the initial stages of drug exposure, is often correlated with reward, or an appetitive or pleasurable effect. Drugs of abuse are thought to exert their rewarding effects predominately through actions in the mesolimbic dopamine pathway. Also referred to as the "reward pathway", this pathway is critically involved in mediating behaviors important to the survival of an organism, such as mating, feeding, and sleeping. In normal circumstances, when an organism engages in these types of behavior, the mesolimbic dopamine pathway is activated and the resulting feelings of reward are reinforcing, meaning that the organism is likely to engage in these beneficial behaviors again. However, when an organism is exposed to certain substances, for example, drugs such as morphine or cocaine, the mesolimbic dopamine pathway is "hijacked", or excessively activated. This pathway not only mediates reward [8], but is also linked to related processes such as learning, motivation, and incentive salience, which have been shown to contribute to the reinforcing effects of drugs [9-11]. Although there is some debate as to how and to what extent dopaminergic systems is involved with the reinforcing effects of drugs [10, 12] it is widely accepted that the rewarding aspect is an important contributor [13, 14].

The mesolimbic dopamine pathway is comprised of dopaminergic neurons originating from the ventral tegmental area (VTA) and projecting primarily to the nucleus accumbens (NAc) [15]. DA concentration within the NAc is positively correlated to the subjective experience of reward [16]. Understandably, as signaling within the mesolimbic DA pathway powerfully mediates behavior, it is tightly regulated. The VTA is comprised of dopaminergic cell bodies,

GABAergic-interneurons [17], and some glutamatergic neurons [18]; it also receives glutamatergic inputs, particularly from the prefrontal cortex (PFC) [19].

Under basal conditions, the inhibitory tone of VTA control over DA cells results in only low levels of DA within the NAc [20, 21]. This tonic, spontaneous DA release arises due to pacemaker-like membrane currents of DA neurons [22], presynaptic glutamate activity on DA terminals [19, 20], and occurs independent of depolarization [20, 23]. Tonic DA release is responsible for creating a baseline level of extracellular DA within the NAc [24]. However, DA can also be released in a phasic manner [22, 25]. In this case, a burst spike firing pattern results in the release of very high concentrations of DA [26]. It has repeatedly been demonstrated that phasic release of DA is functionally relevant and has behavioral consequences[27-31]; further, phasic DA release is sufficient for behavioral conditioning [32]. Both tonic and more recently, phasic, DA signaling have been implicated in drug reward and drug abuse[33]. Although the various classes of abused drugs share the common effect of producing increased DA within the NAc, each differs in the mechanisms by which they do so.

The NAc is comprised predominately of GABAergic medium-spiny neurons [18], and is subdivided into large regions termed the shell, core, and more recently, a small region referred to the rostral pole[34-36]. These regions are distinctly different from one another in receptor and protein expression, as well as cytoarchitecture and density [34]. Both the shell and the core of the NAc send projections back to the VTA [37, 38], thought to function as a feedback circuit, to help regulate basal DA levels [37-42]. In the initial stages of drug exposure, DA concentrations appear to be preferentially increased within the NAc shell compared to the NAc core [43]. Aside from measurements of DA concentrations, there are several reports that support this concept

regarding the particular importance for the NAc shell mesolimbic disturbances contributing to drug reward and reinforcement (for review, see DiChiara, 2002 [44]). The involvement of the NAc core appears to become more important following repeated drug use, demonstrating more sensitization than the NAc shell [45, 46].

Repeated drug use is associated with many long-lasting neuroadaptations, thought to perpetuate changes in behavior observed in advancing stages of drug use. At this point in the drug abuse cycle, drug-taking evolves so that it is not so much voluntary as it is compulsive. There are numerous brain-circuitries where neuroadaptations in various receptors, proteins, transcriptional factors, and epigenetic phenomena have been identified following drug exposure that are implicated in pathological changes associated with addiction [47-50]. Some of the neuroadaptations directly involving the mesolimbic dopamine pathway include alternations in NMDA, AMPA, and GABA receptors [51], plasticity in glutamatergic projections, particularly to the NAc [52], changes in dopaminergic cell and/or dendritic spine morphology [53, 54], as well as a decreases in dopamine receptor expression [16, 55, 56] and changes in dopamine transporter (DAT) sensitivity [16, 55]. Also characteristic of this stage of drug use is physical dependence, evidenced by withdrawal symptoms when drug use stops. The many, complex adaptations associated with repeated drug use underlie withdrawal. Withdrawal symptoms can vary, based on the specific drug, but in general involve anxiety, depression, physical symptoms of illness, and a strong craving or drive to use the drug again, contributing to repeated relapse to drug use.

Unfortunately, although there have been vast improvements in knowledge and understanding of neurobiological mechanisms and consequence of drug use, we are still in need

of effective treatment paradigms. Research shows that combining addiction treatment medications with empirically validated therapies (such as cognitive behavioral therapy) is the best way to ensure success for most patients. However, for some classes of drugs, there are no pharmacotherapies currently approved for treatment. Even with currently existing treatment paradigms, for individuals who do receive treatment for drug abuse and addiction, relapse rates currently range from 40-60% [3]. Treatment approaches that are tailored to each patient's drug abuse patterns and any co-occurring medical, psychiatric, and social problems can lead to sustained recovery and a life without drug abuse. However, the 2012 SAMHSA's National Survey on Drug Use and Health (NSDUH) indicated that only 10% of 23.1 million individuals who met criteria for drug dependence and/or abuse, received treatment [57]. According to several conservative estimates, every dollar invested in addiction treatment programs yields a return of between $4 and $7 in reduced drug-related crime, criminal justice costs, and theft. When savings related to healthcare are included, total savings can exceed costs by a ratio of 12 to 1. Major savings to the individual and to society also stem from fewer interpersonal conflicts; greater workplace productivity; and fewer drug-related accidents, including overdoses and deaths. Therefore, it is currently a high priority of the National Institutes of Health and the National Institute on Drug Addiction to continue to gain a deeper understanding of how drugs affect the brain and central nervous system, and to develop pharmacotherapies that can be administered alongside current, empirically validated psychotherapies. Although there are some commonalities across abused drugs, each drug or class of drug has distinct targets and actions within the brain. In order to develop treatments for drug abuse and addiction, it is necessary to have a thorough understanding of the neurobiological influences of each individual drug.

Classes of drugs

There is a wide range of substances that have addictive and/or abuse liability, ranging from those with widely accepted use (i.e. caffeine), to those that are legal but are well-known to have risks involved with their use (i.e. nicotine or alcohol), to those that are illegal to possess or use (i.e. heroin or cocaine). Substances are generally lumped into classes based on their effects on the central nervous system of an organism. Here, the focus is on illicit substances falling into one of two classes: opioids and stimulants.

Opioids

Opioids are substances originating from the opiate extracts of poppy plants; now, opioids are more commonly synthetically derived. Opioids serve complex roles as substances because their use ranges from appropriate (as medically prescribed), to misuses of prescriptions, to illicit use, including morphine, codeine, hydrocodone, oxycodone, etc. The therapeutic use of opioids predates recorded history and opioids remain the most effective analgesic and are often the first line of defense in severe pain states ranging from acute to chronic. However, not only is the recreational use and misuse of opioids also historical, so are the many unwanted and dangerous side-effects including but not limited to: analgesic and euphoric tolerance, dependence, respiratory depression that can cause death, constipation, itching, and terrible withdrawal symptoms. It has long been believed that both the desired analgesic properties and the unwanted side-effects of opioids originated from signaling through the same mechanism.

There are three traditional classes of opioid receptors (ORs) that opioids interact with [58]; however, the majority of the initial rewarding/reinforcing effects of opioids are attributed to their

actions on μORs[58, 59]. μORs are G protein-coupled receptors, distributed throughout the central nervous system. With regard to the mesolimbic DA pathway, only a very small percentage of DA neurons express μORs [60, 61], whereas there is heavy expression of μORs on GABAergic interneurons in the VTA [62-64] that synapse on DAergic neurons [61, 65]. Opioid binding to μOR results in increased release of GABA [17, 66]. Typically, GABA signaling results in inhibition of the post-synaptic neuron. In the case of opioid reward and reinforcement, the predominate perspective is that opioid initiation of μOR signaling within the VTA results in disinhibition [66], or a release of GABAergic interneuron inhibitory control over dopaminergic cells and consequently allows for increased DA cell firing that produces elevated extracellular DA within the NAc [12]. Overall, this hypothesis is well supported. Local infusions of μOR agonists or opioids into the VTA increases firing rate of DAergic neurons [67-69]. Further, rats will self-administer opioids directly into the VTA [70, 71]. During heroin self-administration, DAergic VTA neurons demonstrate increased firing rate and increased levels of DA in the NAc [72-74]. Lesions of NAc cell bodies disrupt opioid self-administration [75, 76], GABAergic agonists impair intra-VTA opioid-induced DA release in the NAc [77], and rats have been shown to self-administer a GABA antagonist directly into the VTA [78, 79].

However, there are some contradictory findings and, as such, there is not universal agreement upon the DA-dependent hypothesis of opioid reward/reinforcement. For example, rats have also been reported to self-administer opioids into the NAc [80]; interestingly the D2/D3 dopamine receptor antagonist, sulpiride, had no effect on intra-NAc morphine self-administration [81]. Additionally, there are reports that some DAT antagonists do not consistently suppress opioid self-administration [82-84]. Although these suggest that opioids have the ability to exert reinforcing effects through mechanisms that might be DA-independent, it remains the predominate perspective that opioid activities on the mesolimbic pathway the result in elevated

DA levels within the NAc are critically involved in creating the reinforcing and rewarding effects.

The increase of NAc dopamine, as discussed in the preface, has been directly correlated to the euphoric effects of drugs and is a correlate of their abuse liability. In the case of opioids, this effect is non-discriminatory between use of illicit opioids such as heroin, or the administration of prescription opioids, such as oxycodone. The resulting conundrum is that, since opioids are the most effective class of pain relievers, patients and doctors are often fearful of utilizing opioids, meaning that millions of people suffering from pain, whether it is acute or chronic, have little to no pain relief options. In the past decade there has also been an alarming increase of prescription opioid abuse, not just by patients to whom opioids are prescribed, but also others; for example, children or young adults in the house-hold taking opioids without parental knowledge[3, 6, 57, 85].

Unfortunately, use of illicit opioids, such as heroin, also remains problematic, and results not just in high incidences of addiction, dependence, and abuse but also death from respiratory depression. If caught in time, the effects of an opioid over-dose can be reversed with the administration of (-)-naloxone or (-)-naltrexone, potent μOR antagonists, which rapidly displaces opioid binding to μORs and throws the patient into almost instantaneous withdrawal. Because μORs are stereoselective, the (-)-isomers of naloxone or naltrexone are used and because of their antagonistic effects at μORs, can be helpful in preventing relapse to opioid abuse; although difficulties with patient compliance result in limited efficacy [3]. Maintenance doses of methadone or buprenorphine, low-affinity μOR antagonists, can help mitigate withdrawal

symptoms as well as craving, but have many drawbacks such as their own abuse liability and difficulty with compliance[3].

While the existence of medication interventions available for opioid addiction is an improvement over other classes of addictive drugs that have no option for pharmaceutical aids in treatment (such as cocaine or methamphetamine), because of significant limitations, further investigation to develop more effective treatments is certainly warranted.

Psychostimulants

Psychostimulants are another class of drugs that have a high abuse liability, but also have medical applications. This class includes illicit drugs such as cocaine and methamphetamine, but also includes substances used to help treat attention deficit hyperactivity disorder (ADHD) such as amphetamine-based Ritalin or Adderall, or used for their local anesthetic/topical numbing properties such as lidocaine. These drugs are grouped into one class because of their shared, common effects on the central nervous system. Common effects can include enhanced alertness, endurance, motivation, locomotion, heart rate, and blood pressure, suppressed appetite, and euphoria. However, depending on dose and route of administration, effects of stimulant use can also cause anxiety, dysthymia, hyperactivity and potentially heart failure at high doses. Although cocaine and amphetamines have similar effects and mechanisms of action, there are some differences in how they act on central nervous system targets.

Cocaine

Cocaine is derived from the leaves of the coca plant and has a long history of recreational use, leading to abuse and addiction [1]. It is thought to exert rewarding effects through antagonism of the DATs, particularly within the NAc [86, 87]. DATs are the principle mechanism responsible for removing DA from the synapse and transporting it back into the cytoplasm; therefore, the resulting increases of extracellular DA within the NAc are generally attributed to cocaine's antagonistic actions on DATs.

Although DATs within the mesolimbic reward pathway have been the primary focus of research regarding cocaine's rewarding and reinforcing effects, animal studies reveal contradictory findings that imply the pharmacodynamic effects of cocaine are more complex. Decades of research support that cocaine-blockade of DAT contribute to its rewarding and reinforcing effects. Lesions of neurons expressing DATs in either the NAc [88] or the VTA [89] suppress measures of cocaine reward. Structure–activity studies document correlations between psychostimulant properties in tests of reward and their abilities to block DAT, with poorer correlations in regard to their potencies in blocking other transporters [90, 91]. DAT-knockout mice have been described as "indifferent" to cocaine [92] and demonstrated a blunted DA response when administered cocaine. Conversely, it has been shown that cocaine administration in DAT KO mice does produce increases of extracellular NAc [86] and that DAT KO mice will also self-administer cocaine [93]. Further, conditioned place preference (CPP), a measure of the subjective rewarding effects of drugs, can be established in DAT KO mice [94]. These findings led to the speculation that blockade of other monoamine transporters, such as those for norepinephrine and serotonin, might be responsible for the rewarding effects of cocaine [95]; however, in order to block cocaine reward, at least two of the three transporters (for DA, norepinephrine, and serotonin) must be knocked out. However, studies utilizing transporter KO

mice can be difficult to interpret, since there are alterations in basal dopaminergic functioning [96]. Mice with a knock-in functional DAT that is insensitive to cocaine do not demonstrate cocaine-induced increases in NAc DA or CPP [97], lending further support to the importance of DAT underlying cocaine's rewarding effect. It has also been demonstrated that self-administration of cocaine-like drugs correlates with potency of DAT-inhibition [98]; however, several compounds that are potent DAT inhibitors, such as mazindol, fail to demonstrate abuse liability in animals and/or humans [99, 100]. In PET studies, DAT occupancy is positively correlated with the magnitude of self-reported "high" or euphoria in humans [87] that is thought to underlie the high abuse and addiction liability of cocaine. Although it is widely acknowledged that cocaine does have actions on other targets within the brain, the current consensus within the field is that cocaine's actions on DAT are predominately responsible for its rewarding effects [68].

Methamphetamine

Amphetamines and their derivatives are potent central nervous system stimulants, frequently prescribed to treat a wide-range of disorders, such as attention-deficit hyperactivity-disorder, traumatic brain injury, and narcolepsy. However, due to their ability to induce euphoric effects, amphetamines are often diverted to illicit use. Methamphetamine (METH) is one such derivative that is widely abused; like cocaine, it is thought to exert rewarding and reinforcing effects through actions on DAT. Supporting evidence for this arises from an attenuation of amphetamine-induced DA release in the striatum of mice lacking DAT, both tissue slices and *in vivo* [101]. Additionally, administration of DAT antagonists has been shown to attenuate METH-induced DA release in the NAc[102]. However, similar to cocaine, there are contradictory findings regarding the actions of METH and how it might influence the mesolimbic dopamine

pathway. For example, it has also been shown that DAT KO mice will self-administer METH and that amphetamine triggers elevations of DA within the NAc shell[86]. Administration of DAT agonists yield mixed results; some DAT agonists only produce a modest increase of NAc DA, whereas a minor few produce comparable effects to that of amphetamines[103].

However, not only does METH inhibit DA reuptake through DAT antagonism, but it is also is associated with reverse transport, where DA is pumped from the cytoplasm into the extracellular space [104-108]. Interestingly, there are arguments for two different perspectives on reverse transport. One is that binding of substrates such as amphetamine are required to trigger a conformational change on the transporter; that when amphetamine accumulates DA terminals [109, 110] it binds to DAT facilitating a shift in the transporter's conformation from "outward" facing to "inward" facing, leading to reverse transport [108, 111, 112]. However, there are also several intracellular receptors and phosphorylation sites on monoamine transporters such as DAT [113], and some suggestion that the ability to reverse transport serves as a mode of release independent of exogenous substances, likely triggered by increased release/availability of cytoplasmic DA.

This also leads to another interesting effect of amphetamines that is not well understood. Although DAT reverse transport is the predominately accepted mechanism for how amphetamines induce increased extracellular DA concentrations in the NAc, there is also documentation of increased DA cell firing, or a change in firing pattern from the typical, tonic pattern to a burst pattern, triggering increased availability and release of DA [24]. If high levels of cytoplasmic DA are sufficient to trigger reverse DA transport, then reverse transport could be initiated without amphetamine interaction with DAT.

Another relevant mechanism for the effects of METH on the mesolimbic DA pathway is that METH can enter the cell through monoamine transporters to interfere with the ability of vesicular monoamine transporter (VMAT) to "package" DA into vesicles, creating an excess of DA within the cytoplasm[113]. This scenario creates even more available DA to be pumped into the synapse and could contribute to intra-cellular induction of reverse transport.

Treatment approaches for stimulant addiction/abuse

Currently, there are no approved pharmacotherapies for stimulant abuse/addiction [3]. The best options to-date for individuals seeking treatment for stimulant addiction are structured outpatient or, less frequently, inpatient, treatment programs. Treatment programs include teaching skills to help an addicted individual cope with drug cravings and guidelines if they relapse, which is common and is even considered part of the recovery process, as well as general coping and problem solving skills and learning how to recognize susceptibility to relapse. This type of treatment often will also include aid in detoxifying and managing stimulant withdrawal. There are difficulties surrounding these programs because of issues with compliance and expenses, particularly in cases when health insurance may artificially limit treatment coverage. As discussed in the preface, more effective treatments are needed. Because the ideal approach to treatment includes not just psychological interventions but also biological/medical/pharmaceutical intervention, the development of an effective pharamcotherapeutic is an essential tool to help individuals who are motivated to recover from their stimulant addiction. [114]

Although the exact mechanisms and their contributions to the effects of stimulants such as METH and cocaine on the mesolimbic DA pathway are not yet fully elucidated, it is well documented that they are particularly reinforcing/addictive because of their ability to rapidly drive intra-NAc DA levels to extremely high concentrations [115]. Repeated exposure to stimulants is associated with many neuroadaptations involving not just DAergic transmission and a reduction of DAT functioning, but also changes in other brain systems thought to underlie drug craving and impulsive seeking and drug use, even in individuals attempting to recover from stimulant addiction. Although it is beyond the scope of this paper to discuss in detail the myriad of neurobiological consequences of chronic stimulant use, it is important to note that in order to develop effective treatments, a thorough understanding of how stimulants act on the brain to produce neuroplastic events that lead to the development of addiction is necessary. Thus, gaining a better understanding of how frequently abused stimulants like METH and cocaine influence the mesolimbic pathway, even in initial stages of use, could have important implications that direct research that can lead to effective treatment approaches.

Theoretical Considerations

Traditionally, investigation of CNS mechanisms of drug reward and reinforcement has focused on neurons. However, in recent decades other, non-neuronal cells within the brain and spinal cord, collectively referred to as glial cells, have gained attention. Once thought to simply serve as non-signaling "glue" of the CNS whose responsibilities only involved acting as housekeepers for neurons, it is now known that they serve much more complex and dynamic roles[116]. Glial cells are now known to express receptors for many neurotransmitters[117-120], can synthesize and release neurotransmitters and other signaling molecules, and express transporters for reuptake or release transmitters[121, 122].

Microglia generally function as resident macrophages within the CNS. At "rest" or in their quiescent state, microglia are constantly surveying the extracellular space debris and infectious agents[123, 124]. The brain and spinal cord are separated from the rest of the body by a the blood-brain barrier, made of up astrocytes and endothelial cells, that generally prevent infectious or invading agents from entering the CNS. Microglia express a variety of pattern recognition receptors, including the family of toll-like receptors (TLRs), in order to detect invading pathogens, endogenous danger signals released from dead or dying cells, and exogenous small molecules and their metabolites[125-130]. Many TLRs, when activated, initiate a series of intracellular signaling cascades, resulting in the upregulation of the proinflammatory transcription factor NFκB and the production and release of proinflammatory cytokines such a interleukin-1 beta (IL-1β), interleukin-6 (IL-6), tumor-necrosis factor (TNFα) as well as other proinflammatory substances such as nitric oxide, and excitatory amino acids [131]. These proinflammatory substances can have neuroexcitatory actions on neurons [122, 132, 133], the details of which are discussed in subsequent chapters.

Another type of glial cell found within the CNS, astrocytes are now known to form the tripartite synapse because they enwrap the majority of synapses and modulate synaptic excitability [134, 135]. Astrocytes can also become activated by trauma, infection, or inflammation [136]. Microglia are thought to "activate" or react with a proinflammatory response rapidly, and release molecules that, in turn, triggers astrocyte activation, resulting in release of more proinflammatory molecules [131, 137].

Importantly, glial activation and the resulting proinflammatory cascade can have a

powerful effect on behavior. Proinflammatory cytokines and signaling cascades have been shown to mediate wide-ranges in behavior observed in typical sickness responses, such as lethargy and fatigue, alterations in appetite, anxiety and/or depression, anhedonia, and cognitive impairment [138]. As noted by Hutchinson et al. [139], many of the these behaviors depend on multifaceted engagement of the CNS and involve many dimensions of functioning indicating that glial activation and proinflammatory signaling has the ability to influence complex behavior. Dysregulated glial cell functioning has also been implicated in a number of diseases of the brain, such as Alzheimer's and Parkinson's diseases, as well as clinical depression and anxiety-disorders [138, 140-144].

As noted earlier, drug addiction is also considered a disease state of the brain. In recent years, there has been some suggestion that drugs of abuse could engage glial activation/signaling to influence reward/reinforcement [139], but little is known regarding through what mechanisms drugs such as morphine, cocaine, or methamphetamine might initiate central immune signaling. It has been shown that administration of broadly acting glial activation inhibitors attenuate opioid- and cocaine-induced measures of reward and reinforcement[145, 146]. Further, there is documentation of glial activation associated with opioid [146] and psychostimulants [147, 148] administration in animal studies, and post-mortem in brains of human drug users [149]. In the following chapters, evidence is presented indicating that these commonly abused drugs activate glial cells through activation of a specific receptor and that drug-induced activation of central immune signaling is necessary for the rewarding effects of opioids and cocaine, and that it contributes to methamphetamine-reward.

Chapter 2

Opioid Activation of Toll-Like Receptor 4 Contributes to Drug Reinforcement

A.L. Northcutt[1], M.R. Hutchinson[2], T. Hiranita[3], X. Wang[4], S. Lewis[1], T.A. Kopajtic[3], L. Loram[1], C. Sfregola[1], E. Galer[1], N.E. Miles[1], S.T. Bland[5], J. Amat[1], R.R. Rozeske[1], T. Maslanik[6], T. Chapman[1], K. Strand[1], M. Fleshner[6], R.K. Bachtell[1], H. Yin[4], J.L. Katz[3], K.C. Rice[7], S.F. Maier[1], L.R. Watkins[1*]

*

[1]Dept. Psychology & Neuroscience, Center for Neuroscience, University of Colorado-Boulder, Boulder, CO

[2]Discipline of Physiology, School of Medical Sciences, University of Adelaide, Adelaide, South Australia, Australia

[3]Dept. of Health and Human Services, National Institute on Drug Abuse, National Institutes of Health, Intramural Research Program, Biomedical Research Center MDRB, Baltimore, MD

[4]Dept. Chemistry & Biochemistry, Center for Neuroscience, University of Colorado-Boulder, Boulder, CO

[5]Dept. of Psychology, University of Colorado-Denver, Denver, CO, USA

[6]Dept. of Integrative Physiology, Center for Neuroscience, University of Colorado-Boulder, Boulder, CO, USA

[7]Chemical Biology Research Branch, National Institute on Drug Abuse and National Institute on Alcohol Abuse and Alcoholism, National Institutes of Health, Rockville, Maryland, USA

Abstract

Opioid action was thought to exert reinforcing effects solely via the initial agonism of opioid receptors. Here, we present evidence for an additional novel contributor to opioid reward: the innate immune pattern-recognition receptor, toll-like receptor 4 (TLR4), and its MyD88-dependent signaling. Blockade of TLR4/MD2 by administration of the nonopioid, unnatural isomer of naloxone, (+)-naloxone (rats), or two independent genetic knock-outs of MyD88-TLR4-dependent signaling (mice), suppressed opioid-induced conditioned place preference. (+)-Naloxone also reduced opioid (remifentanil) self-administration (rats), another commonly used behavioral mea- sure of drug reward. Moreover, pharmacological blockade of morphine-TLR4/MD2 activity potently reduced morphine-induced eleva- tions of extracellular dopamine in rat nucleus accumbens, a region critical for opioid reinforcement. Importantly, opioid-TLR4 actions are not a unidirectional influence on opioid pharmacodynamics, since *TLR4* - / - mice had reduced oxycodone-induced p38 and JNK phosphorylation, while displaying potentiated analgesia. Similar to our recent reports of morphine-TLR4/MD2 binding, here we provide a combination of *in silico* and biophysical data to support (+)-naloxone and remifentanil binding to TLR4/MD2. Collectively, these data indicate that the actions of opioids at classical opioid receptors, together with their newly identified TLR4/MD2 actions, affect the mesolimbic dopamine system that amplifies opioid-induced elevations in extracellular dopamine levels, therefore possibly explaining altered opioid reward behaviors. Thus, the discovery of TLR4/MD2 recognition of opioids as foreign xenobiotic substances adds to the existing hypothesized neuronal reinforcement mechanisms, identifies a new drug target in TLR4/MD2 for

the treatment of addictions, and provides further evidence supporting a role for central proinflammatory immune signaling in drug reward.

The reinforcing/rewarding effects of opioids contribute to their widespread abuse [150, 151]. Acute opioid reinforcement is traditionally thought to be mediated through the activation of mesolimbic dopamine neurons projecting from the ventral tegmental area to the nucleus accumbens (NAc) shell [152]. However, additional complexities to this system have also been postulated [153, 154].

While there has long been a focus on classical opioid receptors in exploring opioid actions, reconsideration is necessary. The seminal research of Takagi et al. [155] demonstrated the pharmacodynamic relevance of nonclassical nonstereoselective opioid actions, and Goldstein et al. [156] found a 30-fold greater abundance of nonstereoselective but saturable opioid binding sites compared with saturable stereoselective opioid binding. However, until recently there has been little research on these aspects of opioid pharmacology [157]. Reevaluation of these data implies additional sites of opioid action, which are capable of recognizing structurally diverse ligands beyond the more thoroughly studied opioid active (-)-isomers.

Structurally diverse opioids (including stereochemistries) could also be viewed as xenobiotics, akin to detection of chemicals by the liver's pregnane X receptor [158], thus recognized as substances "foreign" to the CNS. Within the CNS, pattern recognition receptors, such as toll-like receptors (TLRs), can serve this sentinel role identifying "molecular patterns" as "nonself" or "danger" signals [159]. TLR4 has recently received increasing attention as it responds to highly diverse molecular patterns associated with gram-negative bacteria and endogenous substances released from stressed/damaged host cells. Such ligands activate the

TLR4 complex, inducing the production and release of proinflammatory, neuroexcitatory mediators via MyD88-dependent intracellular pathways [160].

We have previously examined the xenobiotic-mediated TLR4 actions of opioids using a collection of *in vivo*, *in vitro*, molecular, and *in silico* strategies, demonstrating that various opioids, including morphine, activate TLR4 signaling [128, 161, 162] through binding to an accessory protein of TLR4, myeloid differentiation protein 2 (MD2), thereby inducing TLR4 oligomerization and triggering proinflammation [128]. The potential importance of activation of TLR4 signaling by opioids, in addition to opioid activation of classical neuronal opioid receptors, for opioid reinforcement is unknown, and is explored here for the first time.

The present studies aimed to define whether opioid-induced TLR4 activation contributes to opioid reinforcement and its associated elevations of NAc dopamine [152]. This was conducted using mice deficient in TLR4 and MyD88 signaling and by pharmacological blockade of TLR4 by (+)-naloxone. Importantly, in each condition the analgesic properties of the opioid agonist were assessed to determine whether the TLR4-directed intervention had simply reduced all the pharmacodynamic actions of the opioid agonist, rather than selectively the rewarding properties. It is apparent that an understanding of opioid-TLR4 actions within the mesolimbic dopamine reward system, in addition to the established opioid receptor-dependent response, will have implications for how opioid reinforcement is viewed, and the opportunities that await the use of pharmacological TLR4 blockade in drug reward.

Materials and Methods

Subjects

For studies at the University of Colorado, viral-free adult, male Sprague Dawley rats (250 –325 g; Harlan) were pair-housed in standard Plexiglas cages with *ad libitum* choice food and

water. The colony room was maintained at 21°C on a 12/12 h light/dark cycle. All experiments were conducted during the light phase. Upon arrival, rats were allowed 1 week of acclimation before any procedures. All procedures were approved by the University of Colorado Institutional Animal Care and Use Committee.

For the drug self-administration procedure, performed at the National Institute on Drug Abuse, viral-free adult male Sprague Dawley rats (weighing ~300 g at the start of the study), obtained from Taconic Farms, served as subjects after acclimation to the laboratory for at least 1 week. Food (Scored Bacon Lover Treats, BIOSERV) and tap water were available in their home cages. After acclimation, weights of rats were maintained at ~320 g by adjusting their daily food ration. The animal housing room was temperature and humidity controlled and maintained on a 12/12 h light/dark cycle with lights on at 07:00 A.M. All procedures were approved by the National Institute on Drug Abuse Intramural Research Program Institutional Animal Care and Use Committee. All studies were performed during the light phase.

For mouse studies, conducted at the University of Adelaide, pathogen-free adult male wild-type BALB/c mice were obtained from The University of Adelaide Laboratory Animal Services (Adelaide, SA, Australia), and two null mutant mouse strains, *TLR4* $^{-/-}$and *MyD88* $^{-/-}$, were originally sourced from Professor Akira (Osaka University, Osaka, Japan) via Dr. Paul Foster from University of Newcastle (Newcastle, NSW, Australia). Mice were housed in a 12/12 h light/dark cycle (light on at 7:00 A.M.) in temperature-controlled rooms (23 ± 3°C). Food and water was available *ad libitum*. After arrival, the mice were allowed to acclimate for at least 5 d and were handled at least 3 d before testing commenced. The mice were always tested during the light phase of the light/dark cycle. All procedures were approved by the Animal Ethics Committee of the University of Adelaide. All studies were performed during the light phase.

Drugs

Morphine sulfate was gifted by Mallinckrodt, Inc. (+)-Naloxone was synthesized by Dr. Kenner Rice (Chemical Biology Research Branch, National Institute on Drug Abuse and National Institute on Alcohol Abuse and Alcoholism, National Institutes of Health, Rockville, MD, USA). (-)-Naloxone was purchased from Sigma. Remifentanil (brand name Ultiva) was purchased from Mylan Institutional. Glycine vehicle was purchased from Sigma. Drugs were confirmed to be endotoxin-free by the limulus amebocyte lysate assay (Lonza) conducted per manufacturer's instructions. Drugs doses are reported as free base.

Experiment 1: Rat conditioned place preference

Apparatus

The Plexiglas place preference apparatus measured 72 (L) x 30 (W) x 30 (H) cm and was comprised to two distinct conditioning environments with a neutral space in-between. Each conditioning environment measured 30 (L) x30 (W) x30 (H) cm. One environment had a floor consisting of 5 mm metal bars spaced 1.5 cm apart (edge-to-edge), and walls with alternating 2 cm width black and white stripes. The floor of the second environment was a black anodized aluminum plate, perforated across the surface with evenly spaced 5 mm holes, and the walls were black with evenly spaced 50mm white polka-dots. The neutral area measured 12 x 30 x 30 cm, with sanded, black Plexiglas flooring. During the conditioning phase, Plexiglas partitions matching their respective environments were inserted to restrict the rats to their specific, designated environment.

The activity of each rat was recorded using Logitech Quickcam Pro 5000 webcams mounted 1.0 m above the center of the conditioned place preference apparatus. The cameras

were connected to a computer running AnyMaze (Stoelting Co.), to track and record the time a rat spent in each of the three compartments.

Procedure to assess the effect of (+)-naloxone on morphine conditioned place preference

An unbiased conditioned place preference protocol was used. Rats were handled and weighed the day prior to the start of an experiment. On Day 1, all rats were placed individually in the conditioned place preference apparatus and allowed to freely explore the entire apparatus for 20 min, in order to assess baseline preferences or biases to either environment. Any rat that spent less than 20% or more than 80% of the entire time in either environment was removed from the study. Each rat was then randomly assigned to treatments group and conditioning environment in a counterbalanced fashion, so that half the rats in each treatment group were assigned to the environment they preferred, and half were assigned to the environment they did not prefer. Rats received either (a) saline paired immediately with (-)-morphine vs. saline on alternating days, (b) saline paired immediately with saline (vehicle of morphine) every day, (c) (+)-naloxone paired immediately with (-)-morphine vs. saline on alternating days, or (d) (+)-naloxone paired immediately with saline (vehicle of (+)-naloxone) every day. Upon completion of injections, subjects were placed into the designated conditioning environment for 45 min. Place preference testing occurred on day 10, and was run identically to baseline testing on day 1 (preexposure day 1, days 2–9 conditioning, day 10 preference test). That is, rats were placed in the place preference apparatus, in a drug-free state, and allowed to explore the entire apparatus for 20 min. The time spent in each environment was recorded and conditioning was calculated as a difference of the time spent in the drug-paired environment before and after conditioning.

Procedure to assess the possible aversive effect of (+)-naloxone

The same paradigm was used as above, except that rats received either (1) (+)-naloxone (1 mg/kg, s.c.) versus saline subcutaneously on alternating days, or (2) saline subcutaneously every day. Place preference was then assessed as above.

Experiment 2: Rat self-administration

Apparatus

Experimental sessions were conducted with subjects placed in operant conditioning chambers (modified ENV-008CT, Med Associates) that measured 25.5 x 32.0 x 25.0 cm, and were enclosed within sound attenuating cubicles equipped with a fan for ventilation and white noise to mask extraneous sounds. On the front wall of each chamber were two response levers, 5.0 cm from the midline and 4.0 cm above the grid floor. A downward displacement of a lever with a force approximating 20 g defined a response, which always activated a relay mounted behind the front wall of the chamber producing an audible "feedback" click. Three light-emitting diodes (LEDs) were located in a row above each lever. A receptacle for the delivery of food pellets was mounted behind a 5.0 x 5.0 cm opening in the front wall midline between the two levers and 2.0 cm above the floor. A pellet dispenser (ENV-203, Med Associates) could deliver 45 mg food pellets to the receptacle. A syringe driver (Model 22, Harvard Apparatus) placed above each chamber delivered injections of specified volumes and durations from a 10 ml syringe. The syringe was connected by Tygon tubing to a single-channel fluid swivel (375 Series Single Channel Swivels), which was mounted on a balance arm above the chamber. Tygon tubing from the swivel to the subject's catheter was protected by a surrounding metal spring and completed the connection to the subject.

Procedures

Subjects were placed in chambers during experimental sessions that were conducted daily, 7 d per week. During sessions, subjects were trained with food reinforcement (45 mg of food pellets, BIOSERV) to press the right lever, and were subsequently trained under a fixed-ratio (FR) 5-response schedule of reinforcement (each fifth response produced a food pellet). Food deliveries were followed by a 20 s timeout (TO) period during which all lights were off and responses had no scheduled consequences other than the feedback click. During this training, sessions lasted for 20 min or until 30 food pellets were delivered.

After subjects were responding at a rate sufficiently high that they obtained 30 food pellets within each of three consecutive sessions, they were surgically implanted in the right or left external jugular vein with a chronic indwelling catheter that exited at the mid-scapular region of the animal's back. Catheter implantation was performed under anesthesia (ketamine 60 mg/kg, i.p. and xylazine 12 mg/kg, i.p.). Catheters were infused daily with 0.1 ml of a sterile saline solution containing heparin (30 IU/ml) and penicillin G potassium (250,000 IU/ml) to minimize the likelihood of infection and the formation of clots or fibroids. All animals were allowed to recover from surgery for ~7 d before cocaine self-administration studies were initiated.

Rats were trained to self-administer cocaine first, a standard training paradigm as previously described [163]. Cocaine self-administration sessions were conducted in 2 h daily sessions until the response rates and patterns of responding showed no substantial session-to-session trends. During these sessions, the LEDs above the right lever were illuminated when cocaine injections were available. Completion of five responses turned off the LEDs and activated the infusion pump, delivering a dose of 0.89 mg/kg. A 20 s TO, during which LEDs were off and responses produced no consequences, started with the injection.

After the time out, the LEDs were illuminated and responding again had scheduled consequences. Once rates of responding maintained by cocaine were stable across sessions, the session was divided into five 20 min components, each preceded by a 2 min TO. This arrangement allowed the assessment of a different cocaine dose within each component. By adjusting infusion volumes and durations, the cocaine dose per injection was incremented in the five sequential components in an ascending order as follows: no injection (also referred to as extinction, or EXT, because responses had no scheduled consequences other than turning off the LEDs for 20 s), 0.026, 0.089, 0.29, and 0.89 mg/kg/inj. Infusion volumes and durations were respectively 0, 5.6, 18, 56, 180 µl and 0, 0.32, 1, 3.2 10 s, based on a body weight of 0.32 kg. A response-independent "sample" injection of cocaine at the corresponding dose was administered immediately before each component.

Training continued until: (1) at least 4.5 mg/kg of cocaine was self administered within a session with <20% variation in the total number of cocaine injections compared with the previous session; (2) the dose of cocaine that maintained maximal response rates varied by no more than one-half log unit over two consecutive test sessions; and (3) maximum response rates were at least five-fold higher than response rates maintained during EXT.

Once performances were stable across successive sessions, the effect of substitutions for cocaine of remifentanil (dose range 0.09–2.9 microgram/kg/inj, i.v.) was assessed, with a minimum of 72 h between treatments. Subsequently, the effects of presession intraperitoneal injections of (+)-naloxone on the response rates maintained by remifentanil injection were assessed. The opioid remifentanil was chosen because its ultra-short half-life increases rapidity and stability of bar-pressing for drug [164]. Due to high rates of remifentanil self-administration, infusion durations were reduced to 0, 0.24, 0.75, 2.4, 7.5 s to avoid excessive fluid intake and

emptying of the syringe.

Experiment 3: Rat in vivo microdialysis

Surgery

A single microdialysis guide cannula was stereotaxically implanted per rat under isoflurane anesthesia (MWI Veterinary Supply). Each sterile CMA 12 gauge guide cannula (CMA Microdialysis) was aseptically implanted and aimed at the right or left NAc shell (stereotaxic coordinates relative to bregma: anterior/posterior = +1.7 mm; medial/lateral = ±0.8 mm; relative to dura: dorsal/ventral = -5.6 mm, bite bar = 0; (Paxinos and Watson, 1998) in a counterbalanced fashion. The guide cannula and a tether screw (CMA microdialysis) were attached to the skull using three jeweler's screws and dental cement. After surgery (isoflurane anesthesia), rats were individually housed and allowed to recover for at least 1 week.

In vivo *microdialysis procedures*

The microdialysis study was undertaken with a minimum of 1 week recovery from anesthesia and guide cannula insertion. The afternoon before the microdialysis experiment, the rats were transferred to the dialysis room that was on the same light/dark cycle as the colony room. The rats were placed in separate Plexiglas bowls with *ad libitum* food and water. Microdialysis probes (CMA 12, MW cutoff 20,000 Da, 2 mm active membrane) were inserted through each guide cannula and artificial CSF (145 mM NaCl, 2.7 mM KCl, 1.2 mM CaCl, 1.0 mM KCl) was perfused through the probes using a CMA infusion pump at a rate of 0.2 µl/min overnight. The next morning, the flow rate was increased to 1.5 µl/min where it remained for the rest of the experiment. The rats were given 2 h to acclimatize to the experimental flow rate before any samples were taken. All dialysates were collected in tubes prefilled with 3 µl of

0.02% EDTA (antioxidant) in 1% ethanol. The sample tubes were manually changed every 20 min for a total of 3 h (9 samples total). Three baseline samples were collected for the first hour of the experiment. After the fourth sample tube was inserted, rats began receiving injections. Each rat received two subcutaneous injections, one immediately following the other. The first injection was either (+)-naloxone (1 mg/kg) or saline and the second injection was either morphine (6 mg/kg) or saline. The morphine and (+)-naloxone doses were based on pilot studies. Then the (+)-naloxone dose was similarly based on pilot studies. Following drug administration, samples were taken every 20 min across a 100 min timecourse.

Microdialysis probe placement verification

After completion of the microdialysis study, rats were euthanized with intraperitoneal 65 mg/kg sodium pentobarbital (Abbott Laboratories, North Chicago, IL, USA) prior to brains extraction. The brains were frozen in chilled isopentane and cryostat sectioned (30 μm) at -20°C. Brain sections containing each rat's cannula track were mounted on gelatin-treated slides and stained with creysl violet, cover-slipped, and viewed under a light microscope to define the site of microdialysis sampling. In order to be included in data analysis, at least 75% of the probe had to be within the nucleus accumbens shell. Dialysate samples from rats fulfilling this requirement were analyzed using high performance liquid chromatography (HPLC) along with electrochemical detection, using a method previously described [165].

Experiment 4: Mouse conditioned place preference

Apparatus

The Plexiglas place preference apparatus measured 50 (L) x 25 (W) x 35 (H) cm and

comprised two distinct conditioning environments (22 x 19 x 35 cm divided into 4) with a neutral passage way in-between (16.6 x 4.8 x 35 cm). Each conditioning environment measured 10.9 (L) x 9.3 (W) x 35 (H) cm. One environment had a floor consisting of 5 mm plastic black bars spaced 5 mm apart (edge-to-edge). The floor of the second environment was black plastic perforated across the surface with evenly spaced 5 mm holes. The walls of each environment were black or white (balanced randomized assignment). The neutral passage way measured 16.6 x 4.8 x 35 cm, with sanded, black Plexiglas flooring. During the conditioning phase, Plexiglas partitions matching their respective environments were inserted to restrict the mice to their specific, designated environment.

The activity of each mouse was recorded using Logitech Quickcam Pro 5000 webcams mounted 1.0 m above the center of the conditioned place preference apparatus. The cameras were connected to a computer running AnyMaze (Stoelting), to track and record the time a mouse spent in each of the three compartments.

Procedure

An unbiased conditioned place preference protocol was used. On day 1, all mice were placed individually in the conditioned place preference apparatus and allowed to freely explore the entire apparatus for 20 min, to assess baseline preferences or biases to either environment. Each mouse was then randomly assigned to treatments group and conditioning environment in a counterbalanced fashion, so that half the mice in each treatment group was assigned to the environment they preferred, and half was assigned to the environment they did not prefer. Mice received either (1) oxycodone (20 mg/kg i.p.) versus saline on alternating days, or (2) saline (vehicle of oxycodone) every day. Oxycodone was used here as it produced robust, consistent,

and reliable conditioned place preference in wild-type BALB/c mice, while morphine did not. Upon completion of injections, mice were placed into the designated conditioning environment for 30 min (total of four conditioning sessions, conditioning sessions 1 and 2 separated from conditioning sessions 3 and 4 by a 2 d weekend). Place preference testing occurred on day 8 and was run identically to baseline testing on day 1. That is, mice were placed in the place preference apparatus, in a drug-free state, and allowed to explore the entire apparatus for 20 min. The time spent in each environment was recorded and conditioning was calculated as a difference of the time spent in the drug-paired environment before and after conditioning. All testing was performed using blinded procedures with respect to group assignments.

Phase 1: Control experiments to assess the selectivity of the observed opioid drug response following pharmacological and genetic modification to TLR4

Phase 1A: Rat Hargreaves test for thermal sensitivity

Acute indwelling lumbosacral catheters. Catheter implantations via the L5/L6 intervertebral approach and drug microinjections were performed based on [166]. Rats were briefly anesthetized under isoflurane anesthesia and an 18-gauge needle was placed between L5 and L6 into the intrathecal space to serve as a guide. Polyethylene-10 tubing was threaded rostrally through the guide and terminated over the lumbosacral enlargement. The 18-gauge needle was removed after catheter placement and the tubing secured to the superficial musculature of the lower back with 3-0 silk suture. The tubing was then threaded subcutaneously to exit the nape of the neck and the skin incision closed. Catheters were 75 cm in length, preloaded with drugs at the intrathecal end and the remainder filled with sterile saline, as used previously [167]. This allowed remote injection of drug during behavioral testing without disturbing the animal, and the

injection of a small void volume that ensured delivery of drugs. Behavioral testing began 2 h after intrathecal catheter placement.

Procedure.

Thermal testing measured withdrawal latency to radiant heat applied separately to the tail and the plantar surface of each hindpaw in a modified Hargreaves test [168]. Baseline latencies before drug administration were calculated as the average of three latencies, measured 5 min apart. Following first drug administration, latencies to withdrawal from each paw and the tail were measured at 3 min intervals for 45 min. The intensity of the heat source was adjusted such that predrug latencies to withdrawal were 3– 4 s, with a 10 s cutoff to avoid tissue damage. This allowed both analgesia and hyperalgesia to be measured. All testing was blind with respect to group assignment.

Phase 1B: Mouse hotplate test for thermal sensitivity

Mice received at least three 5 min habituations to the test environment before behavioral testing. Latencies for behavioral responses to the 50°C hotplate were assessed. All testing was conducted blind to group assignment. A cutoff time of 60 s was imposed to avoid tissue damage. Baseline latencies for the hotplate response ranged from 24 to 32 s. Baseline response latencies were recorded before drug administration. Data are expressed as percentage maximum potential effect (% MPE). For the construction of the dose-responses to oxycodone, mice (wild-type and *TLR4* $^{-/-}$) hotplate latencies were assessed before and 20 min after challenge doses of oxycodone (0.01, 0.1, 1, 2, and 5 mg/kg). Each oxycodone challenge dose involved 8 mice. Mice, which displayed freezing symptoms or urinated during hotplate latency testing, were excluded from datasets because of inherent errors in data collection under these conditions. Mouse behavioral

responses that were two SDs or greater than the mean were also excluded (max $n = 2$ per group, and replaced).

Phase 1C: Morphine tissue concentration quantification

Experimental procedure.

(+)-Naloxone (5 mg/kg) or equivolume vehicle (1 ml/kg saline) was administered subcutaneously 10 min before morphine (10 mg/kg, s.c.). The (+)-naloxone and morphine doses and timings were chosen to match those used in studies of reinforcement, below. A series of blood samples (~0.5 ml/sample) were collected via lateral tail vein nick into heparinized tubes. Sampling occurred just before morphine (time 0) and 5, 15, and 30 min after morphine. Heparinized blood samples were kept on ice until centrifugation, collection of plasma, and storage of plasma at -80°C before extraction for analysis of morphine content. Half the rats of each group were killed immediately after the 5 min sample collection. The rest were killed immediately after the 30 min sample collection. Upon death by unanesthetized decapitation, brain samples (hippocampus, cerebellum) were rapidly isolated, flash frozen in liquid nitrogen, and stored at -80°C before extraction for analysis of morphine content.

Morphine extractions and analyses.

Tissue morphine concentrations were quantified by a modification of a HPLC electrochemical detection method previously described [169, 170]. The system consists of an ESA 5600A Coularray detector with an ESA 5014B analytical cell and an ESA 5020 guard cell. The column was an ESA MD-150 (C-18, 3 μm, 150 x 3.2 mm), and the mobile phase was ESA buffer MD-TM. The analytical cell potentials are kept at -100 mV and -250 mV and the guard cell at -300 mV. Tissue was weighed and then sonicated in 1 ml of deionized water, while

plasma samples were diluted in water for a total volume of 1 ml. Samples were then alkalinized with 500 µl of sodium bicarbonate buffer (500 mM; pH 9.6) and extracted with chloroform (6 ml) by vortexing for 120 s followed by centrifugation 1700 x *g*; 10 min). The upper aqueous layer is aspirated to waste followed by a further addition of the sodium bicarbonate buffer. Samples were then vortexed (10 s) and centrifuged (1700 x *g*; 10 min). After aspirating the aqueous layer to waste, morphine was back extracted from 5 ml of chloroform into 300 µl of NaH_2PO_4 (50 mM; pH 2) by vortexing for 120 s. After centrifugation, an aliquot (100 µl) of the aqueous phase was injected onto the system. Calibration standards ranged from 0.25 ng/ml to 400 ng/ml, and samples above this were diluted with water. High (300 ng/ml) and low (1 ng/ml) quality control samples were assayed with each assay and were expected to be within 10% of the nominal concentrations. The lower limit of quantification was 0.25 ng/ml.

Phase 2: Control experiment to define speed of (+)-naloxone effects on mitogen-activated protein kinase phosphorylation in mice following oxycodone

Immediately following hotplate behavioral testing, mice were overdosed with sodium pentobarbital (400 mg/kg), perfused with 0.9% isotonic saline, and then dissected to obtain spinal cord. The spinal cord tissue was homogenized in 1 ml of 1x denaturing buffer and then heated to 100°C in a heating block for 6 min to prevent protein aggregation and degradation. Spinal tissue was stored at -80°C until use. Spinal lysates from wild-type and *TLR4*$^{-/-}$ mice receiving 0.01, 1, and 5 mg/kg oxycodone were tested for levels of p38, JNK, and ERK phosphorylation. Total p38 was not measured because of time limitations for transcription/translation. Before analysis, spinal cord samples were diluted 1:4 using assay diluent and protein concentrations determined using BCA analysis kit (BD Bioscience). Cell lysates were prepared as per BD Cytometric Bead Array kit to label phosphorylated proteins.

Following washing, the samples were analyzed using a BD fluorescence-activated cell-sorting machine and analyzed in a blinded fashion.

Phase 3: Control experiments to define biophysical and in silico interactions of opioids and (+)-naloxone at TLR4/MD2

TLR4/MD2 in silico *docking* To prioritize the docking calculations and to provide a possible mechanistic framework for the *in silico* docking simulations, it was a priori hypothesized that the TLR4 and MD2 could exist in a range of possible conformational states ranging from a preactivation state of individual membrane bound TLR4 and soluble extracellular MD2 through to a complete signaling heterodimer of TLR4 and MD2.

To examine the *in silico* docking of ligands to the TLR4/MD2 complex, the crystal structure of the human TLR4-human MD2-*E.coli* LPS Ra complex program database (pdb) file was obtained from RCSB Protein Data Bank (PDBID: 3FXI) as published by Park et al. (2009). All ligands, water, and cofactors were removed from the file via Molegro Molecular Viewer, thus eliminating exogenous water molecules and artifacts from crystallization from future docking simulations. The modified pdb files were further prepared using MGL Tools1.5.6.RC2 (http://mgltools.scripps.edu) with polar hydrogen atoms added. Ligands for docking were gathered using PubChem isomeric SMILES, then converted to .pdb using a structure file generator (http://cactus.nci.nih.gov/services/translate/), and validated by visual inspection.

The four macromolecules in the MD2-TLR4 heterodimer pdb file were separated into four separate pdb files, resulting in TLR4-A, TLR4-B, MD2-C, and MD2-D facilitating the creation of the range of possible conformational states using Molegro Molecular Viewer. Docking simulations were conducted for all ligands (agonists and antagonists) to each of these

conformational states. Docking was conducted using Vina [version 1.1.2 (Trott and Olson, 2010)] within PyRx [version 0.8 (Wolf, 2009)]. An exhaustiveness factor of 8 was used for all simulations, with the Vina search space dimensions and center defined for each macromolecule using the auto-maximize function.

Fluorescence titrations

An insect expression human MD2-pAcGP67A vector was provided by Dr. Jie-Oh Lee (Korea Advanced Institute of Science and Technology, Daejeon, Republic of Korea). MD2 baculovirus was prepared by cotransfection of SF-9 insect cells with MD2-pAcGP67A vector and bright linearized baculovirus DNA as described by the manufacturer's protocol (BD Bioscience). After 2–3 rounds of amplification, the MD2 baculovirus suspension reached a titer of ~10^{8}/ml virus particles and was used to transfect high 5 insect cells to express MD2. MD2 was secreted into the medium. After 3– 4 d transfection, the medium was harvested and MD2 protein was purified by IgG Sepharose affinity purification.

Fluorescence measurements were performed on a Fluorolog-3 spectrofluorimeter (Horiba Jobin Yvon). All measurements were performed under room temperature using a 2°—10 mm quartz cell (Starna Cells). The wavelength of 280 nm was chosen to excite the Tyr and Trp residues in MD2 fluorescence and measurement at emission of 300 – 450 nm was conducted. For the fluorescent probe Bis-ANS26, 385 nm was chosen as the excitation wavelength and emission at 420–550 nm was recorded. Appropriate baseline signals were subtracted from spectra obtained. Fluorescence was also corrected by the relation, $F_{corr} = F_{obs}$ anti-log ($OD_{ex} + OD_{em}/2$) for the inner filter effect when necessary, where OD_{ex} and OD_{em} are the optical densities at excitation and emission wavelengths, respectively [171].

For naloxone and remifentanil fluorescence quenching assays, 0.5 μM MD2 was titrated with different concentrations of naloxone or remifentanil, and the fluorescence emission at 337 nm was plotted against naloxone or remifentanil concentration. The raw data were fitted by nonlinear least square method using the equation: $F = 0.5 \times (2 \times F_0 - F_{PL} \times (K_D + [L_T] + [P_T] + ((K_D + [L_T] + [P_T])^2 - 4 \times [L_T] \times [P_T])^{0.5}))$, where $[F]$, the observed fluorescence; F_0, initial fluorescence of protein in the absence of ligand; F_{RL}, adjustable parameter for protein–ligand complex molar fluorescence; K_D, dissociation constant; $[L_T]$, total concentration of the ligand; $[P_T]$, total protein concentration. The data were also plotted according to the equation: $\lg (F_0/F - 1) = -\lg K_D + n \times \lg ([\text{ligand}])$ (Lakowicz, 2006), where K_D, dissociation constant; n, stoichiometry. (+)-Naloxone and remifentanil show no fluorescence signal at the tested conditions. Roxithromycin, which has been reported to show no apparent binding to MD2 [172], served as a negative control compound. Protein A was used as a negative control protein to eliminate the possibility of binding to Protein A tag.

For the displacement assay, different concentrations of (+)-naloxone were titrated into MD2 (0.5 μM) and Bis-ANS (0.5 μM) mixture. After overnight equilibrium at room temperature, the Bis-ANS fluorescence intensity was measured. The fluorescence emission at 478 nm was plotted against (+)-naloxone concentration. K_i of (+)-naloxone was determined using the equation: $K_i = K_{app}/(1 + [\text{Bis-ANS}]/K_D\ (\text{Bis-ANS-MD2}))$.

Statistics

Two-way repeated-measures ANOVAs with Bonferroni *post hoc* tests when appropriate were used to determine statistical significance between groups for both the CPP and *in vivo*

microdialysis measures. For the drug self-administration procedure, response rates were determined by dividing responses by elapsed time in each component, excluding the time outs that followed injections. Average values across six subjects (with SEM) are presented below. To determine whether there was a difference in effects of cocaine compared with remifentanil self-administration, a two-way, repeated-measures ANOVA was used (factors were component and substance injected: cocaine or saline). A one-way, repeated measures ANOVA was used to assess the effects of successive components in the substitution for cocaine of remifentanil. A two-way repeated-measures ANOVA was used to assess the effects of presession treatments of (+)-naloxone on remifentanil self-administration. For studies of prior drug treatments on self-administration of remifentanil, a *post hoc* Bonferroni *t* test was used for pairwise comparisons.

For response thresholds to radiant heat (Hargreaves test) and hotplate tests, one-way ANOVAs with appropriate Bonferroni *post hocs* were used to confirm that there were no baseline differences on behavioral measures. Two-way repeated-measures ANOVAs with Bonferroni *post hoc* tests when appropriate were used to determine statistical significance between groups for thermal response threshold measures. $P < 0.05$ was considered significant. Hotplate latencies across the oxycodone dose range were analyzed using Prism, GraphPad 5.0 software with a four parameter dose–response model.

Results

Assessment of the role of TLR4 in opioid reward/reinforcement

Experiment 1: (+)-Naloxone suppresses morphine conditioned place preference

To assess whether systemic (+)-naloxone influences brain mechanisms that underlie opioid reinforcement, the effects of (+)-naloxone on morphine conditioned place preference (CPP; n = 6-11/group) were assessed using procedures previously described [173]. In CPP, rats experience morphine in one context, vehicle in a different context, and are later tested drug-free to determine which context they prefer. The difference in time spent in the drug-paired side, compared with predrug baseline, is then calculated. As expected, control rats displayed preference for the side previously paired with morphine (5 mg/kg i.p.; saline/morphine group; Fig 1). (+)-Naloxone (1 mg/kg, s.c.) administered just prior to each conditioning trial blocked the development of morphine-induced place preference ((+)-naloxone/morphine group). The saline/saline and (+)-naloxone/saline groups were not statistically different from each other, nor were they significantly different from the (+)-naloxone/morphine group, supporting the conclusion that (+)-naloxone effectively blocked morphine induced CPP. A two way ANOVA with Bonferroni post-hoc tests revealed a significant effect of treatment ($p = 0.01$, $F(3, 30)= 4.89$). Thus, morphine-induced TLR4 activation may contribute to morphine reinforcement, as measured by this Pavlovian conditioning paradigm.

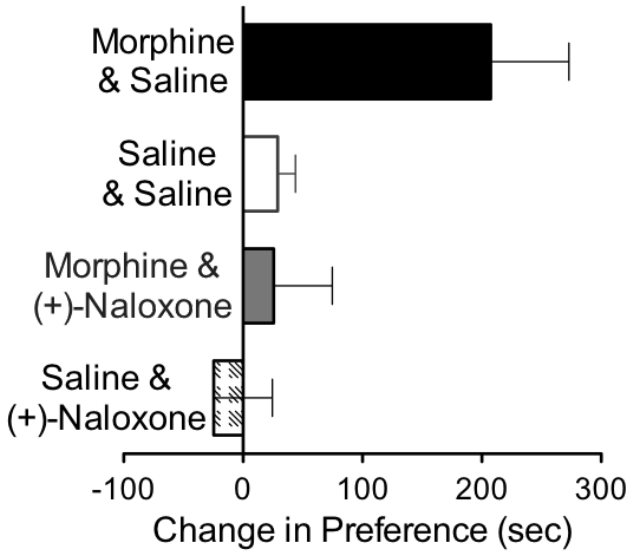

Figure 1. ***(+)-Naloxone blocks the place conditioning effects of morphine.*** Morphine (5 mg/kg, intraperitoneal; 4 pairings) injected with saline (black bar) produced significant place preference (two-way ANOVA with Bonferroni posthoc test, $p<0.01$). (+)-Naloxone (1 mg/kg, subcutaneous) injected just prior to morphine blocked morphine-induced preferences (gray bar). In the absence of morphine, (+)-naloxone and saline were without effect on place conditioning. Data are means per group ±SEMs, $p=0.01$, n=6-11/group

Alternatively, (+)-naloxone could be perceived as aversive, rather than suppressing reinforcement *per se*. To examine this possibility the study was repeated without morphine, with (+)-naloxone paired with one context, rather than both contexts as above (n=5-6/group). (+)-Naloxone failed to condition either aversion or preference (change in preference mean +/SEM for saline: -15.4 ± 46.6 sec; for (+)-naloxone: 1.5 ± 44.35 sec; one way ANOVA, $p>0.05$). Together with the study above, these data support the idea that morphine-induced TLR4 signaling contributes to this measure of opioid reinforcement.

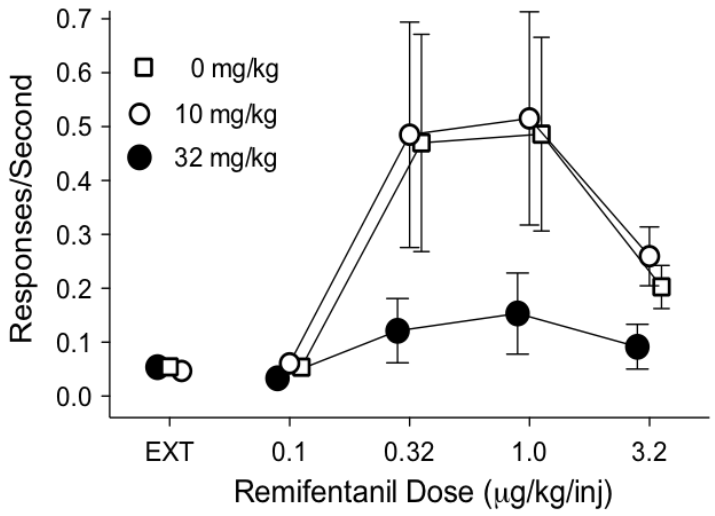

Figure 2. ***Effects of pre-session treatments with (+)-naloxone on responding maintained by remifentanil injection.*** Ordinates, responses per second; abscissae, remifentanil injection dose in ug/kg/injection. Ext; extinction. 0 mg/kg (+)-naloxone (open squares), 10 mg/kg (+)-naloxone (open circles) and 32 mg/kg (+)-naloxone (filled circles). (+)-Naloxone was administered intraperitoneally at 5 min before sessions. Note that (+)-Naloxone dose dependently decreased remifentanil self-administration. Data are means ± SEMs; n=6/group.

Experiment 2: (+)-Naloxone suppresses self-administration of the opioid remifentanil

The effect of the TLR4 antagonist (+)-naloxone was tested on remifentanil self-administration. Remifentanil was chosen for test given its very short half-life increases rate and stability of bar pressing. Rats trained on cocaine self-administration, a standard training paradigm as previously described [163], were tested with remifentanil that reliably maintained self-administration at high rates. The inverted U-shaped dose-effect curve for remifentanil is characteristic of that for other drugs of abuse (Fig. 2) [164]. The highest rate of responding maintained by cocaine was obtained at a dose of 285.6 μg/kg/ inj.

Remifentanil maintained responding in a manner similar to that maintained by cocaine and other abused drugs in all important aspects (Fig. 2). The highest rate of responding was maintained at a dose of 0.9 µg/kg/inj, with lower response rates at higher and lower doses (Fig. 2, open circles). The maximal response rates maintained by remifentanil were two-fold higher than those maintained by cocaine (0.52 ± 0.20 vs 0.19 ± 0.06, respectively), but the shape of the remifentanil dose-effect curve was similar to that for cocaine. Remifentanil was ~320-fold more potent than cocaine. Response rates were significantly ($F_{(4,20)} = 4.20$, $p = 0.013$) affected by dose, and *post hoc* tests indicated that rates maintained by 285.6 and 0.9 µg/kg/inj of cocaine and remifentanil, respectively, were significantly greater than those when responses did not produce injections ($t = 2.81$, $p = 0.043$). Treatment with (+)-naloxone immediately before the self-administration session, dose-dependently suppressed responding maintained by remifentanil (Fig. 2). A two-way repeated measures ANOVA indicated a significant effect of remifentanil dose ($F_{(4,40)} = 5.22$, $p = 0.005$) but a nonsignificant effect of pre-session dose of (+)-naloxone ($F_{(2,40)} = 2.54$, $p = 0.128$). In addition, there was a significant interaction of the two ($F_{(8,40)} = 2.34$, $p = 0.036$). *Post hoc* tests indicated that the effects of 26.2 mg/kg of (+)-naloxone significantly ($p = 0.012$) decreased response rates maintained by the 0.29 ($t = 2.99$) and 0.9 ($t = 2.98$) ug/kg/inj dose of remifentanil.

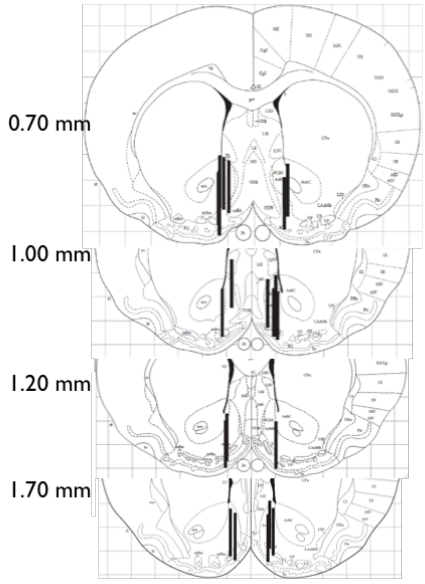

Figure 3. ***Probe placements in the nucleus accumbens shell in the in vivo microdialysis experiment.*** Probe placements are depicted using plates adapted from the atlas of G. Paxinos and C. Watson (Paxinos and Watson, 1998). Not all probes can be seen due to overlapping placements.

Experiment 3: (+)-Naloxone suppresses morphine-induced elevations of Nac shell dopamine

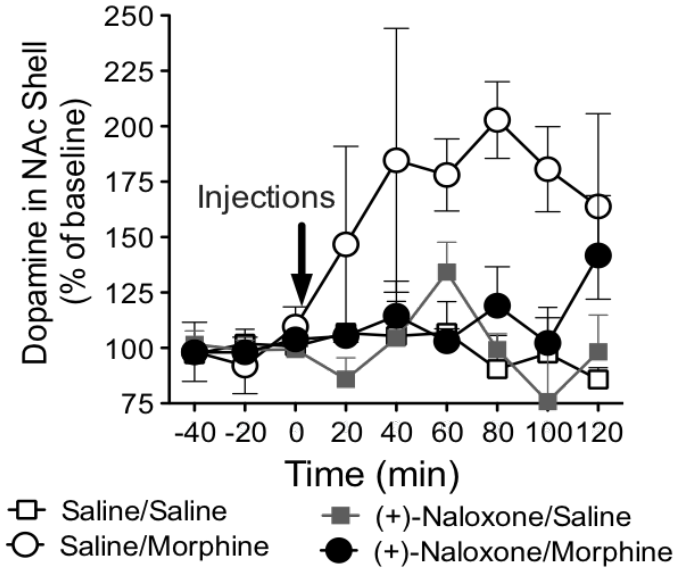

Figure 4. ***(+)-Naloxone suppresses morphine-induced dopamine release in the nucleus accumbens shell***. *In vivo* microdialysis was used to test the effect of (+)-naloxone- (1.22 mg/kg subcutaneously) on morphine- (6 mg/kg subcutaneously) induced increases in extracellular dopamine in the nucleus accumbens shell. After three baseline samples, rats received either saline plus saline, saline plus morphine, (+)-naloxone plus saline, or (+)-naloxone plus morphine. Repeated measures ANOVA revealed a significant effect of treatment condition ($p < 0.01$). Data are means per group ±SEMs; n=4/group.

Given the striking behavioral effects observed with (+)-naloxone in the CPP and self-administration paradigms above, the effect of (+)-naloxone on morphine-induced elevations of NAc shell dopamine, an important neurochemical correlate of opioid reinforcement, was tested to define whether suppression of this measure of reinforcement would also be observed. Dopamine concentrations were assessed by *in vivo* microdialysis, as previously described (Bland et al., 2009), in rats implanted with cannulae confirmed to terminate within the NAc shell (Fig. 3). Before drug treatment, there were no differences in concentrations of extracellular dopamine in the NAc shell recorded from the three baseline time points sampled ($p = 0.05$). As expected, morphine (6 mg/kg, s.c.) injected with saline vehicle increased extracellular concentrations of dopamine in the NAc shell (Fig. 4). (+)-Naloxone (1 mg/kg, s.c.) suppressed this effect. A repeated-measures ANOVA revealed a significant difference in percentage increase of dopamine from baseline based on drug treatment, $F_{(2,128)} = 6.77$, $p = 0.01$. Bonferroni *post hoc* tests supported that the saline/morphine treated rats showed an

increase in dopamine efflux in the NAc shell, whereas the (+)-naloxone/ morphine treated rats were not different from the saline/saline treatment group.

Experiment 4: Mice deficient in TLR4or MyD88-dependent signaling display significantly reduced oxycodone conditioned place preference

Given the above converging lines of evidence, all of which support that a (+)-naloxone-sensitive system is involved in opioid reward/ reinforcement, it was pertinent to assess whether this response could be mirrored using an alternative TLR4-targeted approach. There ore, the role of TLR4 signaling in the behavioral reinforcing actions of oxycodone was examined. Mice deficient in TLR4 or those lacking the TLR4 accessory signaling protein MyD88 were assessed on oxycodone CPP and compared with wild-type control mice. Deficiencies in TLR4 or MyD88 render mice unable to signal via the TLR4MyD88-dependent signaling cascade. Two-way ANOVA revealed main strain ($F_{(2,72)} = 3.21$, $p = 0.046$) and drug effects ($F_{(1,72)} = 3.00$, $p = 0.049$) with a significant interaction ($F_{(2,72)} = 4.76$, $p = 0.01$; Fig. 5). *Post hoc* analyses revealed a significant place preference induced by oxycodone in wild-type mice ($t = 3.8$, $p = 0.001$), but no significant effect of oxycodone in the *TLR4* $^{/}$ or *MyD88* $^{-/}$animals ($t = 0.79$, $p = 0.05$; Fig. 5). Two-way ANOVA

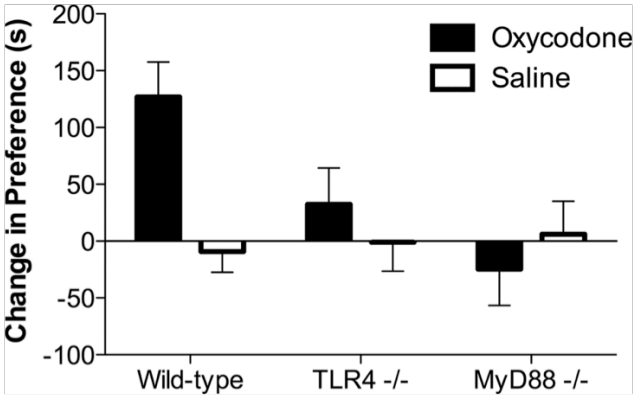

Figure 5: ***Oxycodone conditioned place preference is significantly reduced in TLR4 or MyD88−/− compared with wild-type mice.*** Oxycodone conditioned place preference is significantly reduced in *TLR4* or *MyD88*$^{-/-}$ compared with wild-type mice. Deficiencies in TLR4 or MyD88 render mice with significantly reduced oxycodone conditioned place preference; main strain ($F_{(2,72)} = 3.21$, $p < 0.046$) and drug effects ($F_{(1,72)} = 3.00$, $p = 0.049$) with a significant interaction ($F_{(2,72)} = 4.76$, $p = 0.01$). *Post hoc* analysis revealed a significant place preference induced by oxycodone in wild-type mice ($t = 3.8$, $p < 0.001$), but no significant effect of oxycodone in the *TLR4*$^{-/-}$ or *MyD88*$^{-/-}$ animals ($t < 0.79$, $p > 0.05$). $n = 11–17$ per group. Data are means ± SEMs.

revealed a main effect of drug conditioning ($F_{(1,72)} = 26.55$, $p = 0.0001$) on the total distance traveled, as a measure of activity, but no interaction ($F_{(2,72)} = 0.93$, $p = 0.40$) or effect of strain ($F_{(2,72)} = 1.45$, $p = 0.25$) were observed during the place of preference test.

Experimental controls to assess the selectivity of the impact of TLR4 on the pharmacodynamic actions of opioids

The ability to draw meaningful conclusions from the first four experiments would be significantly hampered if no further assessments were made. Therefore, three additional phases of control experiments were conducted to provide additional validation of the four primary experiments. Phase 1 control experiments assessed the selectivity of the observed opioid drug response following pharmacological and genetic modification to TLR4.

That is, it was first assessed if the previous experiments could simply be explained by a panpharmacodynamic opioid attenuation response, as would be expected if an opioid receptor antagonist had been administered. In fact, based on our previous publications, attenuation of the TLR4-dependent central neuroexcitatory immune signaling, which has been demonstrated to oppose opioid analgesia, should lead to an acute potentiation of opioid analgesia [161, 174]. Phase 1 control experiments also assessed if the coadministration of (+)-naloxone may have altered the access of morphine to the brain, and thus its active sites for producing opioid reward.

Phase 2 control experiments assessed if the opioid-induced TLR4-dependent changes in behavior were temporally associated with established TLR4-dependent downstream signaling activation, thereby providing evidence for the speed of the TLR4 response. Finally, Phase 3 control experiments aimed to determine if these opioid-induced, TLR4-dependent responses were via direct opioid activation of the TLR4 signaling complex or via some other indirect

means. Therefore, *in silico* and *in vitro* biophysical studies were conducted to address each of these concerns.

If remifentanil acts as a TLR4 agonist, then (+)-naloxone should potentiate intrathecal remifentanil analgesia just as (+)-naloxone has previously been documented to potentiate morphine analgesia [161, 174]. There were no baseline latency differences between groups of animals ($F = 1.67$, $p < 0.05$). Very similar patterns were observed on both the left and the right hindpaw withdrawal latencies, and thus results are presented with the two hindpaws averaged. There were significant differences between the drug treatment groups in the tail ($F = 44.8$, $p < 0.05$) and hindpaw ($F = 23.29$, $p < 0.05$) responses. Bonferroni *post hoc* tests showed that intrathecal remifentanil alone produced significant and brief analgesia on the tail (at 3, 6, 18, 21, and 33 min following first remifentanil injection) and hindpaws (at 3 and 33 min following first remifentanil injection), when compared with glycine vehicle alone (Fig. 6). The remifentanil analgesia on both the tail (3, 6, 9, 21, and 36 min following first remifentanil injection) and hindpaws (3, 6, 18, 21,

Phase 1 control experiments: Does pharmacological or genetic modification of TLR4 decrease opioid analgesia parallel to TLR4 blockade reducing opioid reward?

Phase 1A: (+)-Naloxone potentiates acute remifentanil analgesia, in keeping with remifentanil as a TLR4 agonist.

33, and 36 min following first remifentanil injection) was potentiated by administration of (+)-naloxone 10 min before the first remifentanil injection. Thus, as hypothesized, remifentanil acted as a TLR4 agonist causing TLR4-dependent opposition to opioid analgesia, and hence remifentanil analgesia was potentiated by (+)-naloxone acting as a TLR4 antagonist. As such, while (+)-naloxone reduced remifentanil reward (Experiment 2) it increased analgesia.

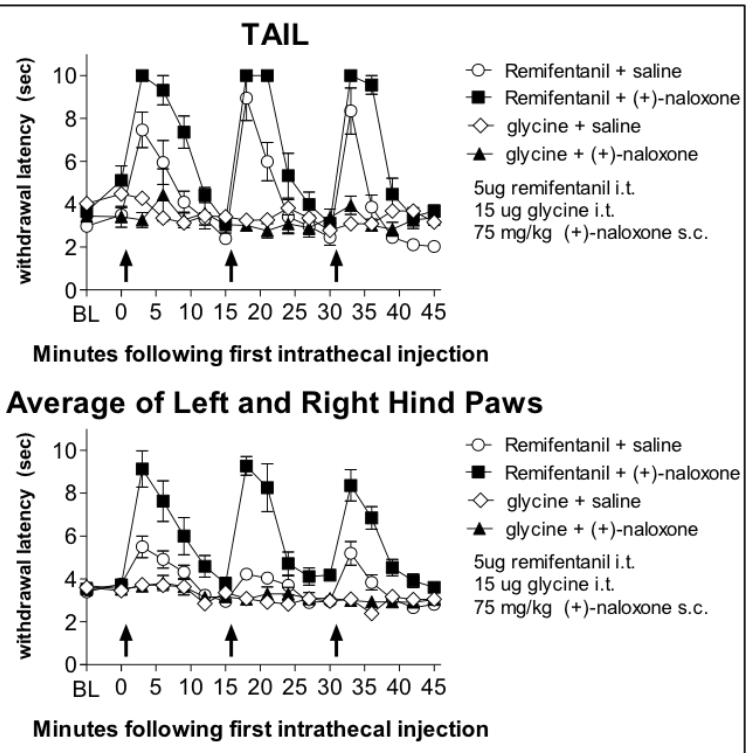

Figure 6. ***Remifentanil analgesia is potentiated by coadministration of (+)-naloxone, as predicted if remifentanil acts as a TLR4 agonist.*** Following baseline (BL) latency assessments with radiant heat to the tail and hind paws, (+)-naloxone (75 mg/kg) or vehicle (saline) was subcutaneously administered, 10 min prior to the first intrathecal dosing. A total of three intrathecal injections of remifentanil or vehicle (glycine) were administered 15 min apart, given the brief half-life of remifentanil. Remifentanil produced a significant and brief analgesia in both the tail (top panel; $F=44.8$, $p<0.05$) and hind paws (bottom panel; $F=23.29$, $p<0.05$) when compared to glycine vehicle. Remifentanil analgesia was robustly potentiated by (+)-naloxone ($F=44.8$; $p<0.05$). Arrows indicate timing of the remifentanil or glycine vehicle intrathecal injections. Data are means ± SEMs; n=6/group.

Phase 1B: Oxycodone is a more potent analgesic in TLR4$^{-/-}$ mice compared with wild-type mice.

TLR4 -/-mice were used to assess the involvement of TLR4 in acute oxycodone analgesia over a range of doses. Pain responsivity was compared for wild-type versus

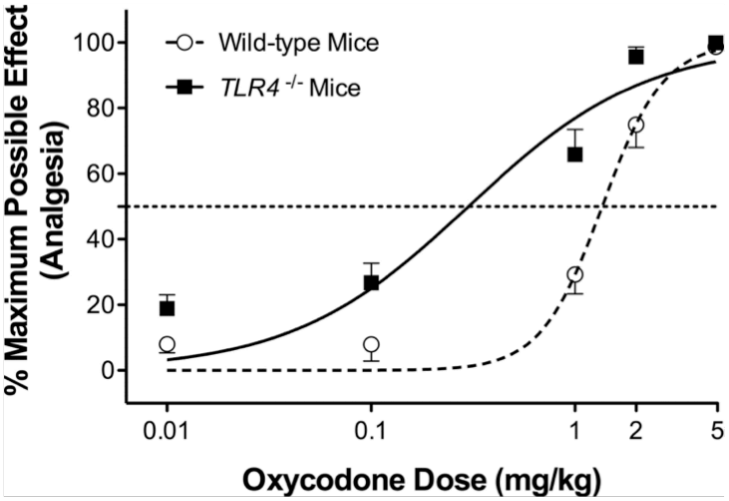

Figure 7: Oxycodone is a more potent analgesic in TLR4−/− mice compared with wild-type mice. Oxycodone is a more potent analgesic in *TLR4*$^{-/-}$ mice compared with wild-type mice. *TLR4*$^{-/-}$ mice demonstrate significantly longer hotplate latencies when administered with oxycodone compared with wild-type controls. ED_{50} wild-type 1.36 mg/kg versus *TLR4*$^{-/-}$ 0.26 mg/kg; $F_{(2,71)} = 24.1$; $p < 0.0001$. $n = 7–8$ animals/dose.

TLR4 $^{-/-}$mice dosed by intraperitoneal injection of oxycodone ranging from no analgesia to maximal analgesia on the hotplate test. As expected, increasing doses of oxycodone resulted in significant increases in hotplate latencies. Further analysis of the oxycodone dose–response curves revealed a main TLR4 effect where *TLR4* $^{-/-}$mice achieved significantly longer hotplate latencies ($p < 0.01$). There was a fivefold leftward shift in the *TLR4* $^{-/-}$oxycodone analgesic dose–response curve (ED_{50} wildtype 1.36 mg/kg vs *TLR4* $^{-/-}$0.26 mg/kg; $F_{(2,71)} = 24.1$; $p < 0.0001$) compared with wild-type mice (Fig. 7). In addition, *TLR4* $^{-/-}$mice had a significantly altered slope of the dose–response curves (wild-type: 2.89 vs *TLR4*$^{-/-}$: 0.85; $F_{(2,71)} = 24.1$; $p < 0.0001$). Once again, as hypothesized, oxycodone acted as a TLR4 agonist causing TLR4-dependent opposition of opioid analgesia, and hence oxycodone analgesia was potentiated in the absence of TLR4. As such, while *TLR4* $^{-/-}$mice had reduced oxycodone reward (Experiment 4), they had increased analgesia.

Phase 1C: (+)-Naloxone does not prevent systemic morphine from reaching the brain.

While the CPP, self-administration, and *in vivo* microdialysis studies above suggest that (+)-naloxone inhibits those centrally mediated opioid-induced effects, an alternative explanation is that (+)-naloxone prevents morphine from reaching the brain, that it is a pharmacokinetic, and not TLR4based, opioid-reward mechanism. Thus, brain morphine concentrations were quantified, as previously described [169, 170], following coadministration with (+)-naloxone. (+)-Naloxone had no effect on morphine concentrations in brain tissue at the time points measured, compared with rats receiving morphine co-administered with vehicle (saline) ($p < 0.05$; Fig. 8). Together with the CPP, self-administration and the *in vivo* microdialysis data above, these results support the conclusion that opioid-induced TLR4 signaling substantially contributes to this neurochemical change considered to play a role in opioid reward independent of pan-pharmacodynamic changes or pharmacokinetic alterations.

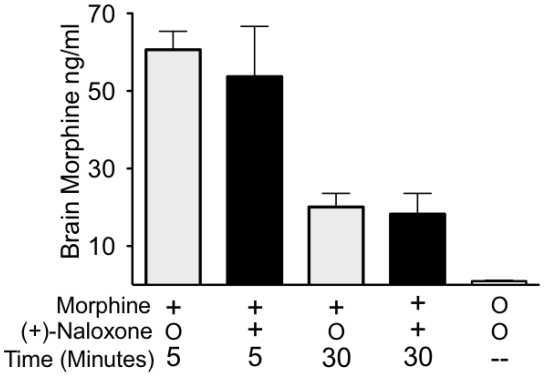

Figure 8. ***(+)-Naloxone does not alter morphine levels in brain (hippocampus).*** To define whether the results from the conditioned place preference or *in vivo* microdialysis studies may be attributed to blockade by (+)-naloxone of morphine reaching the central nervous system, morphine levels were measured in hippocampus, where this brain structure was chosen simply due to its size and ease of isolation. Rats were injected subcutaneously with 1 mg/kg (+)-naloxone or saline 5 min before intraperitoneal 6 mg/kg morphine; naïve rats served as negative controls. Either 5 or 30 min after injection, rats were decapitated, hippocampi were harvested and morphine levels quantified by HPLC (Van Crugten et al., 1997, Doverty et al., 2001). No differences in brain levels of morphine were detected, comparing (+)-naloxone and saline groups administered morphine (two-way ANOVA; $p>0.05$). Data are means ±SEMs; n=4/group.

Phase 2 control experiments: *Are the opioid-induced TLR4-dependent changes in behavior temporally associated with TLR4-dependent activation of mitogen-activated protein kinases?*

It was first necessary to clarify whether opioid-induced TLR4dependent signaling events occurred fast enough to be associated with the altered pharmacodynamic responses. We have previously published that oxycodone is capable of *in vitro* activation of TLR4-dependent NF-κB signaling using a stably transfected cell line and 24 h cell culture [161]. However, to date there is

no evidence for *in vivo* TLR4-dependent oxycodone signaling. Thus, using wild-type and *TLR4* $^{-/-}$mice, quantification of mitogen-activated protein kinase (MAPK) phosphorylation following *in vivo* oxycodone administration was evaluated.

Immediately following analgesia testing in Phase 1 control study 1B (20 min after drug), wild-type and *TLR4* $^{-/-}$mice spinal cord samples were collected to enable quantification of *in vivo* signaling via the TLR4 cascade. Samples were analyzed for downstream TLR4 MAPK phosphorylation. Oxycodone administration caused significant dose-dependent elevations in the phosphorylation of p38 (Fig. 9*A*) and JNK (Fig. 9*B*) in wild-type (t=3.053, p<0.01) but not *TLR4*$^{-/-}$ mice (t = 0.98, p <0.05). For the phosphorylation of p38, a two-way ANOVA resulted in a main strain ($F_{(3,53)}$ = 11.11, p = 0.0016) and oxycodone dose effect ($F_{(1,53)}$ = 6.94, p = 0.0005) with a significant interaction ($F_{(3,53)}$ = 3.71, p = 0.017). *Post hoc* analysis revealed that oxycodone significantly increased p38 phosphorylation in wild-type over *TLR4*$^{-/-}$ mice at 5 mg/kg (t = 3.8, p < 0.01; Fig. 9*A*). Analysis of JNK phosphorylation revealed a main strain ($F_{(3,53)}$ = 9.13, p < 0.0001) and dose effect ($F_{(1,53)}$ = 60.79, p < 0.0001) and significant

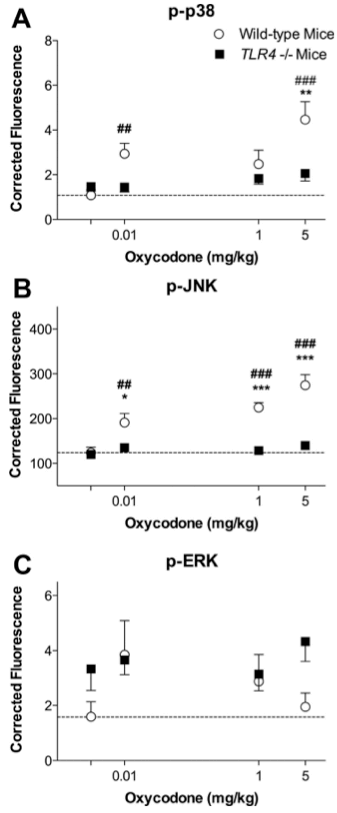

Figure 9: Oxycodone causes TLR4-dependent increases in p38 and JNK phosphorylation. Oxycodone causes TLR4-dependent increases in p38 and JNK phosphorylation. *TLR4*$^{-/-}$ mice had significantly reduced oxycodone-induced MAP kinase signaling. Phosphorylation of MAPK proteins (p38, JNK, and ERK) were measured from wild-type and *TLR4*$^{-/-}$ spinal cords following acute oxycodone administration. Oxycodone caused significant dose dependent elevations in the phosphorylation of p38 (*A*) and JNK (*B*) in wild-type but not *TLR4*$^{-/-}$ mice. An oxycodone effect was not observed in ERK phosphorylation (*C*). n = 7–8 animals per dose. *Post hoc* WT versus *TLR4*$^{-/-}$, $^{*}p < 0.05$, $^{**}p < 0.01$, $^{***}p < 0.001$. *Post hoc* vehicle versus dose, $^{\#\#}p < 0.01$, $^{\#\#\#}p < 0.001$.

interaction ($F_{(1,53)} = 14.73$, $p < 0.001$; Fig. 9*B*). In contrast, there were no dose-dependent elevations in ERK phosphorylation and no TLR4-dependent differences in the response ($p < 0.05$; Fig. 9*C*). Therefore, acute opioid-induced TLR4-dependent p38 and JNK phosphorylation occurred temporally associated with TLR4-dependent alterations in opioid pharmacodynamics.

Phase 3 control experiments*: Can opioid agonists and (+)-naloxone directly act at TLR4 or part of its extracellular signaling complex to induce the TLR4-dependent alterations in opioid reward?*

All the evidence presented thus far implicates an opioid-induced, TLR4-dependent mechanism in altering opioid reward/reinforcement. However, this could occur via either direct opioid action at TLR4 or indirect activation of TLR4 signaling via an undefined mechanism(s). Therefore, a series of experiments were conducted to ascertain if any evidence for direct opioid interactions with TLR4 or its accessory protein MD2 could be found. Our recent publication has already outlined extensive evidence for direct morphine interactions with TLR4 and its accessory protein MD2 [128]. Similar oxycodone *in silico* data and oxycodone-induced TLR4-dependent NF-κB signaling data have also previously been published [161], suggesting a similar mechanism of action to morphine. Here, we sought to examine the direct TLR4 activity of the fully synthetic 4-anilinopiperidine, remifentanil, and the (+)-4,5-epoxymorphinan isomer (+)-naloxone. Two independent lines of evidence were pursued for each compound to address this issue: (1) *in silico* docking of the ligand to the TLR4/MD2 complex, and (2) biophysical assessments of competitive binding of the ligand to MD2.

Phase 3A: Remifentanil and remifentanil acid dock in silico to the TLR4/MD2 complex.

Morphine, remifentanil, and its opioid inactive metabolite, remifentanil acid, were

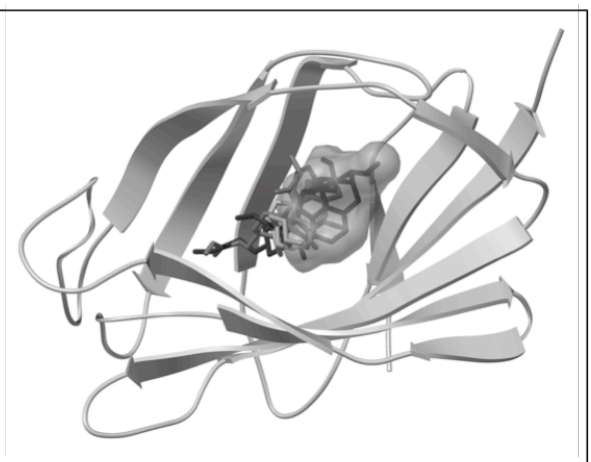

Figure 10. ***in silico of (+)-naloxone docking in the lipopolysaccharide binding pocket of MD2, an essential co-receptor of TLR4***. Morphine, remifentanil and its opioid inactive metabolite, remifentanil acid (displayed as the overlapping stick symbol structures), were determined to dock *in silico* to the lipopolysaccharide binding domain of MD2 (represented as a ribbon peptide), in a conformation that spatially overlap with (+)-naloxone (spacial cloud representing preferred docking conformation) and morphine *in silico* docking.

assessed for their *in silico* docking to various conformational states of the TLR4/ MD2 complex using Vina and previously published TLR4/MD2 pdb files, to assess if any possibly relevant physicochemical interactions occurred. The metabolite of remifentanil was analyzed, in addition to the parent compound, given our prior finding that the opioid inactive metabolite of morphine proved to be a TLR4 agonist [175]. Interestingly, morphine's docking energy did not differ substantially between any of these conformations, but remifentanil and remifentanil acid both displayed lower docking energies when bound to the MD2 portion of the available conformational states. Moreover, all three compounds docked to the critical lipopolysaccharide binding domain of MD2 (Fig. 10). These data suggest that remifentanil and remifentanil acid displayed the physicochemical characteristics that may enable them to interact with the TLR4/MD2 complex.

Phase 3B: Remifentanil binds to MD2.

Following on from the promising *in silico* data results, binding studies were conducted. To investigate whether remifentanil can bind to MD2, a fluorescence quenching assay was performed. As shown in Figure 11*A*, remifentanil caused the quenching of MD2 intrinsic fluorescence upon binding, while the negative control compound roxithromycin caused little quenching of MD2 fluorescence, demonstrating the specific binding of remifentanil to MD2. A dissociation constant (K_D) of 6.0 ± 1.1 μM was derived using a one-site binding model and

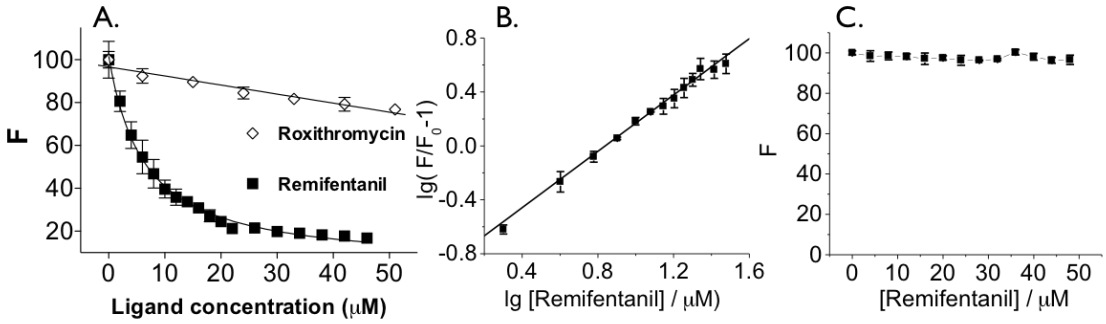

Figure 11. ***Biophysical evidence that remifentanil binds to MD-2 in vitro*****. (A)** Titration curves of MD-2 intrinsic fluorescence assay with the increasing of compound concentration. Remifentanil binds to MD2 and causes the quenching of expressed MD2 intrinsic fluorescence *in vitro*, while roxithromycin, a compound used as a negative control, shows no MD2 binding activity. K_d=6.0±1.1 μM for the remifentanil-MD-2 interaction. **(B)** Replotting the data from Panel A according to the equation: lg (F_0/F-1) = -lgK_D + n×lg ([remifentanil]), revealing a slope of 1.06 ± 0.07 and a K_d=8.2±1.1 μM for the remifentanil-MD-2 interaction. **(C)** Specificity of remifentanil binding is revealed by its failure to bind Protein A. Remifentanil demonstrates negligible binding to a negative control protein, Protein A. 80 nm was used as the excitation and emission at 308 nm (peak position) was plotted against the titrated remifentanil concentration. Note: the binding constants derived here are likely underestimating the affinity constants of remifentanil to MD2 owing to the lack of cofactors found *in vivo*. Data are means ± SEMs; n=2 replications per group.

nonlinear least-squares fit of MD2-remifentanil interaction. Figure 11*B* shows the lg(F_0/F–1) versus lg([remifentanil]/μM) plot. A stoichiometry value of 1.06 ± 0.07 and a K_D of 8.2 ± 1.1 μM were obtained for the binding of remifentanil to MD2, which lends further support to the one-site binding model. To eliminate the possibility that the observed MD2-remifentanil binding was due to Protein A tag-remifentanil interaction, we also tested the binding of remifentanil to Protein A (Fig. 11*C*) and no apparent quenching of Protein A intrinsic fluorescence was observed. The overall result excludes the possible Protein A tag-remifentanil binding. These data suggest that remifentanil is capable of

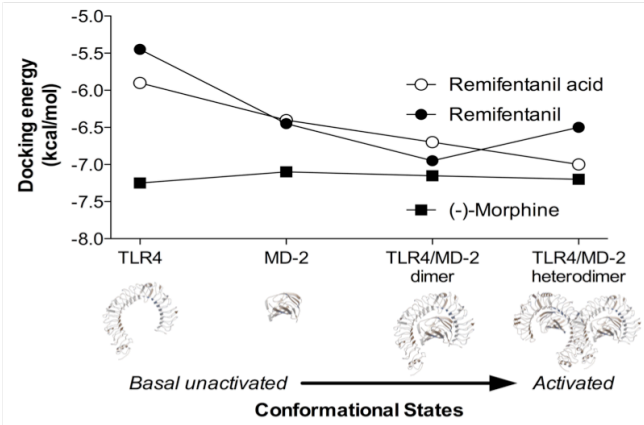

Figure 12. ***Remifentanil, its major metabolite remifentanil acid, and morphine each dock to all states of the TLR4 and MD2 complex.*** Morphine, remifentanil and its opioid inactive metabolite, remifentanil acid, were determined to dock *in silico* to the lipopolysaccharide binding domain of MD2. Remifentanil and remifentanil acid docking were demonstrated to flow down a binding energy gradient estimated from *in silico* docking (y axis), such that the docking conformations preferred the formation of the active signaling herterodimer TLR4/MD-2 complex rather than the MD-2 alone conformation (displayed categorically on the x axis). In contrast, morphine failed to display any such docking energy preference to the TLR4/ MD2 complex states, instead demonstrating high affinity for all states.

direct binding to TLR4/MD2.

Phase 3C: In silico evidence that (+)-naloxone docks to the coreceptor MD2 of TLR4.

Using the approach used in control Experiment 3A, complementary *in silico* data using previously available crystal structures [176, 177] show that docking of (+)-naloxone to MD2 spatially overlaps the docking of both morphine, remifentanil, and remifentanil acid, supporting competition at this binding pocket (Fig. 12). Therefore, (+)-naloxone has the necessary characteristics to allow for blockade of TLR4/MD2 binding to morphine and remifentanil.

Phase 3D: (+)-Naloxone binds to MD2.

As noted above, prior studies have provided support that (+)-naloxone disrupts TLR4 signaling, but failed to identify the location along the TLR4 signaling cascade, even whether this involves an extracellular site versus intracellular site following activation of the TLR4/MD2 receptor complex. Here, the *in vitro* nonstereoselective binding of naloxone to purified expressed MD2 (Hutchinson et al., 2011) was assessed using ligand quenching of MD2 intrinsic fluorescence (Fig. 13*A*). Both (-)-naloxone and (+)-naloxone bound MD2 and quenched MD2 intrinsic fluorescence with comparable affinities (17.7 ± 3.2 μM and 16.6 ± 4.7 μM, respectively). In comparison, the previously reported negative control

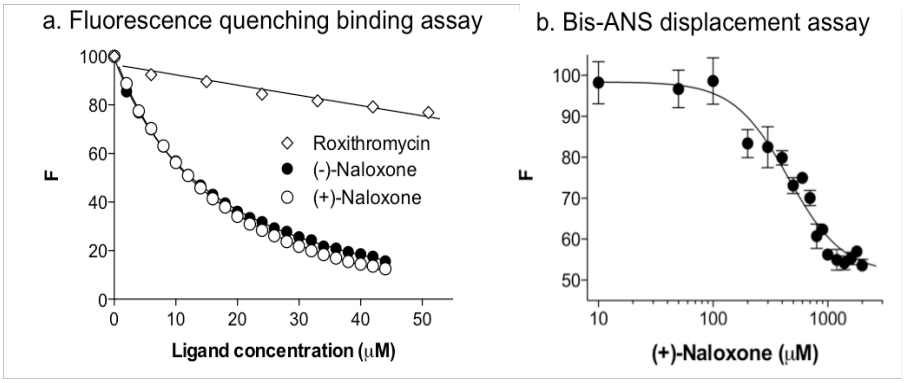

Figure 13. ***(+)-Naloxone binds to MD2 in vitro.*** **(A)** Both (-)-naloxone and (+)-naloxone bind to MD2 and cause the quenching of expressed MD2 intrinsic fluorescence *in vitro*, while roxithromycin, a compound used as a negative control, shows no MD2 binding activity. **(B)** (+)-Naloxone caused the decrease of Bis-ANS fluorescence from the Bis-ANS-MD2 complex, suggesting that (+)-naloxone replaces Bis-ANS binding to MD2. Note: the binding constants derived here are likely underestimating the affinity constants of (+)-naloxone to MD2 owing to the lack of cofactors found *in vivo*. Data are means ± SEMs; n=2 replications/group.

roxithromycin [172] showed no MD2 binding activity, thus demonstrating specific binding of (+)-naloxone to MD2. Bis-ANS, a MD2 molecular probe, binds the lipopolysaccharide binding pocket of MD2 and its fluorescence intensity is enhanced when bound to MD2 [178]. (+)-Naloxone decreased Bis-ANS MD2 complex fluorescence, suggesting that (+)-naloxone replaces Bis-ANS binding to MD2 (Fig. 13*B*). Collectively, these data suggest (+)-naloxone binds to the critical binding domain of MD2.

Discussion

Here, we provide evidence that TLR4 is a novel contributor to opioid reward behaviors and neurochemistry. Specifically, we demonstrated using (+)-naloxone-TLR4 pharmacological blockade, or MyD88-TLR4-dependent signaling genetic knockouts, that opioid-TLR4 signaling is a novel and important contributor to: (1) opioid reward behavior, as measured by CPP and self-administration; and (2) reward neurochemistry, through opioid-induced, but (+)-naloxone-sensitive, NAc shell extracellular dopamine elevations. Critically, these opioid-TLR4 actions are not simply a requirement for all opioid responses, since opioid-induced TLR4 signaling decreased opioid analgesia. We also conclude that opioids of diverse chemical structures can dock with the active domain of MD2, suggesting a direct mode of action of these agents acting as xenobiotic drugs to cause TLR4 signaling. Thus, it is hypothesized that opioids engage inflammatory CNS processes, acting as xenobiotic-associated molecular patterns (XAMPs) to activate TLR4, in addition to their previously characterized neuronal targets, thereby potentiating acute dopamine changes involved in opioid reward.

Several questions arise that warrant discussion regarding the changes in opioid reward: (1) “how” is opioid-TLR4 signaling involved; (2) “what” cell type(s) is/are contributing; and (3) “why” are opioid-TLR4 interactions acting in this manner? The “how” and “what” questions are

indelibly linked, as “how” TLR4 contributes to opioid reward is dependent on “what” cells are expressing TLR4. As such, the two points will be discussed simultaneously.

Which TLR4-expressing cell type(s) contributes to opioid reward is unclear. Preliminary mRNA expression data using flow cytometry-assisted cell sorting of NAc micropunches suggests TLR4 mRNA is only found in microglia and not neurons (S. Bilbo, personal communication). Some examples of neuronal TLR4 expression exist [179, 180], but their functional impact and how the very low MD2 expression by this cell type [181, 182] impacts function is unknown. In contrast, it is clear that TLR4 is constitutively expressed by at least microglia [183], macrophages [184], CNS vascular endothelial cells [183], and some astrocytes [185]. Thus, the highest likelihood is that the TLR4expressing cell type(s) contributing to opioid reward is among these.

Narrowing the list of TLR4/XAMP cellular targets aids in the identification of novel TLR4-dependent signaling pathways that may contribute to opioid reward behaviors and neurochemistry. TLR4 activation in non-neuronal cells leads to MyD88-, MAPK-, and NF-κB-dependent events [182]. It is now apparent all these key signals occur temporally associated with TLR4-dependent altered opioid pharmacodynamic responses, with MyD88 and p38 MAPK [186] specifically implicated in opioid reward behavior. Likely molecular mediators that result from such signaling include proinflammatory cytokines, and these have been proposed as potential contributors to opioid reward [187]; such conclusions are supported by their neuroexcitatory effects [188] of glutamate transporter downregulation [189], GABA receptor downregulation [133], upregulation of AMPA/NMDA expression and function [190], and enhancement of neurotransmitter release [191]. Proinflammatory cytokines could therefore amplify opioid-induced neuronal activity in drug reward circuitry at multiple points, but the

specifics of the underlying mechanisms remain to be determined.

Such a TLR4-dependent proinflammatory hypothesis of opioid reward aligns with prior literature implicating glia. For example, morphine increased NAc astrocyte and microglial activation marker mRNA expression [192] morphine-induced CPP concomitantly induced activation of NAc microglial p38 [186], and NAc microinjection of a microglial or p38 inhibitor blocked both acquisition and maintenance of morphine-induced CPP [186]. These regional specific studies support earlier findings that systemic broad-spectrum glial activation inhibitors suppress morphine-induced dopamine elevations in the NAc shell [ibudilast [165] and morphine-induced CPP [propentofylline, minocycline [173, 193]. Interestingly, morphine reward and dependence/withdrawal may differ regarding TLR4 involvement. Despite broad-spectrum glial attenuators reducing proinflammation-linked opioid dependence/withdrawal [173, 194], *TLR4* $^{-/-}$ mice are not protected against opioid withdrawal, suggestive of a TLR4-independent mechanism [194].

The third point is "why" TLR4 is involved in opioid reward. The evolutionary reasons for TLR4 recognizing XAMPs, including opioids, and this central immune signal interacting with mesolimbic dopamine reward pathways are unknown. It is clear that TLR4 activation by itself does not produce behavioral reward [193]. (+)-Naloxone action is not an evolutionary control measure since (+)-naloxone is a fully synthetic unnatural compound. However, as we have presented here, these small molecules dock to the same domain in MD2 as lipopolysaccharide, suggesting some possible common threat-detection system.

Questions also arise as to why this opioid-TLR4/MD2 interaction has not previously been reported in binding or behavioral studies. Such data have been reported but not followed up. For

example, the seminal research of Takagi et al. [155]demonstrated the relevance of nonclassical nonstereoselective opioid actions, and Goldstein et al. [156] found a 30-fold greater abundance of nonstereoselective but saturable opioid binding sites compared with saturable stereoselective opioid binding. A key issue in *in vitro* systems, which leads to significant variability, is that MD2 is extracellular, and can therefore be easily lost from or not included in assays, as we have exemplified previously [161] .

An important caveat to any pharmacological studies is the specificity of the agonist and the antagonist used. Collaboratively, we have screened (+)-naloxone on over 70 known receptors, enzymes, second messengers, ion channels, and transporters (our unpublished data), finding no significant activity at any of these important targets. These data also extend our prior observation that (+)-naloxone blocks TLR4, but not TLR2, signaling [195]. Other non-TLR4 actions of this agent have been reported that theoretically could alter opioid pharmacodynamics, such as activity at Filamin A [196] and NADPH oxidase [128]. However, given the TLR4-MyD88 dependent signaling required to elicit opioid CPP presented here, and our previous data showing no additional (+)-naloxone-induced potentiation of morphine analgesia in *TLR4* $^{-/-}$ mice [161], suggest that these documented (+)-naloxone actions at Filamin A and NADPH oxidase are not involved in modifying these opioid pharmacodynamic actions. It is possible that other sites of (+)-naloxone action may be downstream from the (+)-naloxone-TLR4/MD2 activity rendering them less relevant to opioid reward, but could prove important for other TLR4 ligands such as PAMPs or DAMPs. Similarly, it is plausible that opioids may be activating other TLRs [197, 198], in a fashion that is codependent on TLR4-MyD88-dependent signaling. Such possibilities will require further evaluation.

Additional studies are needed to understand the *in vivo* (+)-naloxone and opioid

TLR4/MD2 potency in these and other models. It is apparent from the *in vitro* biophysical characterization of ligand-MD2 interactions conducted to date [128] that this is a low affinity site. Moreover, *in vivo* agonist concentrations may fall below the binding constant estimates. Such discrepancies suggest other factors or chaperones may be involved that facilitate this interaction, which are absent in the *in vitro* systems. Other differences in (+)-naloxone requirement were also observed, with morphine CPP and NAc dopamine elevations nearly completely blocked by 1 mg/kg (+)-naloxone, while higher doses were needed for the attenuation of remifentanil self-administration. Some elevations in NAc dopamine were anticipated to occur in the absence of opioid-TLR4 actions, suggesting tonal endogenous TLR4 activity is required for elevated mesolimbic dopamine reward function. Interestingly, Dunwiddie et al. [199] established that hippocampal pyramidal cell spontaneous activity in the CA1 region was nonstereoselectively inhibited by naloxone, providing further impetus to examine the neuronal consequences of this TLR4-opioid response. An additional difference in (+)-naloxone potency across the three different models may reflect the nature of the three models and the opioids studied. The CPP and NAc dopamine microdialysis studies were conducted after limited opioid/XAMP exposure. However, the remifentanil self-administration studies were conducted in rats that had been repetitively trained on cocaine followed by repeated remifentanil. Therefore, if both these treatments were acting as XAMPs, they may have sensitized the TLR4 system [200], which (+)-naloxone had to overcome via higher doses.

If activation of CNS TLR4 signaling by diverse opioid structures reflects an innate immune system response to xenobiotics [157], then other drugs of abuse may be equally viewed as chemical compounds that are foreign to living organisms. Hence, multiple drugs of abuse may cause XAMP-TLR4 signaling that could also contribute to their reinforcing effects. Given that

drugs of abuse including alcohol [201], cocaine [200], amphetamine [202] and methamphetamine [203] are associated with glial activation, and that systemic glial activation inhibitors have been reported to suppress the reinforcing effects of methamphetamine [193, 204, 205], amphetamine [206], and alcohol [207], examining whether XAMP-TLR4 activity contributes to the rewarding properties of diverse drugs of abuse is warranted [187].

Chapter 3

DAT isn't all that:

cocaine reward and reinforcement requires Toll Like Receptor 4 signaling.

A.L. Northcutt[1a], M.R. Hutchinson[2]*, X. Wang[1a,d]*, M.V. Baratta[1c], T. Hiranita[3], T.A. Cochran[1a], M.B. Pomrenze[1c], E.L. Galer[1a], T.A. Kopajtic[3], C.M. Li[4], J. Amat[1a], G. Larson[5], D.C. Cooper[1c], Y. Huang[4], C.E. O'Neill[1a], H. Yin[1b,d], N.R. Zahniser[5], J.L. Katz[3], K.C. Rice[6], S.F. Maier[1a], R.K. Bachtell[1a,c], L.R. Watkins[1a]

[1]Center for neuroscience, University of Colorado-Boulder, Departments of:

[a]Psychology and Neuroscience, [b]Department of Chemistry and Biochemistry, [c]Institute for Behavioral Genetics, [d]Biofrontiers Institute, Boulder, Colorado, USA

[2]Discipline of Physiology, School of Medical Sciences, University of Adelaide, Adelaide, South Australia 5005, Australia

[3]Department of Health and Human Services, Medications Discovery Research Branch, National Institute on Drug Abuse, National Institutes of Health, Intramural Research Program, Biomedical Research Center MDRB, Baltimore, Maryland, USA

[4]Drug Studies Unit, Department of Bioengineering and Therapeutic Sciences, University of California, San Francisco, California, USA

[5]Department of Pharmacology and Program in Neuroscience, University of Colorado Health Sciences Center, Denver, Colorado, USA

[6]Chemical Biology Research Branch, National Institute on Drug Abuse and National Institute on Alcohol Abuse and Alcoholism, National Institutes of Health, Rockville, Maryland, USA

*Equal author contributions

Abstract

Drugs of abuse are traditionally thought to produce their initial rewarding/reinforcing effects by enhancing activity of the mesolimbic dopamine system, resulting in increased extracellular dopamine in the nucleus accumbens (NAc)[208, 209]. Cocaine increases dopamine through its pharmacological antagonism of DAT located on dopamine terminals[87, 98]. While attention has primarily focused on neuronal actions, recent evidence suggests that abused drugs, such as cocaine, activate innate immune signaling within the brain[147, 149]. However, it remains unresolved how cocaine engages the brain's innate immune system, and what pharmacodynamic consequences might result.

Introduction

The innate immune system of the brain is comprised primarily of microglial cells expressing a variety of pattern-recognition receptors. Of these, the prototypic pattern-recognition receptor, Toll Like Receptor 4 (TLR4) and its cell surface binding protein, MD2, detect a range of substances, including endogenous danger signals (substances released by cellular stress and damage; DAMPs), microbes or invading pathogens (MAMPs/PAMPs), and exogenous small molecules and their metabolites (xenobiotics; XAMPs) [125-130]. TLR4-induced microglial reactivity causes the release of proinflammatory substances such as interleukin-1 beta (IL-1β)[125], triggering agent-specific changes in behavior. Interestingly, cocaine and other abused drugs cause increased proinflammatory immune signaling throughout the brain [147, 148, 187], but the mechanism that produces cocaine-induced central immune proinflammatory signaling is unknown. Although specific mechanisms and functional implications are unclear,

proinflammatory central immune signaling has neuroexcitatory effects [132, 133] that could be relevant to cocaine pharmacodynamics.

We hypothesize that cocaine induces central immune signaling through the TLR4-MD2 complex, due to the ability of TLR4 to respond to a diverse range of molecules and its importance in innate immune activation. The present series of studies explores this hypothesis using *in silico*, *in vitro* and *in vivo* paradigms to assess cocaine's interaction with the TLR4 complex, the role of TLR4 signaling in cocaine-induced dopamine increase, and behavioral measures of drug reward and reinforcement. Our findings demonstrate that cocaine induces central immune signaling through activation of TLR4, resulting in proinflammatory signals that contribute to cocaine-induced changes in the mesolimbic dopamine system and cocaine reward. These findings provide evidence requiring a reconceptualization of cocaine neuropharmacology and offer a new target for medication development.

Materials and Methods

Subjects

For rat studies at the University of Colorado Boulder, viral-free adult, male Sprague Dawley rats (275–350 g; Harlan) were pair-housed in standard Plexiglas cages with *ad libitum* choice food and water and maintained on a 12 hlight/dark cycle. Rats were allowed 1 week of acclimation before any procedures. For mouse studies conducted at the University of Colorado Boulder, adult male (25-30 g) C3HeB/FeJ and C3H/HeJ mice (Jackson Laboratories, Bar Harbor, ME) were group-housed until surgery and maintained on a reverse 12 hlight/dark cycle with lights on at 7:00 A.M., with *ad libitum* access to food and water.

For procedures at the National Institute on Drug Abuse, viral-free adult, male ~300g Sprague Dawley rats (Taconic Farms) were single-housed, with food (Scored Bacon Lover Treats, BIOSERV) and water, and allowed at least 1 week acclimation period. After acclimation, weights of rats were maintained at ~320 g by adjusting their daily food ration. The animal housing room was temperature and humidity controlled and maintained on a 12/12 hlight/dark cycle with lights on at 07:00 A.M.

Naïve animals were used for each study. All experimental procedures were approved by the Institute for Animal Care and Use Committee of the University of Colorado Boulder or the National Institute on Drug Abuse Intramural Research Program Institutional Animal Care and Use Committee.

Drugs

Cocaine HCl was obtained from the National Institute on Drug Abuse (NIDA; Research Triangle Park, NC and Bethesda, MD, USA) or Sigma-Aldrich (St. Louis, MO). (+)-Naloxone and (+)-naltrexone were synthesized by Dr. Kenner Rice (Chemical Biology Research Branch, National Institute on Drug Abuse and National Institute on Alcohol Abuse and Alcoholism, National Institutes of Health, Bethesda, MD). Drug doses are reported as free-base where appropriate. LPS-RS (a TLR4 antagonist naturally produced by *Rhodobacter sphaeroides*), IL1ra, and minocycline were purchased from Sigma (St Louis, MO, USA). Neurotensin was purchased from Bachem (Torrance, CA, USA).

***In silico* TLR4/MD2 computer modeling**

In silico docking simulation methods, identical to those previously described[210], used a high-resolution crystalline structure of the dimer of human TLR4 and MD2, and the software suite AutoDock 4. Briefly, the complexed human TLR4 and MD2 pdb file was obtained from RCSB Protein Data Bank database (PDBID: 3fxi). Modified pdb files were inputted into AutoDock 4.0 (http://autodock.scripps.edu), hydrogens added, and resaved in pdbqt format. GA and EtG structures were gathered using PubChem isomeric SMILES then converted to .pdb using a structure file generator (http://cactus.nci.nih.gov/services/translate/). All dockings were executed with Lamarkian genetic algorithms.

Biophysical Characterizations

Materials

Detailed descriptions of materials are as previously described[128]. The murine microglial BV-2 cell line was provided by Dr Rona Giffard (Stanford University). Insect expression human MD2-pAcGP67A vector was provided by Dr Jie-Oh Lee (KAIST, Korea)[176] and high 5 insect cell was provided by Dr Xuedong Liu (University of Colorado, Boulder).

MD2 expression and purification

MD2 expression and purification was performed as described previously[128, 176, 211]. Briefly, baculovirus was prepared by co-transfection of SF-9 insect cells with MD2-pAcGP67A vector and bright linearized baculovirus DNA (BD Bioscience, San Diego, CA, USA). After 2-3 rounds of amplification, the MD2 baculovirus suspension reached a titer of ~10^8/ml virus particles and was used to transfect high 5 insect cells to express MD2. MD2 was secreted into the medium. After 3-4 day transfection, the medium was harvested and subjected to IgG sepharose

affinity purification. SDS-PAGE analysis showed that the purity of the prepared protein was >95%

Biophysical ELISA binding assays

Two different ELISAs were performed to investigate the cocaine and MD2 interaction.

ELISA 1

Indicated concentrations of biotin labeled cocaine aptamer (5'-biotin- GG GAG ACA AGG AAA ATC CTT CAA TGA AGT GGG TCG ACA-3') and cocaine mix were coated onto the streptavidin coated plates in phosphate buffer solution (PBS, 137 mM NaCl, 2.7 mM KCl, 8.1 mM Na_2HPO_4, 1.76 mM KH_2PO_4, pH 7.4) at room temperature for 2 h. The wells were washed 3 times with PBST buffer (PBS supplemented with 0.05% Tween-20) and then blocked with 5% bovine serum albumin solution at room temperature for 1 h. After washing with PBST 3 times, indicated concentrations of MD2-protein A or MD2-protein A and LPS reaction mix were added and incubated for 0.5-1 h at room temperature. After washing with PBST 5 times, mouse IgG-horseradish peroxidase (HRP) conjugate was diluted (1:4000), added into the wells, and incubated at room temperature for 1 h. After washing with PBST 7 times, 100 µl of TMB reagents were added and incubated at room temperature for 10-30 min. 50 µl of 1 M H_3PO_4 was subsequently added to stop the color reaction. The absorbance at 450 nm was measured on a Beckman-Coulter DTX 880 micro-plate reader; the reference wavelength was 620 nm.

ELISA 2

Indicated concentration of MD2-Protein A or BSA were coated onto the polystyrene surface of 96-well ELISA microplate (BD Bioscience, *San Jose, CA, USA*) in 0.1 M acetate

buffer (pH 5.0). The wells were blocked by SuperBlock (PBS) Blocking Buffer (Pierce, Rockford, IL, USA) and washed as described in ELISA 1. Indicated concentration of LPS and/or cocaine were added and incubated at room temperature for 0.5-1 h. After 5 washings, biotin labeled cocaine aptamer and streptavidin coupled HRP conjugate mix were added into the wells and incubated at room temperature for 1 h. After a further 7 washings, the color reaction was developed and measured as described in ELISA 1.

Bis-ANS displacement assay

Fluorescence measurements were performed on a Fluorolog-3 spectrofluorimeter (Horiba Jobin Yvon, Edison, NJ, USA) and were carried out under room temperature in a 2×10 mm quartz cell (Starna Cells, Atascadero, CA, USA). Different concentrations of cocaine were titrated into MD2 (1.0 μM) and Bis-ANS (1.0 μM) reaction mix. After overnight equilibrium at room temperature, Bis-ANS fluorescence intensity was measured. The excitation wavelength of extrinsic fluorescence probe Bis-ANS was 385 nm; emission at 420-550 nm was recorded. Appropriate controls were **s**ubtracted from spectra obtained on the samples. The fluorescence intensity at 478 nm was plotted against cocaine concentration. K_i of cocaine was determined using the equation: $K_i = K_{app}/(1 + [\text{Bis-ANS}]/K_D(\text{Bis-ANS -MD2}))$.

Dual luciferase NF- κB activity

NF-κB dual luciferase reporter glial BV-2 cell line was constructed by Cignal Lenti NF-κB Reporter kit (SABiosciences, MD, USA) as described previously[128]. NF-κB dual luciferase reporter BV-2 cells were cultured in DMEM medium supplemented with 10% FBS, penicillin (50 unit/mL), streptomycin (50 μg/mL) and puromycin (4 μg/mL) and seeded at a density of 1×10^4 cells/well in 96-well plates. After 24 h incubation, medium was changed to

Opti-MEM medium supplemented with 0.5% FBS, penicillin (50 unit/mL), streptomycin (50 μg/mL) and 1% of non-essential amino acid (NEAA) and indicated concentration of cocaine, LPS-RS, or IL-1β; each treatment was run in triplicate. After further 48 h treatment, NF-κB activity was analyzed by Dual-Glo Luciferase Assay System (Promega, Madison, MI, USA). The ratio of Firefly luciferase activity to Renilla luciferase activity represents the NF-κB activity; NF-κB activity of the untreated control group was set as 1.

Real-Time RT-PCR

Collection of tissue micro-punches

After completion of the cocaine and/or (+)-naloxone timecourse injections, rats were euthanized (65 mg/kg sodium pentobarbital, intraperitoneal; Abbott Laboratories, North Chicago, IL, USA), transcardially perfused with ice cold 0.9% saline. Brains were flash frozen in chilled isopentane, frozen on dry ice and stored at -80°C. Brains were cryostat sectioned (30μm) at -20°C. The location of each region, including the VTA, NAc (predominately the NAc shell) and the ventral medial prefrontal cortex (vmPFC) was determined using a brain atlas (Paxinos and Watson). Circular micro-punches of 0.25 cm in length were taken from each region on both hemispheres using the blunt-end of 18-guage, stainless steel hypodermic tubing. Micro-punches were stored in 1.5 ml microcentrifuge tubes, flash frozen in liquid nitrogen, and stored at -80°C until mRNA extraction. Tissue sections were collected and thaw mounted on glass slides for verification of micropunch location; no micropunches were excluded due to incorrect collection sites.

Total RNA extraction

Total RNA was isolated utilizing a standard method of phenol:chloroform. For detailed descriptions of RNA isolation, cDNA synthesis, PCR amplification protocols, and primer sequences, refer to prior publication (Frank et al., 2006)

Quantitative real time polymerase chain reaction (qRT-PCR)

PCR amplification of cDNA was performed using the Quantitect SYBR Green PCR Kit (Qiagen, Valencia, CA). Formation of PCR product was monitored in real time using the MyiQ Single-Color Real-Time PCR Detection System (BioRad, Hercules, CA). Relative gene expression was determined using the $2^{-\Delta\Delta}C_T$ method[212].

In vivo Microdialysis

A detailed description of *in vivo* microdialysis equipment, surgeries, and procedures was published previously[211].

Surgery

Microdialysis guide cannula (CMA Microdialysis) were surgically implanted and aimed at the right or left NAc shell stereotaxic coordinates relative to bregma: anterior/posterior = +1.7 mm; medial/lateral = +/-0.8 mm; relative to dura: dorsal/ventral = -5.6 mm, bite bar = 0; (Paxinos and Watson, 1998) in a counterbalanced fashion.

Procedure

Rats were placed in separate Plexiglas bowls with *ad libitum* food and water in the microdialysis testing room. Microdialysis probes were inserted through each guide cannula and artificial CSF perfused through the probes using a CMA infusion pump at a rate of 0.2 μl/min

overnight. The next morning, the flow rate was increased to 1.5 µl/min for the duration of the experiment. Two hlater, 3 baseline samples were collected and then drug treatments were administered. The sample tubes were changed every 20 min for a total of 4 h (12 samples total) and stored at -80° C until HPLC analysis.

Systemic administration of drugs

All rats received two subcutaneous injections, of either 2.5 mg/kg (+)-naloxone, for a total of 5mg/kg (+)-naloxone or equi-volume saline. 10 min following the first subcutaneous injection, rats received the second identical subcutaneous injection along with an intraperitoneal injection of either 10 mg/kg cocaine HCL or saline.

VTA microinjections

For studies requiring an intra-VTA microinjection, rats received a 1µL of drug (5 µg LPS-RS, 10 µg IL1 receptor antagonist, 10ng LPS, 10nMol neurotensin, or sterile saline) 10 min prior to an intraperitoneal administration of 10mg/kg cocaine or equivolume saline.

Tissue collection and probe placement verification

Rats were euthanized with intraperitoneal 65 mg/kg sodium pentobarbital (Abbott Laboratories) before brain extraction. Brains were cryostat sectioned and sections containing each rat's cannula track were mounted on slides and stained with cresyl violet, coverslipped, and viewed under a light microscope. To be included in data analysis, at least 75% of the probe had to be within the NAc shell. Dialysate samples were analyzed using high performance liquid chromatography (HPLC) along with electrochemical detection using a method previously described[211].

Conditioned Place Preference

Apparatus and equipment

Detailed descriptions including dimensions, etc., of the place preference apparatus were published previously[211]. Briefly, the place preference apparatus comprised of two distinct conditioning environments with a neutral space in-between. One environment had a floor of metal bars and walls with black and white stripes. The floor of the second environment was a black plate, perforated with evenly spaced holes, and the walls were black with white polka dots. The activity of each rat was recorded using Logitech Quickcam Pro 5000 webcams, which were connected to a computer running AnyMaze (Stoelting), to track and record the time a rat spent in each of the compartments.

Procedure

An unbiased conditioned place preference protocol was used. On day 1, all rats were placed individually in the conditioned place preference apparatus and allowed to freely explore for 20 min, to assess baseline preferences. Any rat that spent <20% or >80% of the entire time in either environment was removed from the study. Rats were then randomly assigned to treatments and conditioning environment in a counterbalanced fashion. In studies utilizing (+)-naloxone, for each conditioning session, all rats received two subcutaneous injections, of either 2.5 mg/kg (+)-naloxone, or equivolume saline. Ten min following the first subcutaneous injection, the second identical subcutaneous injection was co-administered with an intraperitoneal injection of either 10mg/kg cocaine HCl or saline. Rats were then immediately placed into their assigned compartment for 30 min. On days 2-4, rats were conditioned twice each day, once in the morning and then in the afternoon, alternating conditioning between the drug-paired

compartment and the vehicle-paired compartment. Place preference testing took place on day 5, and was run identically to pre-exposure testing on day 1. All rats were tested in a drug-free state (i.e. they received no injections). Conditioning was calculated as a difference between time spent in the drug-paired environment before and after conditioning. For studies where minocycline was administered, pre-exposure was conducted to assess baseline preferences as described above. For conditioning, rats received 25mg/kg minocycline dissolved in sterile water or equivolume sterile water via gavage 40 minutes prior to intraperitoneal administration of 10mg/kg cocaine HCL or saline. In this case, rats experienced 4 conditioning sessions once daily, on days 2-5, with alternating treatments. Place preference was assessed on day 6 as described above and all rats were tested in a drug free state.

Self-Administration

Apparatus

Self-administration procedures were performed in operant conditioning chambers (Med-Associates, St Albans, VT) equipped with two response levers and an infusion pump system.

Procedure

After 24–48 h of food restriction, rats were trained with food pellets to lever press with each press producing a pellet, and eventually each five presses (fixed-ratio 5 schedule of reinforcement). Once responses were reliably producing 30 food pellets within a two-hour session, animals were fed *ad libitum* for at least 1 day before surgery. Catheters were implanted into the jugular vein under halothane anesthesia (1–2.5%) as previously described[213].

After recovery from surgery, cocaine self-administration training was conducted in 2-hdaily sessions until criteria for stable cocaine self-administration behavior were met. Cocaine injections, delivered over 5 s concurrent with the illumination of a stimulus light above the active lever, followed by a 15 s time-out period when the house light remained off and responding produced no consequence. Responses on the second lever produced no consequence. The positions of active and inactive levers were counterbalanced. To assess a full range of cocaine doses in a single session, the final phase of training consisted of separating the session into five sequential 20-min components to deliver cocaine injections in an ascending order as follows: no injection (referred to as extinction), 0.03, 0.09, 0.27, and 0.89 mg/kg/inj, each preceded by a 2-min time-out period. A sample injection of cocaine at the corresponding dose occurred independently of responding at the end of each time-out. Training continued until: 1) a minimum of 5.0 mg/kg cocaine was self-administered within a session with < 20% variation in the total number of injections compared with the previous session, 2) the dose of cocaine that maintained maximal response rates varied by no more than one-half log unit over two consecutive test sessions, and 3) maximal response rates were at least 5-fold higher than response rates maintained during extinction.

TLR4 mutant Mouse Self-Administration

Apparatus

Self-administration procedures were performed in operant conditioning chambers equipped with two nose-poke portals located on opposite walls and an infusion pump system[214]. Chambers were modified for sucrose self-administration mounting liquid-dispensing spigots above both ports for mice to freely lick.

Jugular Catheterization

Mice were implanted with chronic intravenous jugular catheters, as previously described[214]. Animals were individually housed and returned to the colony room.

Cocaine Self-administration

Seven days after catheterization mice were trained to nose-poke for intravenous cocaine (0.75 mg/kg/infusion) during daily 3-hsessions over 7 days. Nose-pokes into the active port resulted in a cocaine infusion of 50 μL delivered over 4 s on a fixed-ratio 1 schedule of reinforcement. Each reinforced response resulted in a 10-s timeout period, during which time the active port was illuminated with a white LED. Mice were trained to nose-poke for sucrose (10% in sterile H_2O; Sigma-Aldrich, St. Louis, Missouri) during daily 3-hsessions over 7 days; nose-pokes into the active port resulted in a sucrose delivery of 30 μL delivered over 2 s on a fixed-ratio 1 schedule of reinforcement for mice to freely lick. For both cocaine and sucrose mice, nose pokes into the inactive port were recorded, but had no consequence. If animals' behavior deviated by >30% of the prior day's responding, catheter integrity and access to the jugular vein was examined using 10 mg/kg Sodium Brevital (JHP Pharmaceuticals, Parsippany, New Jersey). If animals did not exhibit sedation within several seconds they were omitted from the study. All genotypes were blind to the investigators.

Progressive ratio

After 7 days of cocaine or sucrose self-administration, mice were challenged to a progressive ratio schedule in which each successive cocaine or sucrose delivery required an increasing amount of nose-poke responses according to the following progression; 1, 3, 4, 5, 7, 9, 12, 15, 19, 23, 28, 33, etc. Breakpoints were determined as the final ratio of responses/infusion

achieved before a 1-hour period when no further infusions were earned; immediately afterwards, catheter integrity was examined using 10 mg/kg Sodium Brevital. If animals did not exhibit sedation within several seconds they were omitted from the study.

HPLC analysis of brain cocaine concentrations in the presence of (+)-naloxone or (+)-naltrexone

Rats were given subcutaneous injections of either saline, 2.5 mg/kg (+)-naloxone or 2.5 mg/kg (+)-naltrexone, followed 10 min later by a second identical saline/(+)-naloxone/(+)-naltrexone injection paired with an intraperitoneal 10 mg/kg cocaine injection. 5 or 20 min later, rats were sacrificed and brains removed. The hippocampus was collected and analyzed for cocaine concentrations using reverse-phase HPLC coupled with ultraviolet detection, as previously described[215].

Pharmacokineticc profile (+)- naltrexone

A protein precipitation method was used to measure (+)-naltrexone content in collected plasma samples, using a blinded procedure, as previously described[216]. 20 mL of rat plasma and additional 20 mL of 50% acetonitrile were mixed prior to the precipitation with 75 mL of acetonitrile containing the isotope-labeled naloxone (naloxone-d5, the internal standard, 5 ng/mL). The mixture was vortexed, centrifuged, then supernatant was analyzed by liquid chromatography tandem mass spectrometry (LC-MS/MS). The standard curve range is 1.00 to 400 ng/mL and the lower limit of quantitation is 1.00 ng/mL. The LC-MS/MS method was validated with 3 inter-day assays (n = 12) and 1 intra-day assay (n = 6); all precision values (coefficient of variation, CV) and accuracy values (relative error) were within 15%, suggesting that the method was sufficiently reproducible for analysis of study samples.

Caliper Life Sciences NovaScreen compound screening assay

(+)-Naloxone was profiled in a NovaScreen compound screening assay 64 radioligand/enzyme assays at two concentrations: 0.1uM and 10uM in duplicate.

DA Transporter, Sigma$_1$ and Sigma$_2$ receptor binding

Detailed descriptions of materials and methods were previously described[217, 218]. For DAT assays, brains from male Sprague-Dawley rats (Bioreclamation, Westbury, NY) were removed, the striata dissected and quickly frozen. Membranes were prepared by homogenizing tissues in 20 volumes (w/v) of ice-cold modified sucrose phosphate buffer (0.32 M sucrose, 7.74 mM Na_2HPO_4, 2.26 mM NaH_2PO_4, pH adjusted to 7.4) using a Brinkman Polytron (setting 6 for 20 seconds; Kinematica AG, Lucerne, Switzerland) and centrifuged at 30,000g for 10 minutes at 4°C. The resulting pellet was resuspended in buffer, recentrifuged, and resuspended in buffer to a concentration of 10 mg/ml. Experiments were conducted in assay tubes containing 0.5 ml sucrose phosphate buffer for 120 minutes on ice. Each tube contained 0.5nM [^{3}H]WIN35,428 (specific activity 76 Ci/mmol) (PerkinElmer Life and Analytical Sciences, Waltham, MA) and 1.0 mg of striatal tissue (original wet weight [OWW]). Nonspecific binding was determined using 0.1 mM cocaine HCl (Sigma-Aldrich, St. Louis, MO).

For σR binding, frozen whole guinea-pig brains (minus cerebellum) were thawed on ice and homogenized in 10 mM Tris-HCl with 0.32 M sucrose, pH 7.4 (10 ml/g tissue). The homogenate was centrifuged at 1000g for 10 min at 4°C. The supernatant was collected into a clean centrifuge tube, and the remaining pellet was resuspended by vortex in 10-ml buffer (10 mM Tris HCl, pH 8.0) and centrifuged again at 50,000g for 15 min at 4°C. The resulting pellet was resuspended in 50 mM Tris-HCl, pH 8.0 buffer to 80 mg/ml OWW. Ligand binding

experiments were conducted in polypropylene assay tubes containing 0.5 ml of 50 mM Tris-HCl buffer, pH 8.0. For σ_1R binding, each tube contained 3 nM [^{3}H](+)-pentazocine (PerkinElmer Life and Analytical Sciences) and 8.0 mg tissue, OWW. Nonspecific binding was determined using 10 mM haloperidol. For σ_2R binding, each tube contained 3 nM [^{3}H]1,3-di-*o*-tolylguanidine (DTG) (PerkinElmer Life and Analytical Sciences), 200 nM (+)-pentazocine, and 8.0 mg tissue, OWW. Nonspecific binding was determined using 100 mM haloperidol. The reaction was started with the addition of tissue, and the tubes were incubated for 120 min at room temperature.

Incubations for all binding assays were terminated by rapid filtration through Whatman GF/B filters (Whatman/GE Healthcare, Maidstone, Kent, United Kingdom), presoaked in polyethylenimine, using a Brandel R48 filtering manifold (Brandel, Gaitherburg, MD). The filters were washed twice with 5-ml ice cold buffer and transferred to scintillation vials. Beckman Ready Safe (3.0 ml) was added, and the vials were counted the next day using a Beckman 6000 liquid scintillation counter at 50% efficiency (Beckman Coulter, Brea, CA).

All assays were typically conducted in at least three independent experiments, each performed in triplicate. From the displacement data, IC_{50} values were computed using a nonlinear, least-squares regression analysis, affinities (Ki values) were calculated using the Cheng-Prusoff equation.

Biogenic amine transporter assays

Brains from rats were removed, striatum dissected and quickly frozen. Membranes were prepared by homogenizing tissues in 20 volumes (w/v) of ice cold modified sucrose phosphate

buffer and centrifuged. The resulting pellet was resuspended in buffer, recentrifuged and resuspended in buffer to a concentration of 10 mg/ml. Nonspecific binding was determined using 0.1 mM cocaine HCl. Incubations were terminated by rapid filtration. The filters were washed twice with 5ml cold buffer and transferred to scintillation vials. The vials were counted the next day using a Beckman 6000 liquid scintillation counter.

Statistics

Statistical tests were run and graphs created in GraphPad Prism Version 5. Data are presented as mean ± SEM. Appropriate statistical analyses were chosen based on experimental design. The specific statistical analysis used is indicated in the text and in each figure caption for all studies. Bonferroni post-hoc tests were used for one-way ANOVAs, two way ANOVAs, and repeated measures ANOVAs. Significance threshold was set to $p< 0.05$ for all analyses. Sample sizes, although appropriate for relative studies, were generally too small to test variance; however, in instances where an unpaired two-tailed t-test was used, there were no differences in variances. No statistical methods were used to pre-determine sample sizes, but our sample sizes are similar to those reported in previous publications[127, 128, 210, 211, 213, 214, 216, 217, 219]. Data collection and quantification was performed blinded whenever possible; final analyses were not performed blind to the conditions of the experiments. However, when possible, behavioral analyses and experiments were performed blind to the experimenter.

Results

Cocaine interacts with the TLR4/MD2 complex

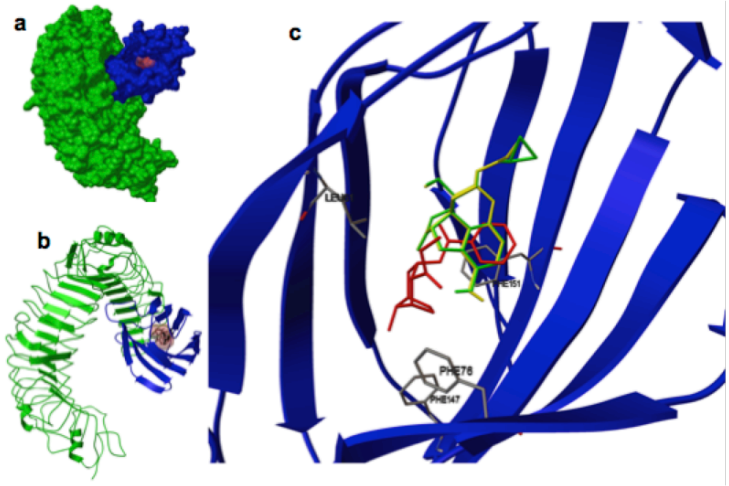

Figure 1: *Computer in silico modeling of cocaine interactions with TLR4-MD2.* (a) Crystalline structure of TLR4 (green) and MD2 (blue). (b) TLR4 (green) and MD2 (blue), the brown fill is the location that cocaine, and TLR4 antagonists (+)-naloxone and (+)-naltrexone prefer to dock. (c) Magnified image of the MD2 structure (blue) and preferred docking location of cocaine (red), (+)-naltrexone (green), and (+)-naloxone (yellow). Images are compositions of individual docking simulations superimposed and indicate that each compound prefers to dock in the same location. Cocaine docking in the presence (+)-naloxone and (+)-naltrexone causes a fundamental shift in docking conformation.

To assess if cocaine possesses relevant physicochemical interactions with the TLR4/MD2 complex, *in silico* and *in vitro* biophysical studies were conducted. *In silico,* cocaine docked to the same binding domain of MD2 as the classical TLR4 agonist lipopolysaccharide (LPS)[176] (Fig. 1). MD2 has been identified as a cell surface protein required for TLR4 signaling[129, 130]. Importantly, recent *in silico* evidence showed that the selective TLR4 antagonists, (+)-isomers of naloxone and naltrexone (non-opioid enantiomers of (-)-naloxone and (-)-naltrexone, respectively), also docked to MD2 [210]. Therefore, to assess the possible utility of novel pharmacological blockade of cocaine-MD2 interactions, docking of (+)-naloxone and (+)-naltrexone was also re-examined. As expected, both compounds docked to this same pocket of MD2. Importantly, when (+)-naloxone or (+)-naltrexone was pre-docked *in silico,* subsequent cocaine docking was disrupted, suggesting that cocaine, (+)-naloxone, and (+)-naltrexone have the physicochemical potential to interact with and affect TLR4/MD2 signaling.

The competitive nature of the docking of the (+)-isomers with cocaine indicates their potential as functional antagonists of cocaine-induced TLR4 activation.

Based on the *in silico* results, cocaine's ability to bind to purified human MD2 was tested using a biotin-labeled aptamer for cocaine, which was immobilized on a streptavidin-coated plate (Fig. 2a[128]). Aptamer-immobilized cocaine bound to human MD2 in a concentration-dependent manner (Fig. 2b). Binding to the negative control, protein A, was negligible. Next, biotin-labeled cocaine aptamer was coated onto a streptavidin plate, bound with cocaine followed by human MD2, or the negative control, protein A. Cocaine-bound MD2 was

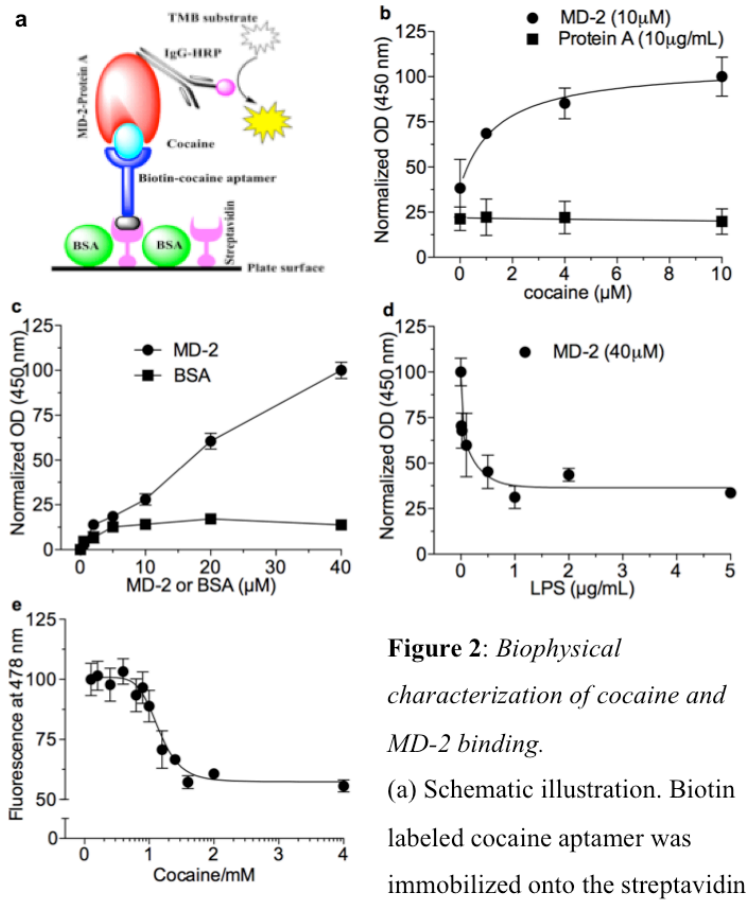

Figure 2: *Biophysical characterization of cocaine and MD-2 binding.* (a) Schematic illustration. Biotin labeled cocaine aptamer was immobilized onto the streptavidin coated plate as the probe for capturing cocaine. Cocaine bound MD-2 was detected by IgG-horseradish peroxidase (HRP) conjugate. It should be noted that the illustration is only a graphic presentation and does not represent the scale of each component. (b) Human MD2 (10 μg/mL) bound varying concentrations of cocaine against 10 μM of biotin labeled cocaine aptamer in a concentration-dependent manner; negative control protein A binding was negligible. c) Varying concentrations of human MD-2 bound cocaine (4μM) in a concentration-depend manner against a fixed concentration of cocaine-aptamer (4μM); the negative control protein, BSA, demonstrated negligible binding. (d) LPS concentration-dependently displaced human MD2 (40μg) binding to cocaine (4μg) against cocaine aptamer (4μg). (e) Florescent competitive binding assay: Bis-ANS fluorescent signaling increases upon MD-2 binding, cocaine decreased Bis-ANS fluorescence in a concentration-dependent manner, indicating that it competitively binds MD2. Data fitting to a one-site competitive model, gives a K_i of 23.9 ± 5.9 μM.

detected by anti-MD2-IgG-HRP conjugate (Fig. 2c). To explore whether cocaine binds competitively to the LPS-binding pocket on MD2 as suggested by the *in silico* data, human MD2 was added to a streptavidin plate coated with biotin labeled cocaine aptamer bound by cocaine and then varying concentrations of LPS were added (Fig. 2d). The resulting decreased signaling indicates that LPS displaced cocaine binding to MD2. When MD2 was titrated into streptavidin-coated plates in the presence of cocaine, human MD2 was captured in a concentration-dependent manner. Protein A binding was again negligible (Supplementary Fig. 1a,b). LPS likewise competed with cocaine for binding to immobilized MD2 (Supplementary Fig. 1c). Lastly, competitive binding of cocaine to MD2 was assessed by fluorescence. The fluorescence intensity of Bis-ANS, a molecular probe that binds to the LPS binding pocket of MD2, increases upon MD2 binding. Cocaine decreased Bis-ANS fluorescence in a concentration-dependent manner, indicating that it competitively binds MD2.(Fig. 2e; data fitting to a one-site competitive model gives a K_i of 23.9 ± 5.9 μM). Collectively, *in silico* and biophysical characterizations demonstrate that cocaine competitively binds to the LPS binding pocket on MD2, providing compelling support for an interaction with the TLR4/MD2 complex.

Cocaine-induced proinflammatory signaling in BV-2 microglial cells is TLR4-dependent

Activation of TLR4 on microglia triggers NFκB nuclear translocation that leads to proinflammatory cytokine production and/or release[220]. We next asked whether cocaine could enhance NFκB activity in a TLR4-dependent manner in BV-2 microglial cells, a murine CNS-derived cell line. Cocaine dose-dependently increased NFκB-dependent luciferase expression in BV-2 microglia (Fig. 3a; $F_{(7,16)}$=45.6; p<0.0001). We tested TLR4-dependency of this effect by administering LPS-RS, a classical TLR4 antagonist from *rhodobacter sphaeroides*, in the presence of cocaine. Co-treatment of cocaine and LPS-RS onto BV-2 microglial cells blocked

cocaine-induced NFκB-dependent luciferase expression (Fig. 3b; $F_{(2,6)}$=27.1, p<0.001). These findings suggest that cocaine activates microglia through a TLR4-dependent mechanism.

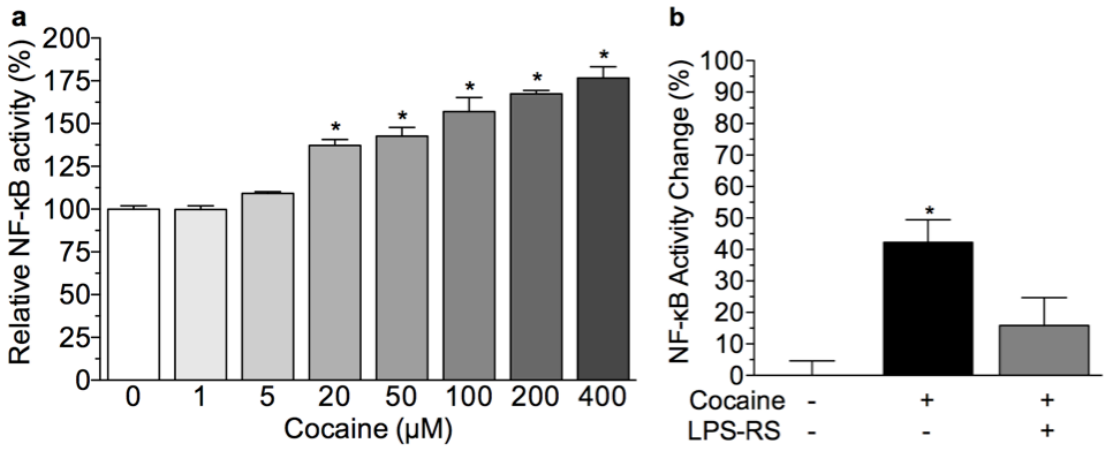

Figure 3: *LPS-RS attenuates cocaine-induced proinflammatory signaling in BV-2 NF-κB reporter cells.*
(a) Cocaine concentration-dependently increases BV-2 dual luciferase NF-κB reporter cell activity ($F_{(7,16)}$=45.6, p < 0.001, one-way ANOVA followed by bonferroni); NF-κB activity of the untreated control group was set as 100%, data are means ± SEMs, n=3. (b) TLR4 antagonist, LPS-RS (1ng/mL) suppresses cocaine (100μM) induced NF-κB activation in BV-2 dual luciferase NF-κB reporter cells ($F_{(2,6)}$=27.1, p < 0.001 one-way ANOVA followed by bonferroni), data are means ± SEMs, n=3.

Cocaine-induced upregulation of interleukin-1 beta mRNA in the VTA is suppressed by systemic (+)-naloxone.

Our *in vitro* data indicate that cocaine interacts with TLR4 to produce a central immune response. We next explored whether *in vivo* cocaine administration would induce proinflammatory changes in brain regions relevant to cocaine reward. Brains were collected 30 min or 2 h after cocaine (10 mg/kg). Micropunches were collected from the ventral medial prefrontal cortex (vmPFC), NAc (predominately NAc shell), and VTA. mRNA for the proinflammatory cytokine, IL-1β, was measured using quantitative RT-PCR. IL-1β mRNA was reliably increased in the VTA (p < 0.01, bonferroni post hoc) 2 h after cocaine. IL-1β mRNA

levels in vmPFC and NAc were unaltered at both time points (Fig. 4a; two way ANOVA, effect of brain region ($F_{(2,38)}$ = 3.7, p = 0.03) and time ($F_{(2,38)}$ = 4.5, p = 0.01).

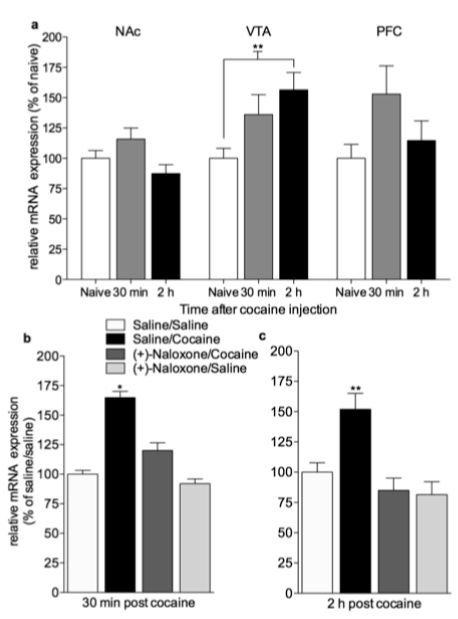

Figure 4: *(+)-Naloxone suppresses cocaine-induced upregulation of interleukin-1 beta (IL1β) mRNA in the VTA.*
(a) Cocaine (10 mg/kg) induced upregulation of IL1β mRNA in the VTA (p < **0.01) but not the NAc or vmPFC. Two-way ANOVA revealed an effect of region (p = 0.034) and time following cocaine injection (p = 0.017), data are means ± SEMs, n = 5-6/group. (b) Cocaine-induced (10 mg/kg) upregulation compared to saline (p = 0.01) of IL1β mRNA within the VTA is attenuated by (+)-naloxone (2.5 mg/kg given in two injections, with the first injection 10 min prior to the second which is paired with cocaine) administration (p <0.05). Bonferroni post-hocs were preceded by two-way ANOVA, indicating a main effects of cocaine ($F_{(1,17)}$=4.61, p=0.001) and (+)-naloxone ($F_{(1,17)}$=4.61, p=0.0447). Data are means ± SEMs, n=5-6/ group. (c) Cocaine-induced (10 mg/kg) upregulation compared to saline (p < 0.01) of IL1β mRNA within the VTA is attenuated by (+)-naloxone (2.5 mg/kg given in two injections, with the first injection 10 min prior to the second which is paired with cocaine) administration (p < 0.01). Bonferroni post-hocs were preceded by two-way ANOVA, indicating main effects of cocaine ($F_{(1,16)}$=5.18, p=0.03) and (+)-naloxone ($F_{(1,16)}$=16.12, p=0.001). Data are means ± SEMs, n=5/group.

To determine if cocaine-induced upregulation of IL-1β mRNA in the VTA is TLR4-dependent we tested the effects of the TLR4 antagonist[211, 216, 219], (+)-naloxone, administered just prior to cocaine. In this instance, reliable upregulation of IL1β mRNA within the VTA was detected at both 30 min and 2 h following cocaine administration. Cocaine-induced increases of intra-VTA IL1β mRNA (Fig 4b; $F_{(1,17)}$=14.6, p < 0.01; Fig4c; $F_{(1,16)}$=5.18, p = 0.03) were blocked by (+)-naloxone both 30 min (Fig. 4b; $F_{(1,17)}$=4.7, p < 0.05) and 2 h (Fig. 4c; $F_{(1,16)}$= 16.1, p = 0.001) after drug administration. Alternately, (+)-naloxone may suppress cocaine-induced IL1β mRNA increases by non-TLR4 mechanisms, rather than through selective TLR4 antagonism. However, extensive screening did not identify any off-target effects of (+)-naloxone (Supplementary Tables 1-3); nor does (+)-naloxone treatment interfere with induction of non-TLR4 dependent proinflammatory signaling (Supplementary Fig. 2a). Therefore, these

results suggest that cocaine initiates proinflammatory central immune signaling in the VTA through a TLR4-dependent mechanism.

TLR4 and IL1β signaling in VTA contribute to cocaine-induced elevations of extracellular NAc dopamine.

Given that a single cocaine administration increases IL1β mRNA in the VTA, we next explored how TLR4 activation and IL1β signaling contributes to cocaine-induced alterations in extracellular NAc dopamine concentrations. Using *in vivo* microdialysis we first tested the effects of the blood-brain barrier permeable TLR4 antagonist, (+)-naloxone, on cocaine-induced dopamine release in the NAc. Cocaine (10 mg/kg) produced robust increases in extracellular NAc dopamine that were blunted to control levels with (+)-naloxone pretreatment (Fig. 5a; $F_{(24,88)}=2.4$; $p = 0.002$). Importantly, (+)-naloxone treatment alone did not influence basal dopamine levels ($p > 0.05$) suggesting that (+)-naloxone did not independently produce effects on dopamine signaling. It remains possible that TLR4 antagonism nonspecifically disrupts dopamine cell responsiveness, leading to what appeared to be a TLR4-mediated suppression of cocaine-induced elevations in NAc dopamine. To explore this potential alternative, (+)-naloxone was tested in the presence of neurotensin, an endogenous mediator of dopamine transmission that is not known to interact with TLR4[221]. An intra-VTA infusion of neurotensin induced increased NAc dopamine that was unaltered by a pretreatment of (+)-naloxone ($p < 0.05$, Supplementary Fig. 3a). These findings suggest that suppression of cocaine-induced elevations of NAc dopamine by (+)-naloxone cannot be dismissed as a global disruption of neuronal responsiveness.

To explore the importance of TLR4 signaling within the VTA on cocaine-induced elevations of NAc dopamine, rats received either intra-VTA treatments of vehicle or LPS-RS, followed by cocaine (10 mg/kg) or vehicle. Although the lipophilic nature of (+)-naoloxone makes it ideal of systemic administration, this same trait becomes problematic for discrete microinjections. Therefore, the classical TLR4 antagonist, LPS-RS, was selected given its well-characterized specificity for the TLR4 complex and comparative lack of diffusion. Intra-VTA LPS-RS attenuated cocaine-induced extracellular NAc dopamine increases (Fig. 5b; repeated measures two way ANOVA ($F_{(3,131)} = 32.0$, $p < 0.0001$), indicating that TLR4 activation in the VTA is necessary for cocaine-induced increases in NAc dopamine. As was the case for (+)-naloxone, intra-VTA LPS-RS had no effect on intra-VTA neurotensin induced elevations of NAc dopamine (Supplementary Fig. 3b).

Since cocaine increased IL-1β mRNA in the VTA, we explored whether cocaine-induced IL-1β signaling in the VTA influences the mesolimbic dopamine system. To test this possibility, intra-VTA IL-1 receptor antagonist (IL-1ra) was administered 10 min prior to cocaine (10 mg/kg) and NAc shell extracellular dopamine quantified. Intra-VTA IL1ra suppressed cocaine-induced elevations of NAc dopamine (Fig. 5c; two way ANOVA, effect of treatment $F_{(3, 104)} = 29.5$, $p < 0.0001$). To ensure that the effect of intra-VTA IL1ra is not due to non-specific disruption of neuronal reactivity, the effects of intra-VTA IL-1ra on intra-VTA neurotensin-induced increases of NAc dopamine were assessed. IL1ra did not alter neurotensin-induced dopamine elevations in the NAc (supplementary Fig. 3c, two way ANOVA, effect of treatment, $F_{(2,82)} = 6.7$, $p = 0.002$). Collectively, results from (+)-naloxone, LPS-RS, and IL1ra indicate that

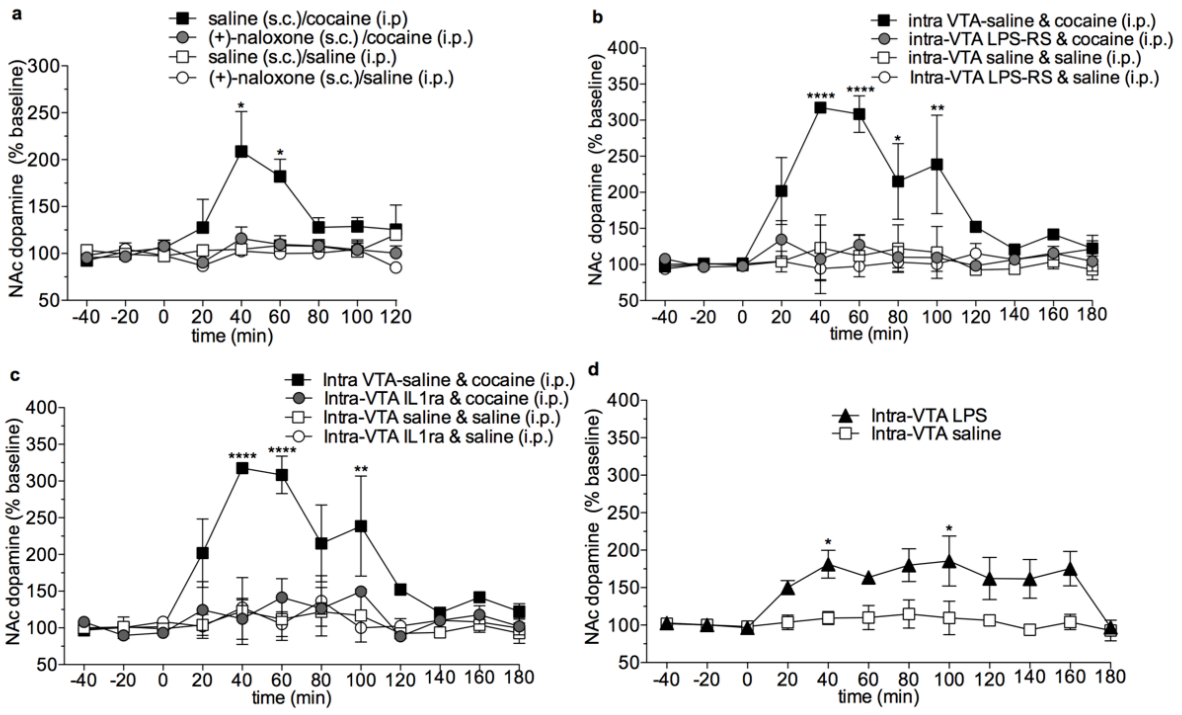

Figure 5: *Cocaine induced increases of NAc DA are dependent on TLR4 and IL-1β signaling within the VTA.* (a) Cocaine (10mg/kg) produces elevated extracellular dopamine in the NAc 40 min ($p < 0.0001$) and 60 min ($p < 0.01$) following drug administration (repeated measures two-way ANOVA with bonferroni post-hocs, time and treatment interaction $p < 0.001$). Administration of (+)-naloxone (2.5 mg/kg in two injections spaced 10 minutes apart) blocked this effect; there were no differences between this group and the saline or (+)-naloxone treated rats. Prior to drug treatment there were no differences in extracellular dopamine concentrations in the NAc shell across all groups. Data are means ± SEMs; n = 4/group. (b) Cocaine (10mg/kg) produces elevated extracellular dopamine in the NAc that sustains for 40-100 min (bonferroni, ****$p < 0.00001$, **$p < 0.01$, *$p < 0.05$) following drug administration. Intra-VTA LPS-RS blocked this effect. There were no differences between other treatment groups. Data are means ± SEMs; n = 4/group. (c) Cocaine (10mg/kg) produces elevated extracellular DA in the NAc that are significant at 40, 60, and 100 min (bonferroni, ****$p < 0.00001$, **$p < 0.01$) following drug administration. Intra-VTA IL1ra suppressed this effect. There were no differences between other treatment groups. Data are means ± SEMs; n = 3- 4/group. (d) LPS (10ng in 1µL) microinjected into the VTA produces increased extracellular DA within the NAc compared to vehicle microinjection-controls (two-way ANOVA, effect of treatment $F_{(1,144)} = 35.83$, $p < 0.0001$ and time $F_{(11,144)} = 2.89$, $p = 0.0018$) 40 min and 100 min post-microinjection ($p < 0.05$, bonferroni post-hoc). Data are means ± SEMs; n = 5- 7/group.

TLR4 and IL1β signaling are powerful mediators of cocaine's effects on the mesolimbic dopamine system.

In order to test whether activation of TLR4 signaling within the VTA is sufficient to produce increased extracellular DA concentrations within the NAc, rats received an intra-VTA microinjection LPS, a the potent and well characterized TLR4 agonist, and NAc DA concentrations were analyzed. Intra-VTA LPS administration produced an increase of

extracellular NAc DA levels (Fig. 5d, two-way ANOVA, effect of treatment $F_{(1,144)}= 35.83$, $p < 0.0001$ and time $F_{(11,144)} = 2.89$, $p = 0.0018$) suggesting that activation of TLR4 signaling within the VTA is sufficient to produce elevated extracellular DA levels within the NAc. Although this is an intriguing phenomenon, it is important to note that while the effect of LPS treatment is highly significant ($p < 0.0001$), DA concentrations are partially elevated, with maximum values at just under 200% of baseline as compared to systemic cocaine, which produces maximum DA peaks of approximately 300% of baseline values. This finding indicates that TLR4 signaling within the VTA could be an important modulator of the mesolimbic dopamine pathway and could have important implications for the rewarding and reinforcing effects of cocaine.

TLR4 signaling contributes to behavioral correlates of cocaine reward and reinforcement.

The present data demonstrate that cocaine-induced TLR4 signaling has a profound influence on the dopamine system, and is particularly dependent on TLR4-induced IL1β increases in the VTA. To explore whether this effect extends to the behavioral effects of cocaine, we tested (+)-naloxone on cocaine conditioned place preference (CPP). Pretreatment with (+)-naloxone blocked the development of cocaine-induced CPP compared to vehicle (Fig. 6a, two-way ANOVA, $F_{(1,27)} = 13.6$; $p = 0.001$). It is important to note that rats were tested for place preference in a drug-free state. Importantly, (+)-naloxone alone produced no appetitive or aversive CPP (p=0.60). Further, we confirmed that brain cocaine concentrations were not altered by similar pretreatment with (+)-naloxone or (+)-naltrexone (Supplementary Fig. 4).

Although TLR4 is predominately located on microglia[183], it is unknown whether it may be expressed on other cell types within the mesolimbic pathway that contribute to drug reward. Our data indicate that *in vitro* cocaine induces activation of microglial cells through a TLR4-dependent mechanism to produce a proinflammatory response; therefore, if (+)-naloxone blockade of CPP is due to antagonism of TLR4 on microglia, then *in vivo* blockade of microglial activation should also result in a suppression of cocaine CPP. We assessed the ability of the putative, blood brain barrier permeable microglial activation inhibitor, minocycline[146, 222], to alter cocaine-induced CPP. Cocaine produced robust CPP that was suppressed by minocycline pretreatment (Fig. 6b; two-way ANOVA, $F_{(1,42)} = 7.7$, $p = 0.008$). Taken with the finding that (+)-naloxone also blocks cocaine CPP, this suggests that cocaine signals through the TLR4 complex to produce microglial activation contributing to the subjective rewarding effects of cocaine.

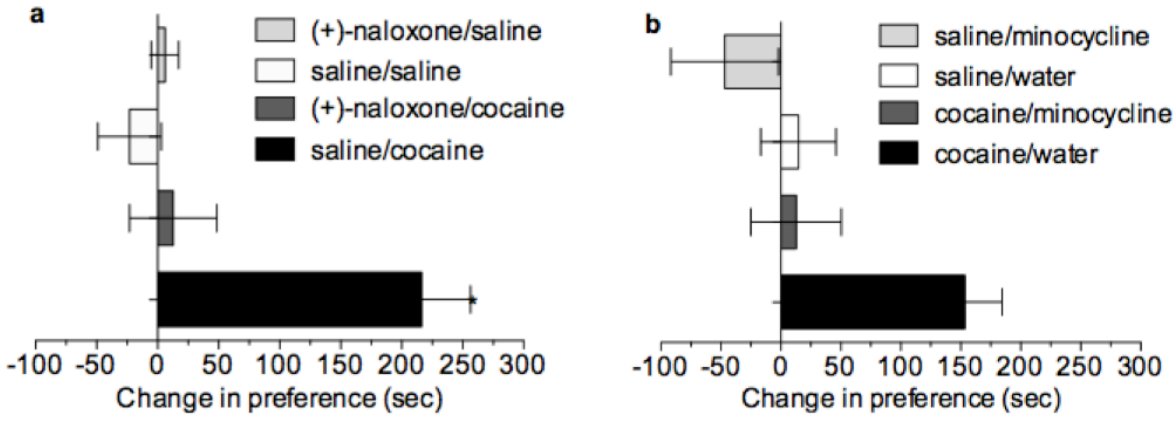

Figure 6: Microglial TLR4 signaling is necessary for the expression of cocaine-induced CPP. (a) Cocaine (10 mg/kg) produces place preference ($p<0.0001$) and (+)-naloxone (5mg/kg divided into two injections spaced 10 min apart) suppresses this effect; no other treatment groups were different from the saline group, nor from one another. Interaction of cocaine and (+)-naloxone ($F_{(1,27)} = 13.6$, $p = 0.001$), with a main effect of each ($n < 0.01$), detected by two-way ANOVA followed by bonferroni, data are mean ± SEMs, n = 7-9/group. (b) Cocaine (10 mg/kg) produces significant place preference ($p < 0.05$, two-way ANOVA with bonferroni). Minocycline (gavage, 50 mg/kg 12 hours prior and 25 mg/kg 45 min prior to conditioning) significantly attenuated cocaine-induced place preference. In the absence of cocaine, neither water nor minocycline altered place preference (main effect of cocaine ($p < 0.01$) and minocycline ($p < 0.01$), data are mean ± SEMs, n = 11-12/group).

Given the robust effects observed using CPP, we next assessed whether TLR4 antagonism would influence cocaine reinforcement in an operant conditioning paradigm. Rats were trained to self-administer cocaine and underwent fixed ratio dose-response testing[217]. Control animals (vehicle treated) yielded the characteristic inverted U-shaped dose-response (Fig. 7a; $F_{4,20} = 6.7$, $p = 0.001$, one-way repeated measures ANOVA). Pretreatment of (+)-naltrexone suppressed responding for cocaine at the peak cocaine doses ($F_{8,40} = 3.7$, $p = 0.003$; effect of cocaine dose, $F_{(4,40)} = 8.3$, $p < 0.001$); in contrast, these doses of (+)-naltrexone failed to suppress responding to food (Fig. 7b; p = 0909). (+)-Naltrexone displays binding and biophysical effects similar to those of (+)-naloxone (Supplementary Fig. 5), but has an extended bioavailability that was preferred for this longer duration behavioral task[223] (Supplementary Fig. 6). These findings suggest that pharmacological inhibition of the TLR4 complex impaired cocaine reinforcement.

In order to expand the assessment of TLR4-signaling on cocaine reinforcement beyond pharmacological blockade of TLR4, we took a genetic approach using C3H/HeJ mice that possess a point mutation that impedes TLR4-NFκB signaling. Acquisition of cocaine self-administration and performance on a progressive ratio schedule of reinforcement for C3H/HeJ mice was compared to the C3H control substrain, C3H/FeJ. C3H/HeJ TLR4-mutant mice self-administered less cocaine across sessions than their TLR4-intact C3H/FeJ counterparts on both fixed and progressive ratio schedules of reinforcement (Fig. 7c-e; repeated measures two-way ANOVA, interaction of genotype and drug, $F_{(1,25)} = 7.1$, $p = 0.01$). No differences in sucrose self-administration were observed between these strains, indicating that there is neither impairment in

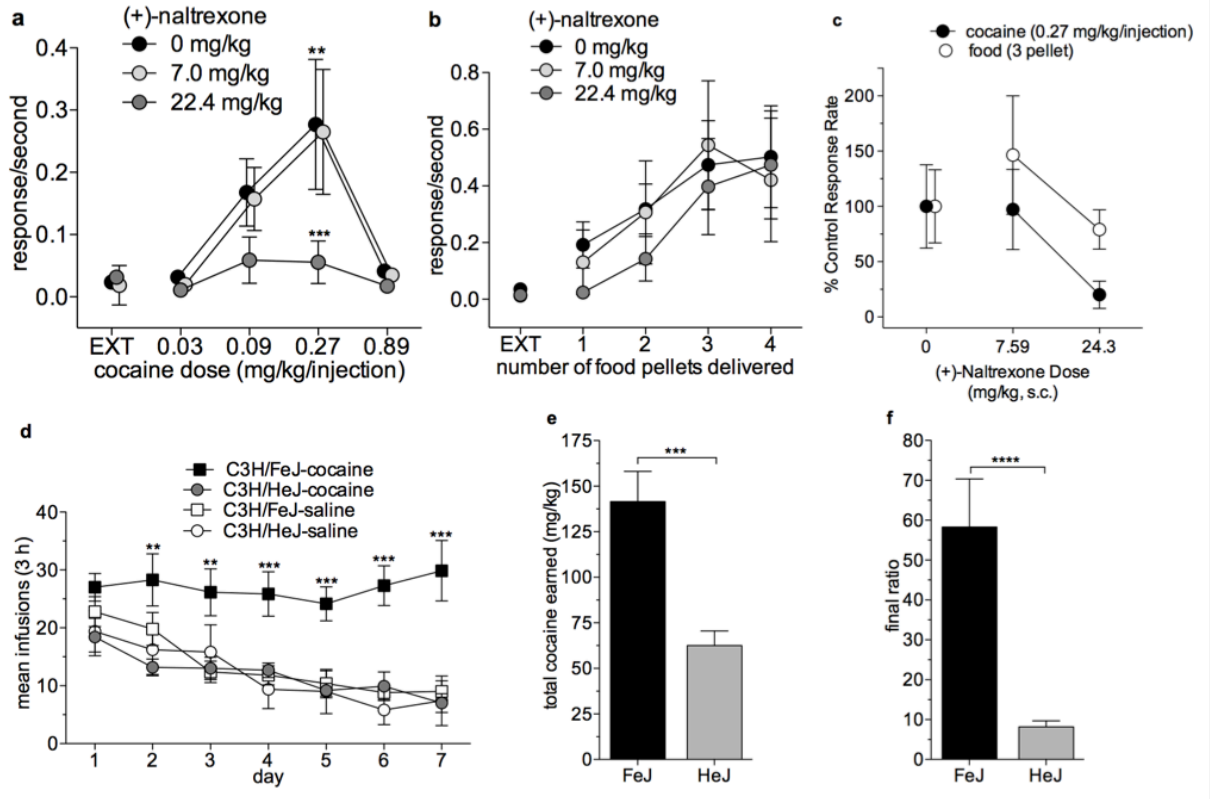

Figure 7: *TLR4 signaling is required for cocaine self-administration.*
(a) Response rates maintained by cocaine injections were affected ($p = 0.001$) by dose and the highest rate of responding maintained by cocaine was at a dose of 0.27 mg/kg/injection ($p = 0.002$), with lower response rates at higher and lower doses. A pre-session dose of 24.3 mg/kg (+)-naltrexone decreases response rates maintained at 0.27mg/kg/injection cocaine ($p < 0.001$). There is a significant interaction of cocaine dose and (+)-naltrexone dose ($p = 0.003$) and a main effect of cocaine dose ($p < 0.001$). Data are means ± SEMs; n = 6/group [**p <0.01 vs. EXT with 0 mg/kg (+)-naltrexone?, ***p<0.001 vs. 0.27 mg/kg/injection cocaine with 0 mg/kg (+)-naltrexone?, bonferroni post-hoc). EXT: extinction. (b) In contrast, food-maintained behavior was virtually insensitive to pre-session treatment with (+)-naltrexone. Data are means ± SEMs; n = 6/ group. EXT: extinction. (c) (+)-Naltrexone was more potent in decreasing responding maintained by the maximal reinforcing doses of cocaine than in decreasing responding maintained by food presentations. Data were from panels a and b. Data are means ± SEMs; n = 6/group. (d) C3H/ HeJ TLR4 mutant mice do not self-administer cocaine, while their normal C3H/FeJ normal TLR4 counterparts demonstrate normal cocaine self-administration. Repeated measures two-way ANOVA revealed a significant interaction of genotype and drug ($p = 0.0134$) and a main effect of both drug ($p = 0.0143$) and genotype ($p = 0.0029$). On days 2-7, FeJ mice self-infused significantly more cocaine than HeJ TLR4 mutant mice, whereas HeJ mice demonstrated no difference in cocaine self-infusions than either FeJ or HeJ saline groups (**p <0.001, ***p<0.0001, bonferroni post-hoc). (e) Over the 7 days of testing HeJ TLR4 mutant mice self-administer less cocaine (***$p < 0.0001$, unpaired t-test) and (f) nose-poked less (***$p < 0.0001$, unpaired t-test) than their FeJ normal TLR4 counterparts. However, there are no differences in sucrose self-administration between either the FeJ or the HeJ mice (supplementary figure 7). All data are ± SEMs; n = 7-11/group.

operant learning nor a generalized disruption of motivated behavior (Supplementary Fig. 7). The parallel results from both the pharmacological and genetic blockade of TLR4 signaling on cocaine self-administration offers profound evidence of the importance of TLR4 signaling in cocaine reinforcement.

Discussion

The present studies demonstrate that cocaine interacts with TLR4 to induce proinflammatory signaling that is necessary for the rewarding effects of cocaine. These findings, combined with previous work, provide the foundation for our recently proposed xenobiotic hypothesis[139]. This hypothesis suggests that in serving its immune-surveillance role, TLR4 detects and identifies drugs of abuse, such as cocaine, as foreign compounds and initiates proinflammatory immune signaling in response to the perceived threat.

Proinflammatory cytokines are neuroexcitatory in that they upregulate surface expression of AMPA and NMDA receptors, increase conductivity of NMDA receptors[122, 132, 133], increase spontaneous neurotransmitter release[133], and increase glutamate transmission[224]. Nitric oxide, released as part of the proinflammatory cascade, has been shown to inhibit dopamine uptake[225], potentially contributing to increased extracellular dopamine concentrations in the NAc. Dopamine neurons express IL-1 receptors[226, 227] and IL-1β microinfused into rat anterior hypothalamus augmented the release of dopamine[228]. Here we show that systemic cocaine administration induces upregulation of IL1b mRNA within the VTA and that selective intra-VTA blockade of either TLR4 or IL1b signaling suppresses cocaine-induced increases of DA concentrations within the NAc. Further, we show that activation of intra-VTA TLR4 signaling increases NAc DA concentrations. Thus, it is possible that cocaine

activates TLR4 to induce IL-1β release that in turn enhances dopamine signaling via IL-1 receptors expressed on dopamine neurons in the VTA. Interestingly, although activation of TLR4 signaling within the VTA produces increases of DA within the NAc, our findings also demonstrate that NAc DA did not accumulate as rapidly nor to such extreme concentrations as with systemic administration of cocaine. Further, it has been shown that cocaine-induced DA elevations within the NAc are preserved in DAT KO mice[86], suggesting that there is an alternate or a second co-mechanism by which cocaine produces high concentrations of DA within the NAc.

It might be that the neuroexcitatory influence of IL-1β/TLR4 signaling within the VTA drives the shift from typical phasic DA cell firing to burst firing observed in the presence of cocaine. Perhaps this increased DA cell firing when paired with blockade of DAT, results in robust increases of extracellular concentrations of dopamine within the NAc, enhancing the rewarding properties of cocaine. Essentially, it appears that in order for cocaine to exert its dramatic effects on the mesolimbic pathway both TLR4 signaling and DAT blockade are necessary.

Recent evidence suggests that proinflammatory TLR4-dependent mechanisms also extend to opioids. We have shown that opioids induce proinflammatory signaling via TLR4[127, 210]. Like cocaine, morphine reward and reinforcement are TLR4 dependent[211, 223]. In the case of morphine, it might be that activation of proinflammatory signaling through TLR4, paired with disinhibition of dopamine signaling via mu-opioid receptor stimulation, increases NAc dopamine levels. Based on evidence presented here, it appears that the xenobiotic hypothesis can now be extended to encompass multiple drug classes. This implies that a required synergism between neuronal systems and central proinflammatory immune signaling may be the rule rather

than the exception underlying the rewarding and reinforcing effects of opioids, cocaine, and potentially other abused substances, such as methamphetamine[148, 149] and alcohol[187, 194].

While our data suggest that microglia are the primary mediators of the central proinflammatory response, there are other related processes that could also influence the rewarding effects of abused drugs. Astrocytes are another non-neuronal cell type in the brain that have been implicated in the effects of abused drugs[229]. In addition to being immunocompetent and participating in proinflammatory signaling[230], astrocytes are important modulators of synaptic activity, formation, function, plasticity, elimination and glutamate transmission[135]. Although there is some controversy regarding TLR4 expression on astrocytes, under basal conditions, cultured astrocytes express low levels of TLR4 mRNA, which upregulates when exposed to TLR4 ligands[231]. Importantly, astrocyte functioning is closely tied to microglial activity. TLR4 signaling rapidly triggers a microglial proinflammatory response, subsequently activating astrocytes[122, 232]. This shift in activity can impact neuronal excitability and functioning, as astrocytes begin to release proinflammatory cytokines and glutamate[122, 233]. Alterations in glutamatergic signaling are frequently associated with the neuroplasticity thought to underlie the addictive effects of cocaine[234]. Additionally, excessive extracellular glutamate can have neurotoxic consequences[235]. Therefore, cocaine-induced activation of microglial TLR4 may trigger a broader proinflammatory response involving astrocytes, instigating glutamatergic dysregulation.

Microglia and proinflammatory cytokines may also have neurotoxic effects[236] and chronic activation of TLR4 by drugs of abuse may have effects on the brain that contributes to drug-induced neuropathologies. Brains of human stimulant users show increased activated

microglia[149], potentially contributing to decreased numbers of dopamine neurons and cortical deficits observed in chronic psychostimulant users[237, 238]. IL-1β, in particular, contributes to dopamine cell death following TLR4 stimulation with LPS[227], and dopamine neurons may be particularly susceptible to microglial-mediated neurotoxicity[236]. Blockade of proinflammatory signaling through IL1ra administration or TLR4 antagonism has protective effects[227, 239]. Additionally, microglia form positive feedback loops[240]; when repeatedly activated, microglia can become primed[241], so that with subsequent stimulation the proinflammatory response becomes stronger. While the initial proinflammatory central immune signaling paired with actions on neuronal targets might be sufficient to produce increased dopamine signaling associated with reward and reinforcement, repeated exposure to cocaine might begin to prime microglia. Augmentation of proinflammatory responding with each subsequent drug exposure might lead to disruptions in astrocyte modulation of synaptic excitability, driving neuroplasticity, leading to the development of addiction, and eventually triggering neurotoxic levels of proinflammatory and glutamatergic signaling.

It is becoming evident that abused drugs are proinflammatory and drug addiction should be conceptualized within the realm of neuro*immuno*pharmacology[139]. The xenobiotic hypothesis of drug abuse incorporates these concepts and suggests that the rewarding, and possibly addictive, effects of abused drugs requires stimulation of both neuronal and glial cell functioning. The data presented here indicate that cocaine-induced activation of TLR4 triggers proinflammatory signaling that is required to produce cocaine-induced neurochemical and behavioral changes. Further, we demonstrate that TLR4 activation within the VTA is sufficient to produce increases of NAc DA, indicating that TLR4 signaling potently influences mesolimbic dopamine activity. The role of glial cells, TLR4, and proinflammatory mediators in dopamine

cell functioning and toxicity has overarching implications for numerous diseases affecting dopamine systems that could guide the development of pharmacotherapies aiming to treat these pathologies. Altogether, we provide compelling evidence that the xenobiotic hypothesis could encompass both the initial stages of drug use driven by rewarding effects of drugs, as well as the drug-induced changes in the brain associated with chronic use.

Supplementary Figures

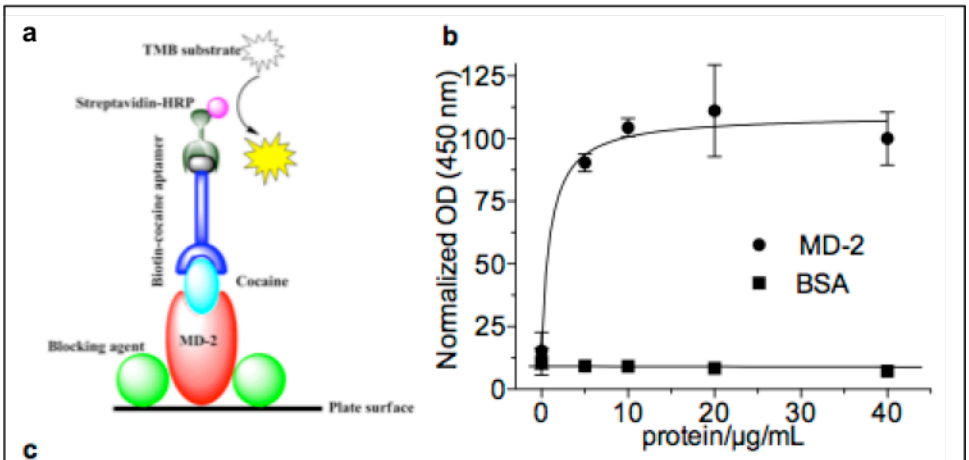

Supplementary Fig 1: *Cocaine captures human MD-2 in a concentration-dependent manner.* (a) Schematic illustration; MD-2 was immobilized onto the polystyrene surface of 96-well plate. The unoccupied surface was blocked with a blocking Agent. Cocaine was added and unbound cocaine was removed by washing. The MD-2 bound cocaine was recognized by biotin labeled cocaine aptamer and detected by streptavidin-HRP conjugate, which catalyze TMB substrate into detectable catalyze TMB substrate into detectable form. (b) Immobilized human MD-2 concentration dependently captured cocaine; cocaine capture by negative control protein BSA was negligible. (c) LPS displaced cocaine binding to MD2 in a concentration dependent manner.

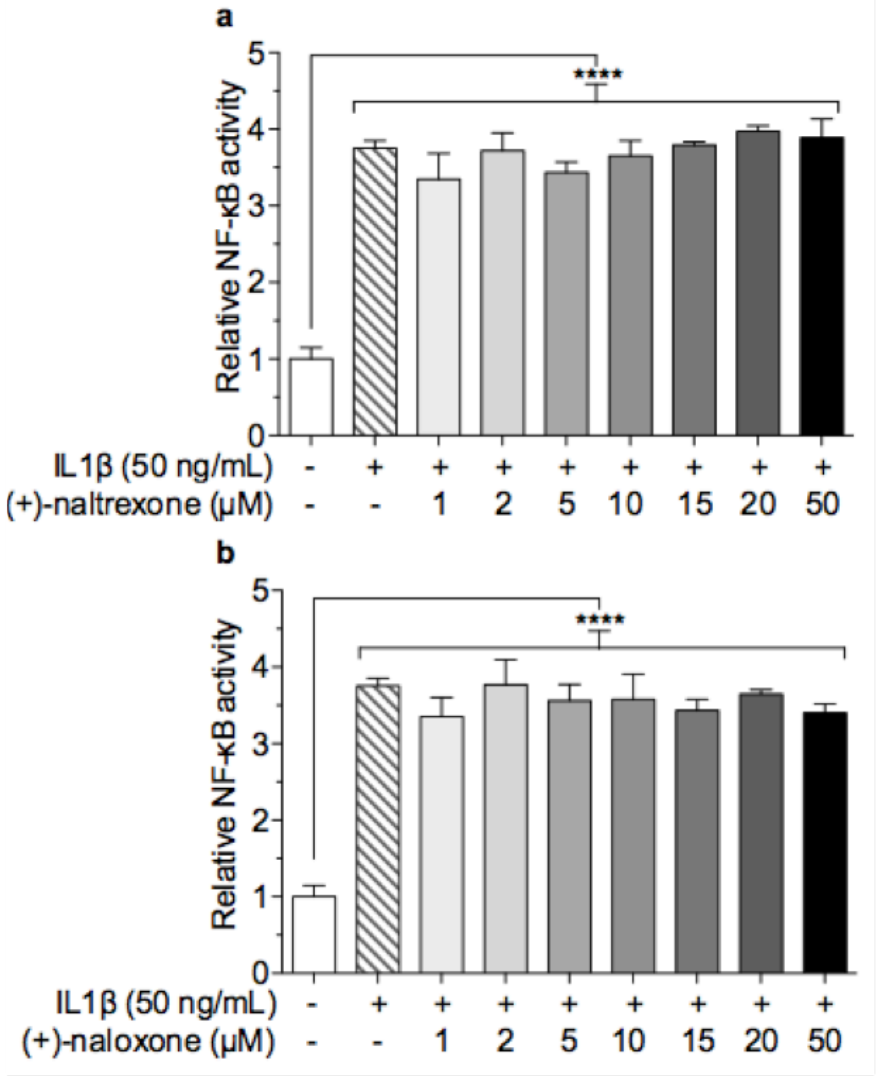

Supplementary Fig 2: *Neither (+)-naloxone nor (+)-naltrexone treatment interfere with induction of non-TLR4 dependent proinflammatory signaling.*
IL-1β induced activation of microglia BV-2 NF-κB reporter cells in regardless of (a) (+)-naltrexone (one-way ANOVA, $F_{(8,18)}$=23.27, $p < 0.0001$, bonferroni post hocs) or (b) (+)-naloxone ($F_{(8,18)}$=17.18, $p < 0.0001$, bonferroni post hocs) treatment. NF-κB activity in the untreated cells was set as 1; data are ± SEMs; n = 3/group.

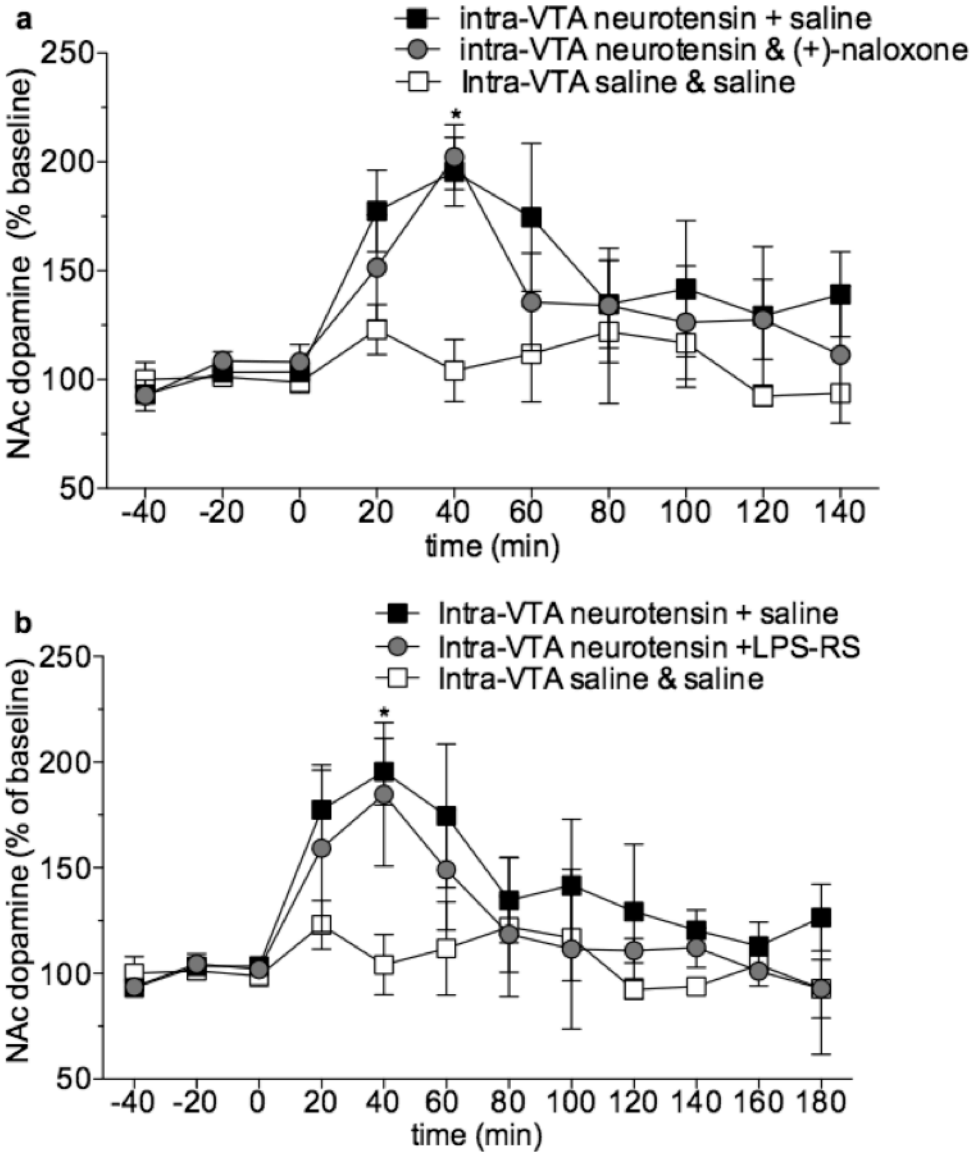

Supplementary Figure 3: *Neither (+)-naloxone nor LPS-RS alter neurotensin-induced increases of NAc dopamine.*
(a) Intra-VTA administration of neurotensin elicits increased extracellular levels of dopamine in the nucleus accumbens shell ($p < 0.05$, bonferroni) and is unaffected by s.c. administration of two doses of 2.5 mg/kg (+)-naloxone, spaced 10 minutes apart (repeated measures ANOVA, effect of treatment, $F_{(2,72)}=6.76$, $p = 0.002$). (b) Similarly, intra-VTA administration of LPS-RS did not alter neurotensin induced DA increases (repeated measures ANOVA, effect of treatment $F_{(2,82)}=6.67$, $p = 0.002$).

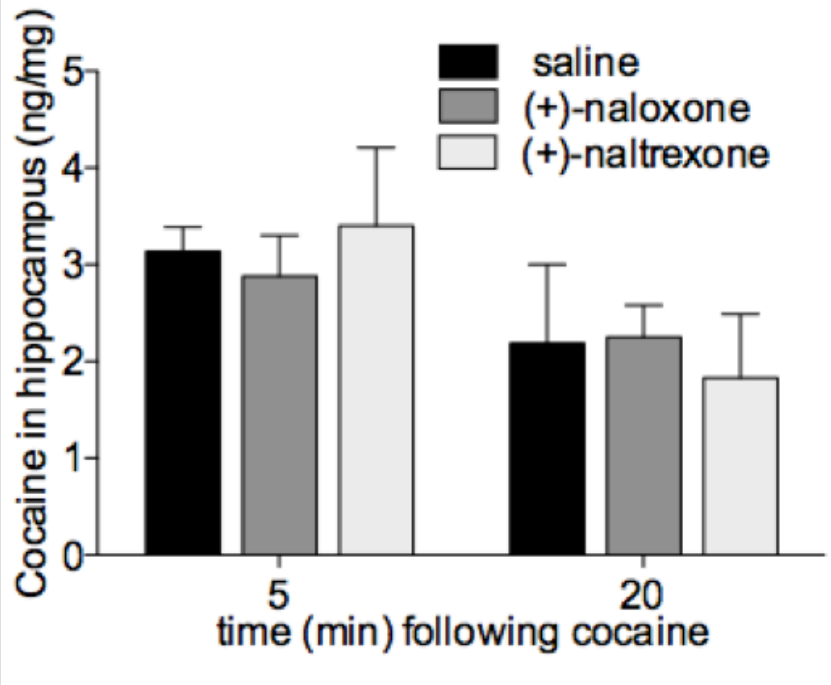

Supplementary Figure 4*: Neither (+)-naloxone nor (+)-naltrexone alter cocaine levels in the hippocampus following systemic administration.* Injections were administered exactly as in microdialysis and CPP studies: a primary injection of 2.5 mg/kg (+)-naloxone or (+)-naltrexone or equivolume saline was followed by a second identical subcutaneous injection of 2.5 mg/kg (or saline) co-administered with 10 mg/kg intraperitoneal cocaine. All rats in this study received cocaine. When compared to saline controls, neither (+)-naloxone nor (+)-naltrexone, had any effect of cocaine levels within the hippocampus at either 5 minutes or 20 minutes following cocaine administration (two-way ANOVA, $p = 0.75$, $n = 4$/group).

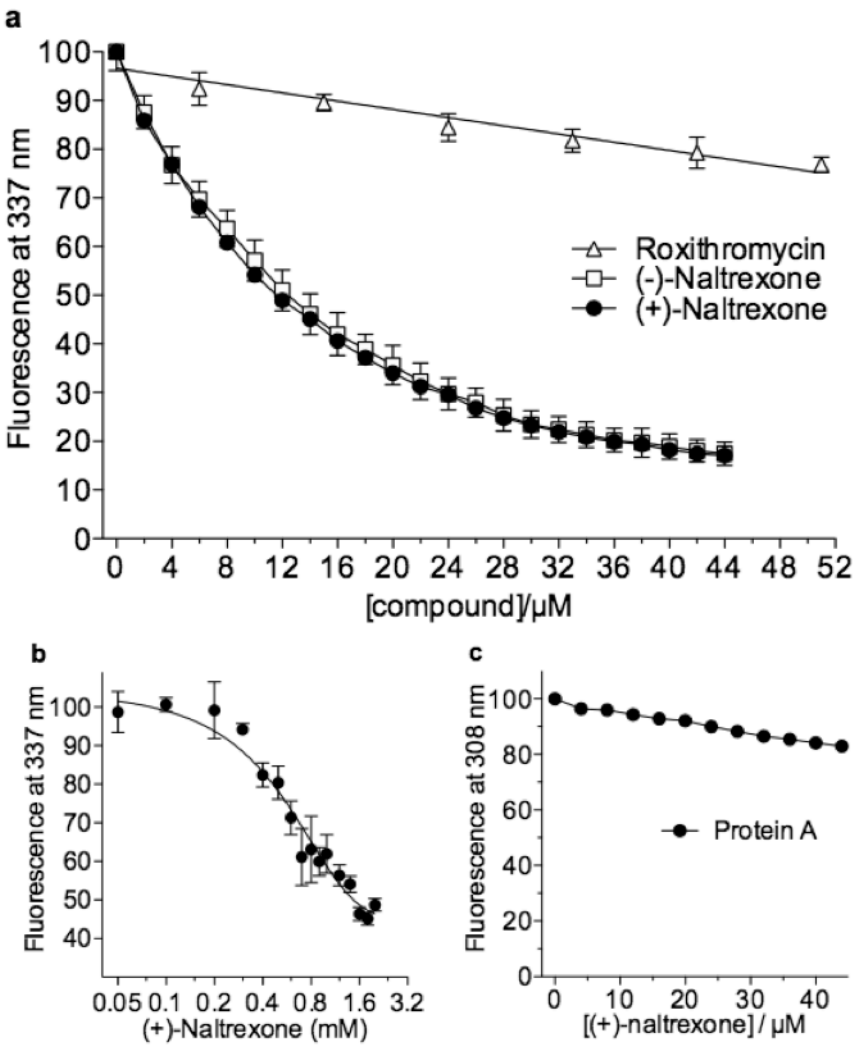

Supplementary Figure 5*: (+)-Naltrexone binds to MD-2*
(a) Titration curves of naltrexone binding to MD-2. The negative control compound, roxithromycin, shows no apparent binding to MD-2. Both isomers of naltrexone bind MD2 By fitting the curves by nonlinear least-square regression, the K_D of 13.7 ± 0.3 μM ((+)-naltrexone) and 15.5 ± 3.5 μM ((-)-naltrexone) were obtained. (b), the (+)-naltrexone binding curve shown in (a) was plotted according to the equation: lg (F_0/F-1) = -lgK_D + n×lg ([Naltrexone]). K_D = 16.1 ± 1.8 μM and n =1.15 ± 0.06. (b) (+)-Naltrexone displaces Bis-ANS binding to MD-2. Data fitting to a one-site competitive model gives a K_i of 21.2 ± 4.1 μM. (c) Selectivity of (+)-naltrexone binding is revealed by its failure to bind protein A.

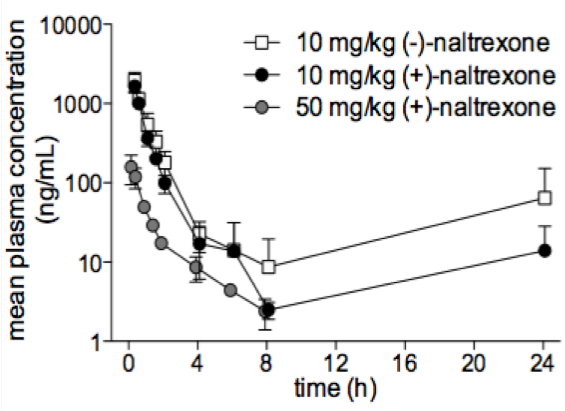

Supplementary Figure 6: *Pharmacokinetic studies of (+)-naltrexone and (-)-naltrexone.*
The pharmacokinetics of (+)-naltrexone was assessed in rats after oral (50 mg/kg) and s.c. (10 mg/kg) administration; s.c. (-)-naltrexone (10 mg/kg) was also examined for comparison. (+)-Naltrexone was absorbed very rapidly (t_{max} was found at first time point; 0.25hr). The half-life values of (+)-naltrexone were 2.10 ± 0.405 and 1.19 ± 0.063 hours (mean ± standard deviation) for oral (50 mg/kg) and s.c. (10/mg/kg)administration, respectively. Subcutaneous administration of (-)-naltrexone showed similar PK profile with (+)-naltrexone. Although plasma exposure to (-)-naltrexone was slightly higher than that to (+)-naltrexone, overall, the PK properties of (+)-naltrexone and (-)-naltrexone were similar.

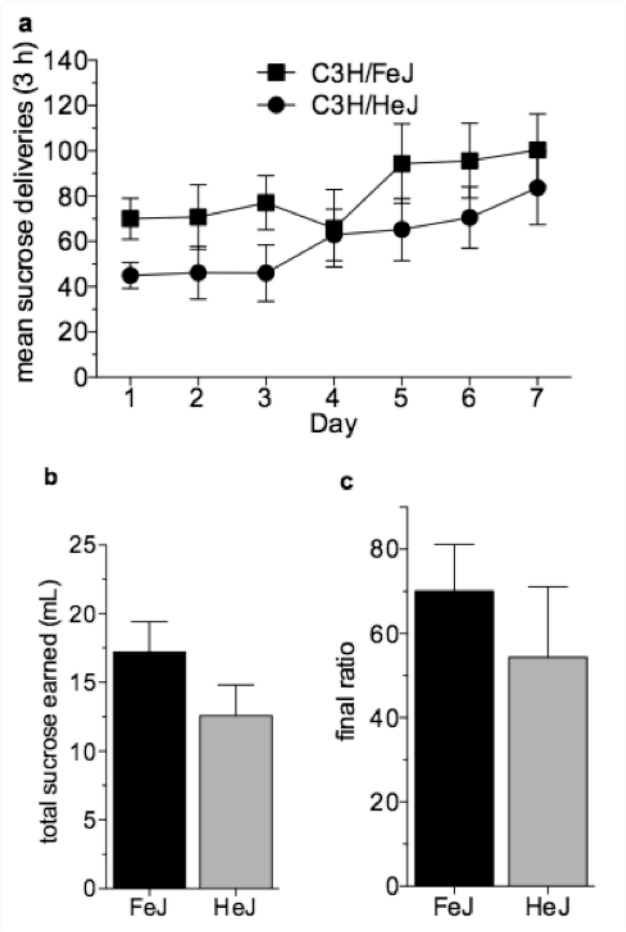

Supplementary Figure 7: *TLR4 mutant C3H/HeJ mice self-administer sucrose no differently than their normal TLR4 C3H/FeJ counterparts.* (a) There are no differences in the daily number of sucrose (10%) deliveries between C3H/FeJs and C3H/HeJs (two-way ANOVA, p = 0.80), (b) the total amount of sucrose earned over the 7-day testing period (two-tailed, unpaired t-test, p = 0.16), or (c) the final ratio of nose-pokes (two tailed, unpaired t-test, p = 0.44). All data are ± SEMs; n = 9/group.

Supplementary Tables

Supplementary Table 1. *NovaScreen assay.* (+)-Naloxone (0.1 uM and 10 uM) has no reliable activity at a broad range of neuronal targets, including neurotransmitters, steroids, ion channels, second messengers, growth factors, hormones, peptides, and enzymes. Values are expressed at the percent inhibition of specific binding; % control values below 50% are considered inactive by the contract laboratory (Caliper Life Sciences).

	(-)- Naloxone		(+)- Naloxone	
% Inhibition at:	1×10^{-7} M	1×10^{-5} M	1×10^{-7} M	1×10^{-5} M
Neurotransmitter Related				
Adenosine, Non-selective	-4.6%	-7.5%	4.2%	-0.8%
Adrenergic, Alpha 1, Non-selective	3.7%	9.8%	0.6%	2.6%
Adrenergic, Alpha 2, Non-selective	0.4%	5.6%	-6.8%	0.9%
Adrenergic, Beta1	7.4%	22.1%	7.6%	17.6%
Cannabinoid, CB1	2.2%	7.0%	3.5%	15.0%
Cannabinoid, CB2	12.3%	18.7%	9.2%	13.1%
Dopamine, D4.2	25.2%	28.3%	10.6%	-11.1%
GABA A, Agonist Site	0.8%	-0.6%	1.6%	2.2%
GABA A, BDZ, alpha 1 site	0.04%	11.4%	1.6%	0.7%
GABA-B	8.3%	-2.3%	15.4%	14.3%
Glutamate, AMPA Site (Ionotropic)	-0.3%	-1.0%	-0.4%	2.6%
Glutamate, Kainate Site (Ionotropic)	4.9%	-0.9%	-0.4%	2.4%
Glutamate, NMDA Agonist Site (Ionotropic)	-2.5%	4.2%	9.7%	8.4%
Glutamate, NMDA, Phencyclidine Site (Ionotropic)	8.5%	4.6%	4.1%	2.5%
Glutamate, mGluR1 (Metabotropic)	-4.0%	5.9%	-0.3%	0.8%

	(-)- Naloxone		(+)- Naloxone	
% Inhibition at:	1×10^{-7} M	1×10^{-5} M	1×10^{-7} M	1×10^{-5} M
Neurotransmitter Related				
Glutamate, mGluR5 (Metabotropic)	-12.2%	-2.0%	4.7%	5.1%
Glutamate, NMDA, Glycine (Stry-insens Site) Ionotropic)	-8.2%	-11.8%	5.7%	5.7%
Glycine, Strychnine-sensitive	9.0%	6.5%	25.1%	40.7%
Histamine, H1	2.7%	5.0%	5.8%	5.7%
Histamine, H2	10.8%	19.6%	-12.1%	9.7%
Histamine, H3	-3.2%	15.9%	-13.0%	10.9%
Muscarinic, M1 (	-5.5%	1.6%	-4.1%	8.3%
Muscarinic, M2 (	-0.3%	17.4%	6.4%	3.9%
Muscarinic, Non-selective, Central	0.8%	3.7%	1.1%	4.2%
Muscarinic, Non-selective, Peripheral	9.8%	-2.6%	-9.2%	9.9%
Nicotinic, Muscle (a-BnTx sensitive)	2.5%	10.7%	-6.8%	-5.6%
Nicotinic, Neuronal [a-BnTx insensitive]	-0.5%	9.7%	-14.0%	-3.0%
Opioid, Kappa 1	93.9%	97.4%	6.1%	26.3%
Opioid, Mu (h)	94.9%	100.0%	13.7%	13.0%

	(-)- Naloxone		(+)- Naloxone	
% Inhibition at:	1×10^{-7} M	1×10^{-5} M	1×10^{-7} M	1×10^{-5} M
Steroids				
Estrogen	11.5%	1.6%	-9.6%	-2.0%
Glucocorticoid	-1.0%	20.0%	-3.1%	0.8%
Testosterone (cytosolic)	-1.8%	-12.0%	12.7%	7.7%
Ion Channels				
Calcium Channel, Type L (Benzothiazepine Site)	10.3%	13.6%	17.0%	19.8%
Calcium Channel, Type L (Dihydropyridine Site)	13.6%	9.1%	-5.8%	14.4%
Calcium Channel, Type N	-4.4%	-2.0%	-2.9%	3.0%
Potassium Channel, ATP-Sensitive	10.3%	13.6%	17.0%	19.8%
Potassium Channel, Ca2+ Act., VI	13.6%	9.1%	-5.8%	14.4%
Sodium, Site 2	-4.4%	-2.0%	-2.9%	3.0%
Second Messengers				
Nitric Oxide, NOS (Neuronal-Binding)	9.9%	11.2%	-0.8%	-0.9%
Prostoglandins				
Leukotriene, LTB4 (BLT)	-8.8%	1.6%	-1.7%	1.9%
Leukotriene, LTD4 (CysLT1)	-17.0%	-13.1%	-3.9%	-11.4%
Thromboxane A2	8.5%	1.4%	-5.3%	1.9%

	(-)- Naloxone		(+)- Naloxone	
% Inhibition at:	1×10^{-7} M	1×10^{-5} M	1×10^{-7} M	1×10^{-5} M
Growth Factors/Hormones				
Corticotropin Releasing Factor, Non-selective	-5.4%	-3.6%	3.1%	1.6%
Oxytocin	6.6%	1.9%	-3.9%	4.5%
Platelet Activating Factor, PAF	-19.5%	-7.3%	11.4%	4.2%
Thyrotropin Releasing Hormone, TRH	12.2%	-0.5%	-3.4%	6.4%
Brain/Gut Peptides				
Angiotensin II, AT1 (h)	-1.2%	-1.6%	5.9%	-6.1%
Angiotensin II, AT2	7.3%	3.4%	0.9%	10.6%
Bradykinin, BK2	-4.8%	-9.0%	-3.9%	-9.4%
Cholecystokinin, CCK1 (CCKA)	-4.5%	3.0%	-13.3%	-8.1%
Cholecystokinin, CCK2 (CCKB)	0.9%	3.0%	5.0%	6.4%
Endothelin, ET-A (h)	-12.8%	4.9%	0.0%	-0.3%
Endothelin, ET-B (h)	1.0%	-2.7%	-12.0%	-2.9%
Galanin, Non-Selective	-3.0%	-16.9%	-6.8%	-14.1%
Neurokinin, NK1	0.0%	-0.6%	-1.4%	-1.4%
Neuroknin, NK2 (NKA) (h)	-9.9%	8.5%	-3.4%	-10.5%
Neurokinin, NK3 (NKB)	6.9%	9.7%	16.3%	16.4%
Vasoactive Intestinal Peptide, Non-selective	13.2%	14.7%	0.6%	2.2%
Vasopressin 1	7.1%	7.9%	-2.2%	-11.9%

	(-)- Naloxone		(+)- Naloxone	
% Inhibition at:	1×10^{-7} M	1×10^{-5} M	1×10^{-7} M	1×10^{-5} M
Enzymes				
Decarboxylase, Glutamic Acid	1.5%	-6.0%	1.0%	3.6%
Esterase, Acetylcholine (h)	3.8%	4.8%	4.5%	2.4%
Oxidase, MAO-A, Peripheral	4.7%	7.2%	1.2%	6.4%
Oxidase, MAO-B, Peripheral	0.0%	9.0%	-4.2%	-1.6%
Transferase, Choline Acetyl	6.8%	26.8%	1.1%	4.0%

Supplementary Table 2. *Dopamine transporter and sigma1 receptor assays support that (+)-naloxone does not reliably bind to those sites***.** Both (+)- and (-)-naloxone failed to displace [^{3}H]WIN 35,428 and [^{3}H](+)-pentazocine from the dopamine transporter in rat striatum and sigma receptors from guinea pig brain, respectively. Historical values for cocaine and haloperidol are also provided for DAT and sigma receptor binding as positive controls. As indicated by the table values, (+)-naloxone failed to reliably binding at any of these sites. *Historical values from previously conducted studies in this laboratory using identical conditions. ^Values from previously conducted studies in this laboratory using identical conditions (Garces-Ramiriez, et al., 2011)

Compound	DAT Ki Value (nM)	$Sigma_1$ Receptor Ki Value (nM)	$Sigma_2$ Receptor Ki Value (nM)
(+)-Naloxone	>10,000	>10,000	>10,000
(-)-Naloxone	>10,000	>10,000	>10,000
Cocaine	76.6 (72.6-80.5)^	5,190 (3,800-7060)	19,300 (16,000-23,300)
Haloperidol	NT	2.91 (2.69-3.14)*	19.6 (15.6-24.6)*

Supplementary Table 3. *Biogenic amine transporter assays support that (+)-naloxone does not reliably affect their binding or function.* (+)-Naloxone and cocaine (positive control) were tested (2-3 tests/dose) by a contract research laboratory (Research Service, R&D22, Dept. of Veterans Affairs Medical Center, Portland, OR) for their effects on radioligand ([^{125}I]RTI-55) binding to, and transporter specific neurotransmitter uptake by, human dopamine (hDAT), serotonin (hSERT), and norepinephrine (hNET) transporters stably over-expressed in human embryonic kidney (HEK) cells. The Ki value for [^{125}I]RTI-55 displacement and, when significant displacement was found, the Hill coefficient were calculated. When [^{125}I]RTI-55 displacement was measurable (i.e., <10 uM), the IC_{50} for radiolabeled neurotransmitter uptake was also calculated. As indicated by the table values, (+)-naloxone failed to reliably affect the binding or function of any of the biogenic amine transporters.

HEK-hDAT cells	**33,113**	**Cocaine**
[^{125}I]RTI-55 Binding Ki (nM)	>10 μM	411 ± 61
Hill coefficient		-1.2 ± 0.1
[^{3}H]Dopamine Uptake IC_{50} (nM)		
HEK-hSERT cells	**33,113**	**Cocaine**
[^{125}I]RTI-55 Binding Ki (nM)	>8,300	385 ± 66
Hill coefficient		-1.12 ± 0.1
[^{3}H]Serotonin Uptake IC_{50} (nM)	>10 μM	319 ± 36
HEK-hNET cells	**33,113**	**Cocaine**
[^{125}I]RTI-55 Binding Ki (nM)	>7,100	632 ± 51
Hill coefficient		-1.0 ± 0.1
[^{3}H]NE Uptake IC_{50} (nM)	>10 μM	445 ± 43

Chapter 4

Methamphetamine activates TLR4 to induce central immune signaling within the VTA and contributes to increases in NAc dopamine concentrations: implications for methamphetamine reward and neurotoxicity.

Northcutt A.L., Wang, X., Cochran, T.A., Fabisiak, T.J., Haas, M.E., Amat, J., Rice, K.C., Maier, S.F., Hutchinson, M.R., Watkins, L.R.

Introduction

Methamphetamine (METH) is a globally abused, highly addictive stimulant. Its behavioral effects and high abuse potential are derived from its ability to dramatically increase extracellular dopamine levels within the nucleus accumbens shell (NAc) [115], due to blockade and reversal of dopamine transporters (DAT) [104, 107]. In addition to the complications of drug abuse and addiction, repeated METH exposure has neurotoxic effects and results in the reduction of dopaminergic functioning [234, 242-245]. While investigation regarding the addictive or rewarding effects of METH has primarily focused on neuronal actions, evidence suggests that the neurotoxic effects of METH are related to activation of innate central immune cells, including microglia and astrocytes, resulting in the release of proinflammatory mediators [203]. However, it remains unknown via what mechanism that METH activates central immune signaling.

Recently, a role for central immune signaling underlying the rewarding effects of other drugs of abuse has emerged. The pattern-recognition receptor, Toll-Like Receptor 4 (TLR4)

detects and responds to morphine [127, 210, 211] and cocaine *[246]* triggering a proinflammatory central immune signaling cascade. Blockade of TLR4 suppresses morphine- and cocaine-induced proinflammatory signaling, as well as several measures of drug reward and reinforcement, including conditioned place preference, drug-induced DA increases within the NAc, and self-administration [211, 246]. Further investigation of cocaine-TLR4 interactions revealed that cocaine-induced DA increases are dependent on IL1 signaling produced by TLR4 activation within the ventral tegmental area (VTA) [246]. Collectively, these findings resulted in our newly proposed xenobiotic hypothesis of drug abuse [139, 246], suggesting that while functioning in its role as a detector of endogenous danger signals (substances released by cellular stress and damage; DAMPs), microbes or other invading pathogens (MAMPs/PAMPs), and exogenous small molecules (xenobiotics; XAMPs) [125-128], TLR4 recognizes cocaine and morphine as "foreign" and triggers proinflammatory central immune signaling.

METH has also been shown to activate central immune signaling [148, 203, 247], though the ensuing proinflammatory response has typically been linked to its neurotoxic consequences rather than its rewarding effects. Here, we explore our hypothesis that METH initiates central immune signaling via interaction with TLR4 and that the ability of METH to increase NAc extracellular DA concentrations is, in part, dependent on TLR4-induced immune signaling.

Materials and Methods

Subjects

Viral-free adult, male Sprague Dawley rats (275–350 g; Harlan) were pair-housed in standard Plexiglas cages with *ad libitum* choice food and water and maintained on a 12 h

light/dark cycle. Rats were allowed 1 week of acclimation before any procedures. Naïve animals were used for each study. All experimental procedures were approved by the Institutional Animal Care and Use Committee of the University of Colorado Boulder.

Drugs

Methamphetamine was obtained from the National Institute on Drug Abuse (NIDA; Research Triangle Park, NC and Bethesda, MD, USA. (+)-Naloxone was synthesized by Dr. Kenner Rice (Chemical Biology Research Branch, National Institute on Drug Abuse and National Institute on Alcohol Abuse and Alcoholism, National Institutes of Health, Bethesda, MD). Curcumin was purchased from Sigma-Aldrich (St. Louis, MO, USA). Drug doses are reported as free-base where appropriate.

Biophysical Characterizations

Materials

Detailed descriptions of materials and where they were obtained are as previously described [128]. The murine microglial BV-2 cell line was provided by Dr. Rona Giffard (Stanford University). Insect expression human MD2-pAcGP67A vector was provided by Dr Jie-Oh Lee (KAIST, Korea)[176] and high 5 insect cell was provided by Dr Xuedong Liu (University of Colorado, Boulder).

MD2 expression and purification

MD2 expression and purification was performed as described previously [128, 176, 211]. Briefly, baculovirus was prepared by co-transfection of SF-9 insect cells with MD2-pAcGP67A vector and bright linearized baculovirus DNA as described by the manufacturer's protocol (BD

Bioscience, San Diego, CA, USA). After 2-3 rounds of amplification, the MD2 baculovirus suspension reached a titer of ~10^8/ml virus particles and was used to transfect high 5 insect cells to express MD2. MD2 was secreted into the medium. After 3-4 days after transfection, the medium was harvested and subjected to IgG sepharose affinity purification. SDS-PAGE analysis showed that the purity of the prepared protein was >95%

Biophysical ELISA binding assays

2 μg/mL of rabbit anti-MD2 antibody was coated onto the 96-well ELISA microplate (BD Bioscience, San Jose, CA, USA) in 0.1 M carbonate-bicarbonate buffer (pH 9.6) at room temperature for 2 h as the capturing antibody. The wells were washed 3 times with PBST buffer (PBS supplemented with 0.05% Tween-20) and then blocked with 5% BSA solution at room temperature for 1 h. 5 μg/mL of MD2 (protein A tag were removed) and different concentrations of METH or roxithromycin (served as the negative control) were added and incubated at room temperature for 1 h. After washing with PBST 5 times, 0.1 μg/mL of mouse anti-MD2 antibody (9B4), which specifically recognizes free MD2, was added and incubated at room temperature for 1 h. Following an additional 5 washings, goat anti-mouse IgG-HRP conjugate was diluted at the ratio of 1:2000 and added and incubated at room temperature for 1 h. After 7 additional washings, the color reaction was developed and measured as described in ELISA 1. The absorbance at 450 nm here represents the free MD2, not METH/roxithromycin bound MD2.

Bis-ANS displacement assay

Fluorescence measurements were performed on a Fluorolog-3 spectrofluorimeter (Horiba Jobin Yvon, Edison, NJ, USA). All measurements were carried out under room temperature in a 2×10 mm quartz cell (Starna Cells, Atascadero, CA, USA). Different concentrations of cocaine

were titrated into MD2 (1.0 μM) and Bis-ANS (1.0 μM) reaction mix. After overnight equilibrium at room temperature, the Bis-ANS fluorescence intensity was measured. 385 nm was chosen as the excitation wavelength of extrinsic fluorescence probe Bis-ANS and emission at 420-550 nm was recorded. Negative controls were **s**ubtracted from spectra obtained on the samples. The fluorescence intensity at 478 nm was plotted against methamphetamine concentration. K_i of cocaine was determined using the equation: $K_i = K_{app}/(1 + [\text{Bis-ANS}]/K_D(\text{Bis-ANS -MD2}))$.

Dual luciferase NF- κB activity

NF-κB dual luciferase reporter glial BV-2 cell line was constructed by Cignal Lenti NF-κB Reporter kit (SABiosciences, MD, USA) as described previously [128]. Firefly luciferase gene was placed under the control the NF-κB transcriptional response element and the constitutively expressing Renilla luciferase was placed under the control of CMV promoter. The internal control Renilla luciferase overcomes technical variability and increases data reliability. NF-κB dual luciferase reporter BV-2 cells were cultured in DMEM medium supplemented with 10% FBS, penicillin (50 unit/mL), streptomycin (50 μg/mL) and puromycin (4 μg/mL). BV-2 reporter cells were seeded at a density of 1×10^4 cells/well in 96-well plates. After 24 h incubation, medium was changed to Opti-MEM medium supplemented with 0.5% FBS, penicillin (50 unit/mL), streptomycin (50 μg/mL) and 1% of non-essential amino acid (NEAA) and indicated concentration of methamphetamine and/or LPS-RS or TAK-242 (TLR4 antagonists, Invivogen; San Diego, California); each treatment was run in triplicate. 48 h later, NF-κB activity was analyzed by Dual-Glo Luciferase Assay System (Promega, Madison, MI, USA). The ratio of Firefly luciferase activity to Renilla luciferase activity represents NF-κB activity. NF-κB activity of the untreated media control group was set as 1.

Real-Time RT-PCR

Collection of tissue micro-punches

After completion of the cocaine timecourse and (+)-naloxone/cocaine timecourse injections, rats were euthanized with i.p. 65 mg/kg sodium pentobarbital (Abbott Laboratories, North Chicago, IL, USA) followed by transcardial perfusion with ice cold 0.9% heparinized saline. The brains were flash frozen in chilled isopentane, frozen on dry ice and stored at -80°C until the collection of tissue micropunches. Brains cryostat sectioned (30µm) at -20°C. The location of each region (VTA, NAc, PFC, C/P, St) was determined using a brain atlas (Paxinos and Watson). Circular micro-punches of 0.25 cm in length were taken from each region on both hemispheres using the blunt-end of 18-guage, stainless steel hypodermic tubing. Tissue micro-punches were stored in 1.5 ml microcentrifuge tubes, flash frozen in liquid nitrogen, and stored at -80°C until the mRNA extraction.

Total RNA extraction

Total RNA was isolated from each tissue micro-punch by utilizing a standard method of phenol:chloroform (Chomczynski and Sacchi, 1987). Detailed descriptions of RNA isolation, cDNA synthesis, PCR amplification protocols, and primer sequences are as previously published (Frank et al., 2006).

Quantitative real time polymerase chain reaction (qRT-PCR)

PCR amplification of cDNA was performed using the Quantitect SYBR Green PCR Kit (Qiagen, Valencia, CA). Formation of PCR product was monitored in real time using the MyiQ

Single-Color Real-Time PCR Detection System (BioRad, Hercules, CA). Relative gene expression was determined using the $2^{-\Delta\Delta}C_T$ method[212].

In vivo Microdialysis

A detailed description of *in vivo* microdialysis equipment, surgeries, and procedures has been previously described [211].

Surgery

Microdialysis guide cannulae (CMA Microdialysis) were surgically implanted, aimed at the right or left NAc shell using stereotaxic coordinates relative to bregma: anterior/posterior = +1.7 mm; medial/lateral = +/-0.8 mm; relative to dura: dorsal/ventral = -5.6 mm, bite bar = 0; (Paxinos and Watson, 1998) in a counterbalanced fashion.

In vivo microdialysis procedure

Rats were placed in separate Plexiglas bowls with *ad libitum* food and water in the microdialysis testing room. Microdialysis probes were inserted through each guide cannula and artificial CSF perfused through the probes using a CMA infusion pump at a rate of 0.2 µl/min overnight. The next morning, the flow rate was increased to 1.5 µl/min for the duration of the experiment. Two h later, 3 baseline samples were collected and then drug treatments were administered. The sample tubes were changed every 20 min for a total of 4 h (12 samples total) and stored at -80° C until high performance liquid chromatography (HPLC) analysis along with electrochemical detection using a method previously described [211].

Drug administration

All rats received two subcutaneous injections, of either 2.5 mg/kg (+)-naloxone, for a total of 5 mg/kg (+)-naloxone, 7.5 mg/kg (+)-naloxone for a total of 15 mg/kg, or equivolume saline. 10 min following the first subcutaneous injection, rats received the second identical subcutaneous injection along with an intraperitoneal injection of either 1 mg/kg METH or saline.

Tissue collection and probe placement verification

Rats were euthanized with intraperitoneal 65 mg/kg sodium pentobarbital (Abbott Laboratories) before brain extraction. Brains were cryostat sectioned and sections containing each rat's cannula track were mounted on slides and stained with cresyl violet, coverslipped, and viewed under a light microscope. To be included in data analysis, at least 75% of the probe had to be within the NAc shell..

Statistics

All statistical tests were run and graphs created in GraphPad Prism Version 5. Data are presented as mean ± SEM. Appropriate statistical analyses were chosen based on experimental design. The specific statistical analysis used is indicated in the text and in each figure caption for all studies. For all ANOVAs (one-way ANOVA, two way ANOVA, and repeated measures ANOVA) bonferroni post-hoc tests were used. As is standard, significance threshold was set to $p< 0.05$ for all analyses. Sample sizes, although appropriate for relative studies, are generally too small to test variance; however, in instances where an unpaired two-tailed t-test was used, there were no differences in variances. No statistical methods were used to pre-determine sample sizes, but our sample sizes are similar to those reported in previous publications [127, 128, 210, 211, 213, 214, 216, 217, 219]. Data collection and quantification were performed blinded, final analyses were not performed blind to the conditions of the experiments.

Results

Experiment 1: METH Interacts with the TLR4-MD2 complex

We first determined whether METH interacts with the TLR4-MD2 complex. MD2 is an important co-factor responsible for the recognition of the classical TLR4 agonist, lipopolysaccharide (LPS) [126]. Binding of METH to MD2 was assessed using a monoclonal

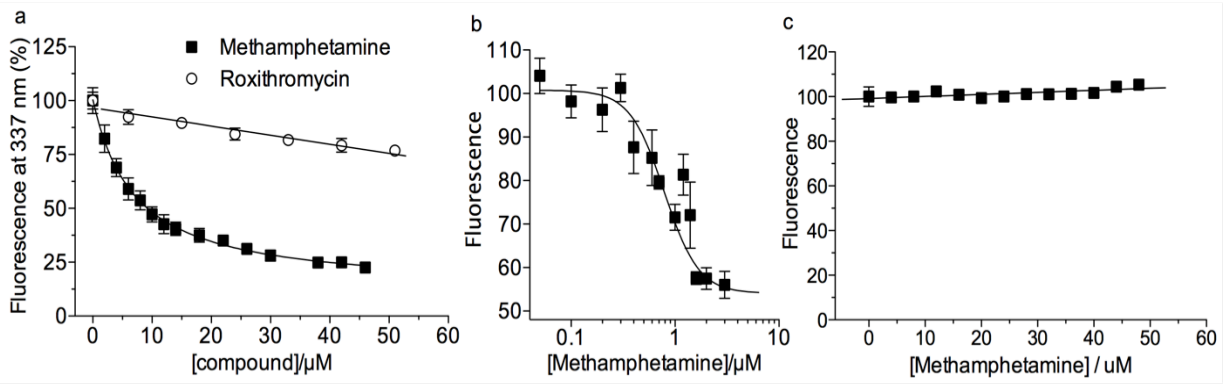

Figure 1*: Methamphetamine binds to MD-2*
(a) Titration curves of methamphetamine (METH) binding to MD-2. MD-2 (1 μM) was titrated with different concentrations of METH or the control compound, roxithromycin. Roxithromycin shows no apparent binding to MD-2. METH binds MD2 by fitting the curves by nonlinear least-square regression were obtained. The wavelength of 280 nm was chosen as the excitation wavelength of MD-2 intrinsic fluorescence. The fluorescence signal at 337 nm, after correction with the basal fluorescence subtracted, was plotted against titrated drug concentrations. Fluorescence intensity of MD-2 at the absence of ligand was normalized as 100%. (b) Methamphetamine displaces Bis-ANS binding to MD-2 in a florescent competitive binding assay. Bis-ANS fluorescent signaling increases upon MD2 binding, cocaine decreased Bis-ANS fluorescence in a concentration-dependent manner, indicating that it competitively binds MD2. Methamphetamine binding curve was plotted according to a one-site competitive model. (c) Methamphetamine does not bind to protein A, indicating a lack of non-specific binding/interaction.

antibody that specifically recognizes unbound MD2 (apoMD2), but not MD2 with bound LPS. This assay detected decreased antibody binding to MD2 in the presence of METH (Fig. 1a). In comparison, the negative control roxithromycin [128], showed no MD2 activity.

As shown in Figure 1b, METH caused a concentration-dependent decrease of Bis-ANS fluorescence from the Bis-ANS-MD2 complex, suggesting that METH competitive ly replaces Bis-ANS binding to MD2. Figure 1c demonstrates that METH does not bind protein A, serving

as a negative control and indicating a lack of nonspecific binding.

Experiment 2: METH induced proinflammatory signaling in BV-2 microglial cells is TLR4-dependent

The results of Experiment 1 indicate that METH can interact with the TLR4-MD2 complex, so we next tested whether this interaction results in activation of TLR4. TLR4 activation on microglia triggers an intracellular signaling cascade resulting in nuclear translocation of nuclear-factor kappaB (NF-κB), a transcription factor that coordinates production and release of proinflammatory cytokines [220]. BV-2 microglial cells, a murine CNS-derived cell line expressing TLR4, were incubated with METH (400 μM) alone or paired with either the TLR4 antagonists, TAK-242 (200 nM) or LPS-RS (2 ng/mL). As shown in Figure 2, METH treatment increased NF-κB activity ($p < 0.01$ bonferroni post-hoc; one-way ANOVA, $F_{(1,8)} = 5.81$, $p = 0.02$). When paired with TAK-242 ($p < 0.05$) or LPS-RS ($p < 0.05$), METH had

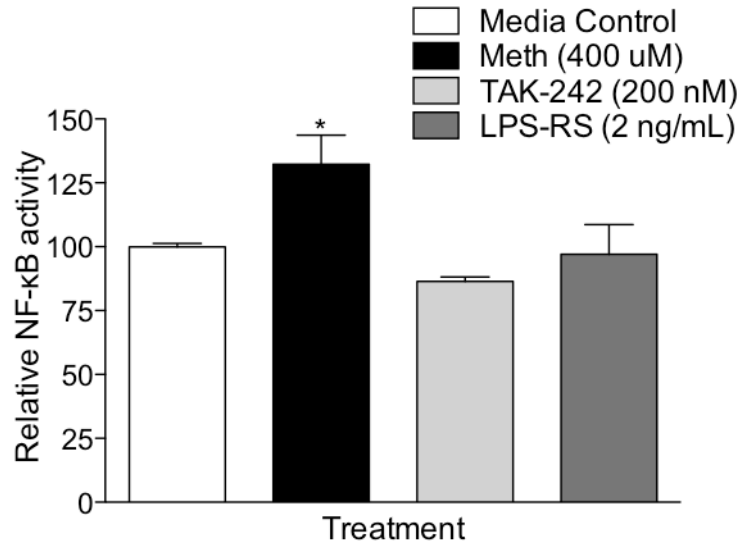

Figure 2: *TLR4 antagonism blocks METH-induced NF-κB signaling.*
One-way ANOVA revealed a main effect of treatment ($F_{(3,11)} = 5.81, p = 0.02$) followed by bonferroni post-hoc tests. METH alone increases NF-kB signaling compared to saline ($p < 0.05$). NF-kB signaling is significantly blunted when METH is paired with TAK-242 ($p < 0.05$) or LPS-RS ($p < 0.05$). The media group, TAK-242, and LPS-RS groups are not different from each other ($p > 0.05$). We have previously demonstrated that neither LPS-RS or TAK-242 alone alter BV-2 signaling (Northcutt et al., 2014; Hutchinson & Northcutt et al., 2012). Data are means ± SEMs; n = 3/group.

no effect on NF- κB signaling. There were no differences between media control, METH plus TAK-242, or METH plus LPS-RS ($p > 0.05$). Together, biophysical characterization and BV-2 cell culture studies indicate that METH activates TLR4 signaling through competitive binding to the TLR4-MD2 complex.

Experiment 3: METH induced increases of dopamine within the NAc is partially dependent on TLR4 signaling.

Our *in vitro* data indicate that METH binds to MD2 and thereby activates TLR4 signaling. Our previous findings with morphine and cocaine indicate that drug-induced TLR4 activation is a critical component of the ability of these drugs to elicit increased concentrations of DA within the NAc. Using *in vivo* microdialysis, we tested the effects of TLR4 antagonism on METH-induced dopamine levels within the NAc. We have recently characterized the non-opioid, (+)-isomer of naloxone as a selective, competitive TLR4 antagonist. It is readily blood-brain-barrier permeable and thus far has demonstrated a notable lack of side-effects or off-target actions [211, 216, 219, 246]. As shown in Figure 3, METH (1 mg/kg) produced robust increases in extracellular NAc dopamine compared to saline controls ($p < 0.0001$) that were dose-dependently attenuated with (+)-naloxone (15 mg/kg: $p < 0.01$; 5mg/kg: $p > 0.05$). Two-way ANOVA revealed a main effect of treatment ($F_{(4,17)} = 17.57$, $p < 0.0001$) and time ($F_{(8,136)} = 20.82$, $p < 0.0001$) and was followed by bonferroni post-hocs. Importantly, (+)-naloxone treatment alone did not alter basal dopamine levels ($p > 0.05$) suggesting that (+)-naloxone did not independently produce effects on dopamine signaling. We have previously established that (+)-naloxone treatment does not interfere with dopaminergic cell functioning, and that non-TLR4 stimulation of increased DA within the NAc is preserved in the presence of (+)-naloxone [246].

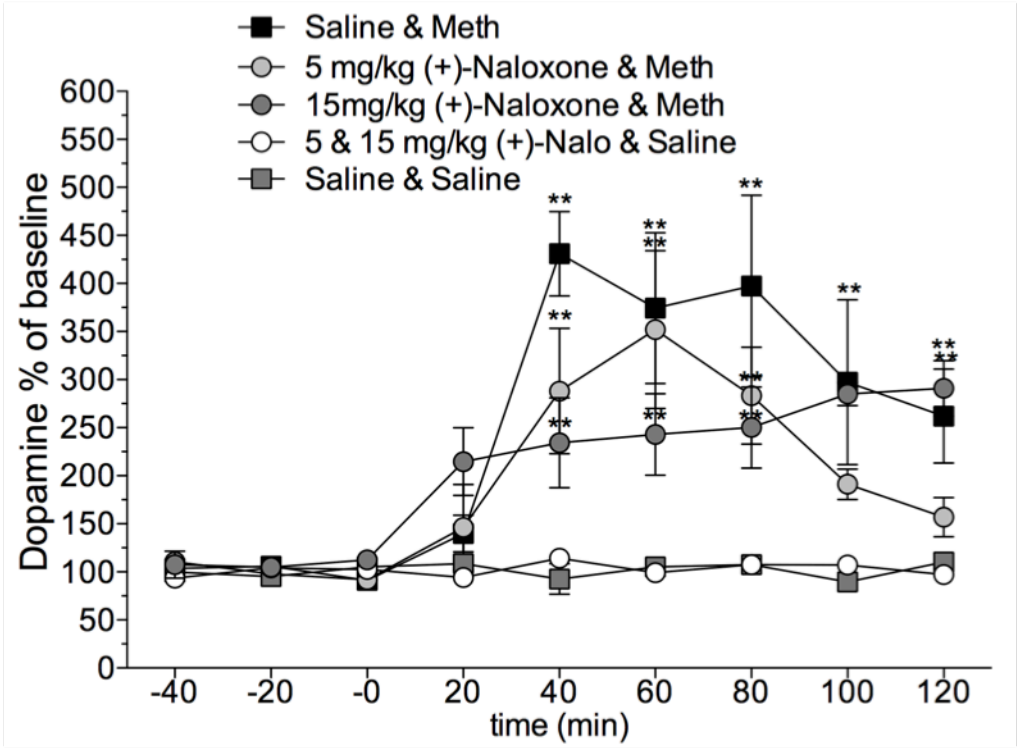

Figure 3: *(+)-Naloxone attenuates METH-induced increases of extracellular DA within the NAc shell.*
METH (1 mg/kg) produces elevated extracellular dopamine in the NAc following compared to saline controls ($p < 0.0001$) that were dose-dependently attenuated with (+)-naloxone (15 mg/kg: $p < 0.01$; 5mg/kg: $p > 0.05$). Two-way ANOVA revealed a main effect of treatment ($F_{(4,17)} = 17.57$, $p < 0.0001$) and time ($F_{(8,136)} = 20.82$, $p < 0.0001$) and was followed by bonferroni post-hocs. Prior to drug treatment there were no differences in extracellular dopamine concentrations in the NAc shell across all groups ($p > 0.05$). There were no differences between this group and the saline or (+)-naloxone treated rats ($p > 0.05$). Data are means ± SEMs; n = 4/group.

Collectively, these findings indicate that METH-induced increases of NAc dopamine are partially dependent on systemic TLR4 signaling.

Experiment 4: A single systemic administration of METH induces upregulation of mRNA markers indicative of central immune activation within the VTA.

Although our findings indicating that TLR4-methampetamine signaling influences dopaminergic signaling are intriguing, they do not indicate whether TLR4 signaling is site-specific or if this is a more global CNS phenomenon. In order to examine if TLR4 signaling is

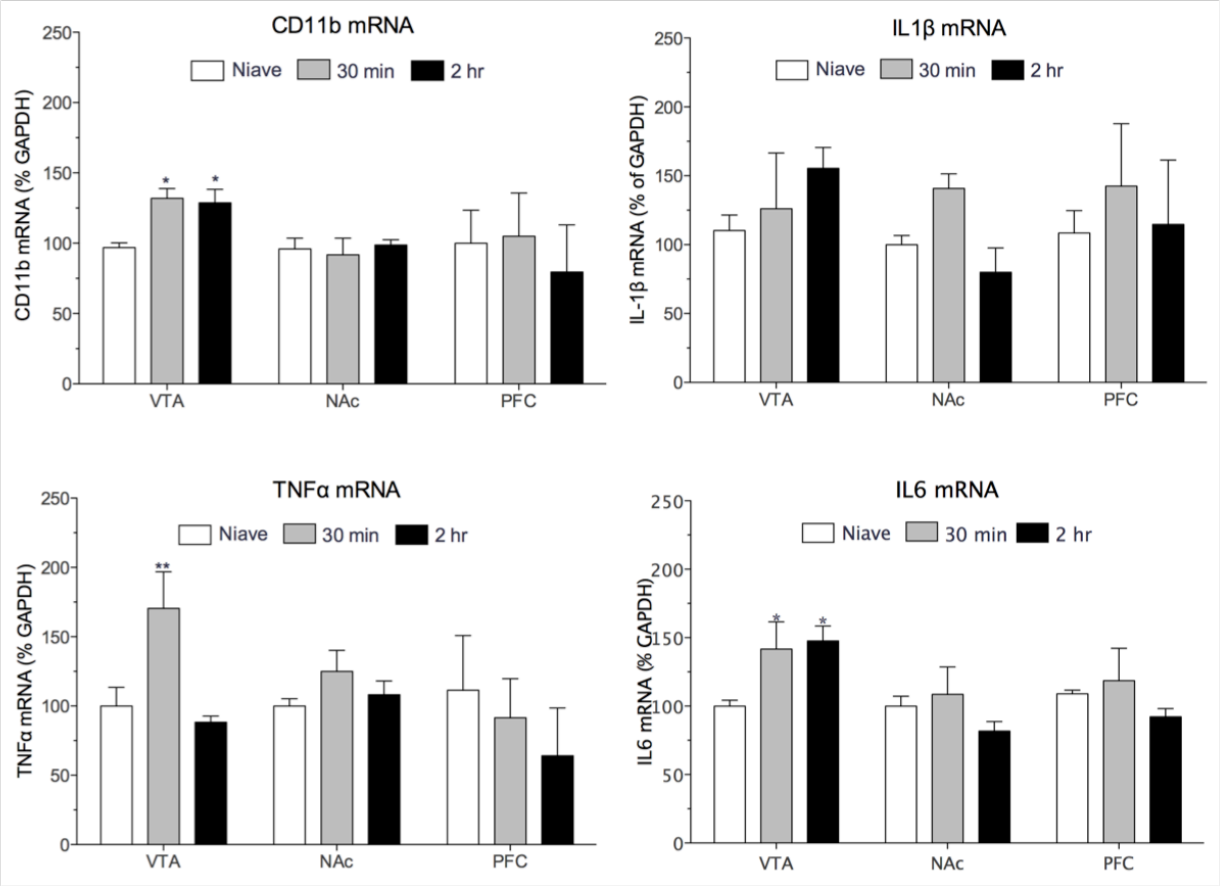

Figure 4: *A single systemic injection of 1 mg/kg METH upregulates mRNA markers of central immune activation within the VTA, but not within the vmPFC or NAc.*
(a) METH upregulated VTA mRNA expression of CD11b at both 30 min ($p < 0.05$) and 2 hr ($p < 0.05$) following treatment; however in the vmPFC and the NAc CD11b mRNA was not altered ($p > 0.05$); two way ANOVA revealed a main effect of brain region ($F_{(2,32)} = 4.69$, $p = 0.016$) and was followed by bonferroni post-hocs. (b) A two-way ANOVA revealed no effect on IL1β within the VTA, NAc, or vmPFC 30 min or 2 hrs following METH administration ($F_{(4,28)} = 1.53$, $p = 0.222$). (c) METH produced an increase of TNFα expression within the VTA at 30 min ($p < 0.01$) which returned to baseline by 2 hrs ($p > 0.05$); there were no effects within the NAc or the vmPFC ($p > 0.05$); bonferroni post-hocs were preceeded by two way ANOVA detection of a main effect of time ($F_{(2,31)} = 6.15$, $p = 0.006$) and brain region ($F_{(2,31)} = 3.70$, $p = 0.036$). (d) A two way ANOVA revealed that METH produced an upregulation of IL6 mRNA within the VTA (bonferroni, $p < 0.05$) but not the vmPFC or the NAc ($p > 0.05$); there was an effect of brain region ($F_{)(2,27)} = 4.74$, $p = 0.0173$).

activated within the regions comprising the mesolimbic dopamine pathway, rats were administered a single intraperitoneal injection of METH (1 mg/kg) and brains removed 30 min or 2 h later. Micropunches were collected from the ventral medial prefrontal cortex (vmPFC), NAc, and VTA; mRNA markers for proinflammatory cytokines were measured using quantitative RT-PCR for each region. A two-way ANOVA with bonferroni post-hocs was used to analyze all

PCR data. CD11b, a microglial activation marker, was upregulated in the VTA following METH administration (Fig.4a, 30 min $p < 0.05$) but was unaffected in either the NAc or the vmPFC. Interleukin-1beta (IL1β) mRNA was unaffected at all time-points in all three brain regions (Fig 4e, $p > 0.05$); however, mRNA for the proinflammatory cytokines tumor necrosis alpha (TNFα) and interleukin-6 (IL-6) were upregulated in the VTA (respectively, fig 4c, $p < 0.01$ at 30 min and Fig 4d, $p < 0.05$ at 30 min and 2 h) but not within the NAc ($p > 0.05$) or the PFC ($p > 0.05$). Collectively, these data indicate that systemically administered METH induces proinflammatory central immune signaling specifically within the VTA.

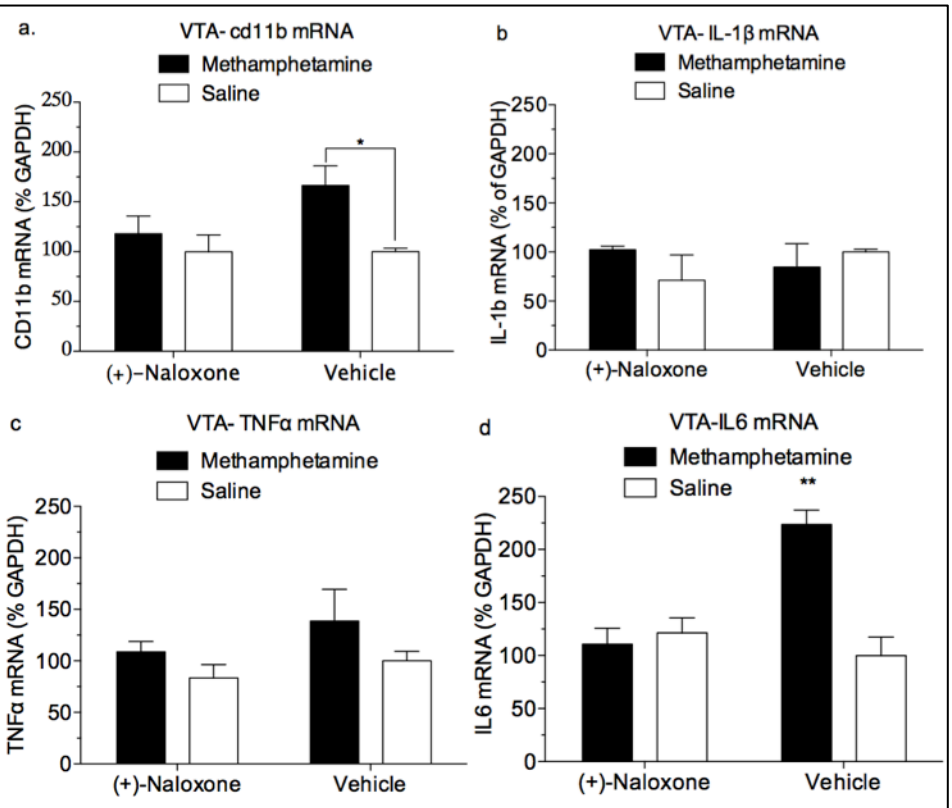

Figure 5: *Systemic TLR4 antagonism via (+)-naloxone prevents METH-induced upregulations of mRNA for cd11b and IL6.*
(a) Two-way ANOVA followed by bonferroni indicates that, within the VTA, IL6 is upregulated 2 h following methamphetamine, and that (+)-naloxone suppressed this effect. (Interaction: $F_{(1,9)} = 19.27$, $p = 0.001$; Main effect of methamphetamine ($F_{(1,9)} = 13.74$, $p = 0.005$) and (+)-naloxone ($F_{(1,9)} = 8.99$, $p = 0.015$), $^{**}p < 0.01$. (b) Methamphetamine had no effect on mRNA expression of IL1b within the VTA (interaction: $F_{(1,9)} = 0.16$, $p = 0.703$) or on (c) TNFα (interaction: $F_{(1,10)} = 0.11$, $p = 0.75$) within the VTA two hours following METH injection (c) METH administration upregulated mRNA expression for CD11b within the VTA 2 h following administration ($F_{(1,9)} = 6.06$, $p = 0.034$). In the presence of (+)-naloxone, methamphetamine is not different from saline control ($p > 0.05$) or (+)-naloxone alone ($p > 0.05$).

In order to determine if METH-induced upregulation of mRNA markers of central immune signaling within the VTA is TLR4-dependent *in vivo* another PCR study was conducted. In a two-by-two design, just prior to either METH or vehicle (saline) administration, rats received (+)-naloxone (15 mg/kg, sub-cutaneous) or vehicle; brains were removed, micropunches of the VTA were collected and processed for PCR. As shown in Figure 5a, a two-way ANOVA with bonferroni post-hocs revealed that following METH treatment, mRNA for CD11b, a microglial activation marker, was upregulated (Fig. 5a, $F_{(1,9)}= 6.05$, $p= 0.034$) and in the presence of (+)-naloxone, mRNA expression is not different from saline and vehicle control groups ($p > 0.5$). IL1β was, once again, unaffected by METH administration (Fig. 5b, $p= 0.703$) whereas METH treatment induced IL6 mRNA expression within the VTA ($F_{(1,9)}= 13.74$, $p = 0.005$) and (+)-naloxone administration suppressed this effect ($F_{(1,9)}= 8.99$, $p= 0.015$). Additionally (+)-naloxone administration alone did not produce any alterations in CD11b mRNA ($p > 0.05$).

Discussion

The data presented here indicate that, *in vitro,* METH activates proinflammatory signaling by competitively binding to MD2, thereby activating TLR4 signaling. Further, we demonstrate that METH-induced TLR4 activation contributes to increased dopaminergic extracellular levels implicated in the rewarding effects of METH. And finally, systemic METH administration induces upregulation of mRNA expression for CD11b and IL6. Interestingly, mRNA levels for IL1β were unaffected by METH treatment.

Although there are reports of increased activated microglial cells in the brains of human METH addicts [149] as well as central immune activation in animal models [148], including activation

of microglia [203], the mechanism by which METH exerted this effect was unknown. Here, our data suggest that METH may signal via the TLR4-MD2 complex to initiate proinflammatory signaling. We have recently demonstrated that other drugs of abuse, including opioids [211] and cocaine [246] competitively bind to MD2, inducing the activation of TLR4 signaling. This TLR4 signaling contributes to drug reward and in the case of cocaine, induce central immune signaling [246]. Here, we observed that TLR4 blockade antagonized both METH-induced DA increase and METH-induced upregulation of mRNA markers of proinflammatory activation. These findings provide further support for our recently proposed xenobiotic hypothesis of drug abuse [139, 211, 246]. This hypothesis suggests that: (1) in serving its immune-surveillance role, TLR4 detects and identifies drugs of abuse, such as morphine, cocaine, and now methamphetamine, as foreign compounds and initiates proinflammatory immune signaling in response to the perceived threat and (2) drug-induced proinflammatory signaling paired with unique neuronal actions of each drug of abuse synergize to create their rewarding effects.

Reports of microglial activation and proinflammatory signaling tend to focus on the neurotoxic consequences of METH [203, 248-250]. We have recently demonstrated for that another member of the psychostimulant drug class, cocaine, TLR4 signaling is required for its rewarding effects [246]. Similar to METH, our *in vitro* studies indicate that cocaine competitively agonizes the TLR4-MD2 complex and depends on TLR4 signaling to induce NK-κB activation of BV-2 cells. Further, we have recently showed that TLR4 antagonism abolishes both cocaine-induced [246] and morphine-induced [211] DA increases within the NAc. Here we demonstrate that TLR4 antagonism attenuates METH-induced increases of extracellular DA concentrations within the NAc. Taken together, these findings suggesting that TLR4 signaling may be an important mediator in drug-induced dopaminergic effects. Further, our data indicate

that METH, like cocaine [147, 246], induces upregulation of central immune activation markers, specifically within the VTA. Upregulation of mRNA suggests the possibility that these proinflammatory mediators were released. In order to verify this, further study is required.. However, if METH administration triggers the release of proinflammatory cytokines, there could be important implications for neuronal functioning, that might explain how TLR4 signaling influences dopaminergic functioning. Proinflammatory cytokines, released following TLR4 activation, can have neuroexcitatory actions. For example, proinflammatory cytokines can upregulate surface expression of AMPA and NMDA receptors, increase conductivity of NMDA receptors [122, 132, 133], increase spontaneous neurotransmitter release [133], and increase glutamate transmission [224]. However, many of these findings particularly involve IL-1β and TNFα. Although TNFα upregulation is evident 30 min following METH, no alternations in IL-1β were detected. This is surprising considering our recent finding that intra-VTA IL-1β signaling, induced via TLR4, is required for cocaine to influence neuronal functioning. Although IL6 mRNA was upregulated following METH administration, less is known about its ability to influence neuronal functioning. Certain neuronal populations throughout the brain express IL6 receptors [251] and IL6 has been shown to mediate neuronal differentiation [252], so it is reasonable to postulate that IL6 can influence neuronal signaling, but how relevant this signaling might be to the mesolimbic dopamine pathway is unknown. It may be that the lack of IL-1β signaling partially explains the differences between our cocaine findings (where TLR4 blockade abolishes cocaine-induced DA increases) and the METH data presented here (where TLR4 attenuates, but does not block, METH-induced DA increases). It is also important to note that METH has the ability to more dramatically effect DA concentrations through its actions on DATs than cocaine, given that it triggers reverse transport. So while it may be that METH also activates dopaminergic signaling through proinflammatory mechanisms in the VTA, initiated

through TLR4 agonism that drive increased DA cell firing, given METHs reversal of DAT, its mesolimbic dopaminergic effects are likely less dependent on possible proinflammatory activation in the VTA.

TLR4 is predominately expressed on microglial cells within the CNS, therefore most of its effects are attributed to microglial responses. However, astrocytes are also are immunocompetent and can participate in proinflammatory signaling [230]. Although there is some controversy regarding TLR4 expression in astrocytes, under basal conditions, cultured primary murine astrocytes have been shown to express low levels of TLR4 mRNA, but demonstrate marked upregulation when exposed to TLR4 ligands [231]. Astrocytes have received attention regarding their role in the tripartite synapse [134], where they serve as important modulators of pre- and post-synaptic activity, synapse formation, function, plasticity, elimination as well as regulation of glutamate transmission [135]. Importantly, astrocyte functioning can be closely tied to microglial activity; TLR4 signaling rapidly triggers a microglial proinflammatory response, subsequently activating astrocytes [122, 232]. When astrocytes shift a basal state to an activated, proinflammatory state, they can release proinflammatory cytokines, D-serine (co-agonist of glutamate on NMDA receptors) and glutamate [122, 233]. *In vitro,* incubation with METH for 3 days has been shown to activate astrocytes [253]. Narita et al. demonstrated that when conditioned media from cortical astrocytes isolated from neonates following stimulation with METH is microinjected into the NAc, METH reward was potentiated. They also demonstrated that administration of a glial activation inhibitor, propentofylline, attenuated astrocyte activation *in vitro* and when administered intraperitoneally diminished the METH-induced (1mg/kg) conditioned place preference. [229, 253]. Although the findings of Narita et al. point toward the NAc, it is

important to note that these effects are all with prolonged or repeated treatments. In our case, a single systemic injection of METH, induces upregulation of mRNA markers of proinflammatory activation within the VTA but not the NAc. Further, via what mechanism METH exerts this proinflammatory effect in the NAc is unknown. As noted in the prior paragraph, since astrocytes have been shown to upregulate expression of TLR4 with exposure to TLR4 ligands, it might be initially, TLR4-mediated responses to METH are microglial, but that with repeated METH exposure, astrocytes begin upregulate TLR4 expression. Further investigation is required to examine this possibility.

Whether drug-induced astrocyte activation might occur directly (for example, if TLR4 is expressed on astrocytes) or indirectly (downstream from TLR4-induced microglial activation) remains to be explored. Given that astrocytes are involved in mediation of neuroplasticity within brain systems where alterations in glutamatergic signaling is implicated in the addictive effects of cocaine such as the prefrontal cortex [234], it is likely that disruption of basal functioning in astrocytes contributes to not only the acute rewarding effects of METH, but also to disturbances in impulse control, decision making, etc. that underlie the development of addiction [238, 254] and neurotoxicity [253, 255].

Neurotoxicity associated with chronic METH use is well-documented within humans [244, 256, 257] and rodents [258], but mechanistically, is not a well-understood phenomenon. It has been shown that within the striatum, microglia activation precedes and/or coincides with markers of neurotoxicity in rats administered a neurotoxic regimen of METH [203, 249]. Given the findings presented here from our laboratory it is possible that METH-induced TLR4 activation resulting in glial activation and central immune signaling contributes to these neurotoxic effects. Here, our mRNA time-course study revealed that 1 mg/kg METH upregulated

mRNA markers of central immune activation within the VTA in a TLR4 dependent manner. Of particular interest is the upregulation of IL6 but not IL1β, paired with cd11b suggestive of coinciding microglial activation. A similar pattern of proinflammatory mRNA expression was described in mice. Within the striatum, 30 min and 1 h following 30 mg/kg METH administration, mRNA for IL6 but not IL1β was upregulated [148]. IL6 has been linked to pathologies overlapping or similar to those also reported following chronic METH use including depression, anxiety, anorexia/loss of appetite, obsessive-compulsive behaviors, Parkinson's Disease, and neurotoxicity [143, 144, 245, 259-264]. In fact, IL6 has been directly implicated in METH neurotoxicity. Transgenic mice expressing a null mutation for IL6 were protected from METH-induced reduction of DATs, gliosis, and apoptosis demonstrated in wild-type mice [248]. We found that systemic TLR4 antagonism blocked upregulation of both CD11b and IL6 mRNA, suggesting that METH signals through TLR4 to activate microglia and trigger proinflammatory signaling, potentially related to METH induced neurotoxcity.

We also found that TNFα mRNA is upregulated within the VTA, 30 min following a single administration of METH, but returns to control-group levels by 2 hrs. Our METH dose (1 mg/kg) is based on drug reward rather than neurotoxicity. However, there are reports of TNFα upregulation within the frontal cortex, following higher doses of METH [148, 265]. Findings regarding the role TNFα might play in METH neurotoxicity are contradictory as to whether TNFα is protective [250] or neurotoxic [265, 266]. TNFα regulates both apoptotic and anti-apoptotic signaling and is clearly involved in central immune signaling as it is released as part of a proinflammatory cascade and induces activation of NF- κB [267, 268]. Beyond the induction and participation in proinflammatory signaling, TNFα also stimulates over-production and release of glutamate from glial cells [263] and excessive extracellular glutamate can have

neurotoxic consequences [235]. Additionally, TNFα can increase conductivity of AMPA receptors [190], and increases cell-surface expression of AMPA receptors, particularly those permeable to calcium [133]. Although TNFα appears to play a role in METH-induced neurotoxicity, the specific mechanisms and consequences following acute and chronic METH exposure remain to be elucidated.

A prominent hypothesis for METH-associated neurotoxicity involves nitric oxide (NO) and reactive oxygen species (ROS). METH not only reverses dopamine transport to produce substantial increases of extracellular DA within the NAc, it can also enter neurons through DATs, interfering with the vesicle monoamine transporter ($vMAT_2$) [104], resulting in the increase of cytoplasmic dopamine levels. There is support for both an intracellular and extracellular role for DA oxidation resulting in the production of ROS contributing to neurotoxicity, as well as a role for increased glutamate levels triggering NMDA activation to produce ROS and NO. [269]. Therefore, for the most part, the production of ROS and NO following METH exposure have been primarily linked to these neuronal interactions. Although it is beyond the scope of the present series of studies to explore these mechanisms in detail, it is important to note that, NO and ROS are components of a proinflammatory cascade triggered by TLR4 activation and glial activation [122, 128, 188]. Once again, this implies a possible synergism or positive feedback loops between neuronal systems and innate immune activation that might underlie neurotoxicity related to NO and ROS signaling following METH exposure, and the potential for glial cells to contribute significantly to these mechanisms cannot be overlooked.

With repeated stimulation, glial cells can become primed; meaning that with each subsequent activation, the ensuing proinflammatory cascade becomes increasingly stronger [240].

The result is a central innate immune system that exists in a perpetual state of readiness; glial cells are not fully engaged in their basal activities and when stimulated, demonstrate an exaggerated proinflammatory response. While the initial proinflammatory central immune response to METH paired with actions on neuronal targets might be sufficient to produce increased DA signaling associated with reward and reinforcement, repeated exposure to METH might begin to prime microglia. In fact, DA has been shown to increase basal IL6 as well as augment TLR4-agonist induced release of IL6 [270]. As a natural extension of our recently proposed xenobiotic hypothesis of drug abuse, if repeated METH use does prime glial cells, this phenomenon could have important implications for chronic METH exposure, related to both neurotoxic consequences as well as disruptions in astrocyte modulation of synaptic excitability, contributing to plasticity involved in the development of addiction. Initially, METH use may produce reward through a synergistic effect of TLR4 activation resulting in neuroexcitatory, innate immune activation paired with DAT reversal. However, with repeated METH exposure, if glial cells become primed, positive, continually escalating feedback loops between TLR4 signaling, microglial and astrocyte activation, DAT reversal, and DA release may form leading to the development of addiction, and eventually triggering neurotoxic levels of proinflammatory, dopaminergic, and glutamatergic signaling; however, further exploration is required to determine whether METH induces glial priming.

Our findings indicate that a mechanism by which METH initiates central immune activation, which until now was not known, is likely through TLR4 activation. Further, TLR4 signaling induced via METH appears to be initially selective to the VTA and contributes to METH-induced increases of extracellular NAc DA, a correlate of drug reward. The present findings have important implications for drug reward and merit further investigation as to how

these mechanisms may contribute to the development of addiction and other pathological effects of METH. They also provide further support for our newly proposed xenobiotic hypothesis of drug abuse. TLR4 may be a novel target for the development of pharmacotherapies to aid in the treatment of METH abuse and addiction. Additionally, the role of glial cells, TLR4, and proinflammatory mediators in dopamine cell functioning and toxicity have overarching implications for numerous diseases and/or neuropathic states effecting dopamine systems that could guide the development of pharmacotherapies aiming to treat these pathologies.

Chapter 5

Discussion

The data presented here identify TLR4 as a novel target that opioids, cocaine, and methamphetamine bind to, and activate, thereby initiating central immune signaling. Further, this induction of TLR4 signaling appears to be an important element contributing to drug-induced alterations in mesolimbic DA functioning that is associated with the rewarding and reinforcing effects of opioids and psychostimulants, as well as linked to their high abuse potential. Collectively, our findings give rise to our newly proposed xenobiotic hypothesis of drug reward. In addition, data described herein further characterize the (+)-isomers of naloxone and naltrexone as selective, competitive TLR4 antagonists that show promise in terms of pharmacotherapeutic development to aid in the treatment of opioid and/or psychostimulant abuse.

In the case of opioids, we show that systemic TLR4 antagonism with (+)-naloxone suppresses morphine-induced increases of extracellular concentration of DA in the NAc. Systemic (+)-naloxone also suppressed morphine induced CPP as well as opioid self-administration, further demonstrating the relevance of opioid signaling at TLR4 in opioid reward and reinforcement. To extend our findings beyond pharmacological blockade of TLR4, Hutchinson et al. tested TLR4 KO mice and found that opioid-induced CPP was significantly reduced compared to wildtype mice.

If TLR4 activation triggers the MYD88-dependent intracellular signaling cascade, the result is nuclear translocation of the transcription factor NFκB, which then results in the production and/or release of proinflammatory molecules. MYD88 is an adaptor protein that is

recruited very early within the intracellular cascade; therefore, another way to examine whether it is opioid-interactions with the TLR4 receptor rather than some other downstream signaling mediator, MyD88 KO mice were examined for opioid CPP. Consistent with the TLR4 KO mice and with (+)-naloxone treatment, MyD88 KO mice showed a significant reduction of opioid place preference compared to wildtype mice. We also report herein that opioid administration activates TLR4 intra-cellular signaling pathways in wild-type mice but not TLR4(-/-). Together, these results indicate the importance of TLR4-opioid signaling, and also indicate that the NFκB pathway is likely involved. Evidence for proinflammatory signaling is further supporting by *in vitro* studies demonstrating that opioids induce upregulation of markers of proinflammatory signaling and trigger the release of proinflammatory molecules in TLR4-dependent manner (citation). Collectively these data suggest that opioid-induced TLR4 signaling is a necessary component of opioid signaling for reward/reinforcement.

There is also evidence pointing towards TLR4 and/or proinflammatory glial involvement in the effects of chronic opioid use. Administration of (+)-naloxone or glial activation inhibitors suppresses opioid-withdrawal behaviors [271-273]. Further, chronic delivery of (+)-naltrexone attenuates incubation of heroin craving, a phenomenon where the craving for a drug increases in a time-dependent manner [223]. When an individual or organism overdoses on opioids, the result is respiratory depression that can lead to death. However, administration of minocycline (which broadly blocks microglial activation) has also been shown to alleviate respiratory depression[146] induced by opioids.

While illicit opioids, such as heroin, have high rates of use and abuse, there is a growing problem with prescription opioids being diverted from their intended use to abuse settings.

Interestingly, blocking opioid-TLR4 signaling doesn't interfere with the desired analgesic effects of opioids. In fact, blocked of opioid-induced TLR4 signaling has been shown to *improve* the analgesic efficacy in opioids and protects against analgesic tolerance[210, 219]. The consensus is that because opioids can initiate proinflammatory signing, this creates an opponent process where alleviation of pain signaling through neuronal binding targets are constantly being counteracted by the proinflammatory actions of opioids [274]. Essentially, allowing opioids to bind to their neuronal/non-TLR4 targets, while simultaneously interfering with their proinflammatory actions, appears to protect against the unwanted side-effects of opioids while simultaneously improving its analgesic effects.

Due to the finding that opioid-activation has important contributions to the rewarding/reinforcing effects of opioids, we wanted to investigate whether proinflammatory signaling might be similarly involved with other classes of drugs of abuse. *In silico* computer modeling demonstrated that, like opioids, cocaine preferentially docks in the MD-2 binding pocket where other TLR4 agonists bind, such as LPS. Cocaine docking is displaced when (+)-naloxone is pre-docked. Biophysical characterization of cocaine-interactions with MD-2 support that cocaine competitively binds the agonist-binding pocket and *in vitro* studies demonstrate that cocaine activates NFκB signaling in BV-2 microglial cells in a TLR4-dependent manner. *In vivo*, acute cocaine administration induces upregulation of IL1b mRNA within the VTA; systemic (+)-naloxone administration suppresses this effect. That cocaine has proinflammatory effects in the brain has recently been investigated [147, 275], but the mechanism by which cocaine activates central immune signaling within the brain were unknown. Collectively, our findings support that cocaine does have proinflammatory actions in the brain and demonstrate that it may do so through TLR4 activation.

Cocaine induced TLR4 signaling also has important implications for the neurochemical reflection of cocaine reward; that is, systemic TLR4 antagonism blocked cocaine-induced elevations of NAc DA. Given our finding that systemic cocaine also induces upregulation of IL1b mRNA in the VTA, and the importance of VTA modulation of the mesolimbic DA pathway, we investigated whether TLR4 signaling within the VTA was necessary for cocaine-induction of increase DA concentrations in the NAc. Indeed, intra-VTA blockade of TLR4 signaling prevented cocaine-induced DA increases within the NAc. Additionally, intra-VTA administration of IL1ra, had the same effect, indicating that IL1β release is particular important in modulating cocaine's neurochemical effects in the mesolimbic pathway. How IL1β and other proinflammatory cytokines might exert neuroexcitatory effects was addressed within the discussion of Chapter 3. However, this finding also helps address the conundrum in the literature as to how DAergic cell firing might be altered/increased by cocaine (citation) regarding the widely held view that it primarily influenced the mesolimbic dopamine pathway through its DAT-blocking actions on DAergic neuron terminals. These results led to the logical next step of exploring whether TLR4 activation alone within the VTA would be sufficient to produce elevated DA within the NAc. Although intra-VTA microinjection of LPS did significantly increase DA levels within the NAc, it did not produce the extreme increases seen with systemic cocaine administration. Our findings, as discussed in Chapter 3, suggest a synergistic effect, that both cocaine activation of TLR4 in the VTA and cocaine blockade of DAT in the NAc to produce rapid and extreme increases of extracellular DA.

Although it is well known that extracellular DA concentrations within the NAc are linked to the subjective rewarding effects of cocaine, in order to examine whether our neurochemical studies

translated to behavioral measures of reward and reinforcement we utilized cocaine CPP and self-administration paradigms. Systemic blockade of TLR4 via (+)-naloxone administration suppressed cocaine CPP. Further, we found the same effect with systemic administration of minocycline, which has been shown to block microglial activation. These findings extended to cocaine self-administration in rats, which was suppressed by systemic (+)-naltrexone. Given that all the findings were based on pharmacological blockade of TLR4 or microglial signaling, we assessed a naturally occurring mutant mouse line with a point mutation that interferes with TLR4 signaling. These TLR4 mutant mice do not self-administer cocaine, whereas their wildtype counterparts did.

Interestingly, the involvement of TLR4 in cocaine reward also appears to extend beyond acute actions and into chronic cocaine exposure. Chapter 4 includes a detailed discussion of how repeated cocaine use is associated with neuroplasticity leading to a shift from recreational drug use seen in the early stages of the cycle of drug abuse to compulsive drug use characterizing drug dependence and addiction. Thus, it could be possible that as drug-induced neuroplasticity in the brain progresses, the relevancy of TLR4 signaling could be altered or diminished. Therefore, in order to explore the clinical utility of targeting TLR4, we wanted to test the effect of TLR4 signaling in reinstatement, a self-administration animal model analogous to relapse in human drug users. A collaboration with our colleagues, Bachtell et al., (*in preparation)* demonstrated that (+)-naltrexone administration dose dependently suppresses cocaine-primed reinstatement to cocaine seeking in rats It is important to note that these rats acquired cocaine self-administration and extinguished cocaine-self administration without (+)-naltrexone exposure and that a single injection just prior to the cocaine-priming injection intended to trigger reinstatement to cocaine seeking, was effective in blocking subsequent lever pressing observed in control groups. Bachtell

et al., (*in preparation)* also demonstrated that intra-VTA TLR4 antagonism with LPS-RS attenuated cocaine-primed reinstatement. Finally, the Bachtell laboratory found that intra-VTA LPS microinjections served to prime reinstatement to cocaine self-administration. This suggests that initiating TLR4 signaling within the VTA is sufficient to stimulate relapse to cocaine seeking. It is possible that administration of another drug that activates TLR4 signaling, for example, morphine, could trigger drug-craving, based on the finding that intra-VTA LPS primed reinstatement. While these findings do have interesting implications for mechanisms underlying relapse to drug use, it is important to note that it is not yet known whether non-pharmacological (i.e. non-xenobiotic) induced-reinstatement would be susceptible to TLR4 signaling. For example, the presentation of a cue associated with cocaine taking has been documented to trigger reinstatement in animals[276, 277] as well as craving/relapse in human drug users [278-280]. Whether or not TLR4 signaling contribute to this phenomenon remains to be explored.

Given the robust data from our investigation of the effect of cocaine-induced TLR4 signaling on drug reward and reinforcement, we wanted to explore if this would hold true for other types of psychostimulants, such as methamphetamine. Paralleling the cocaine and opioid findings, *in silico* data indicate that METH interacts with the agonist-binding-site of the MD-2/TLR4 complex. Further, METH also displaced the Bis-ANS probe from MD-2. *In vitro*, METH induces increased NFκB signaling in BV-2 migroglial reporter cells, indicative of glial activation; this effect is dependent on TLR4 signaling, as TLR4 antagonists co-incubated METH blocks NFkB activation. These *in silico* and *in vitro* findings support that METH can bind and activate TLR4 signaling, analogous to cocaine. However, it is important to note that METH not only blocks DATs, but also initiates reverse transport, releasing extra DA into the synapse; therefore, we wanted to explore if METH was dependent on TLR4 signaling to produce

increased DA concentrations in the NAc. Interestingly, *in vivo* microdialysis studies revealed that although administration of (+)-naloxone significantly attenuated METH-induced DA increases within the NAc, but did not fully block it, as observed with cocaine.

In order to explore if this effect of TLR4 antagonism might be localized to a specific brain region involved in modulating the mesolimbic DA pathway, mRNA levels of profinflammatory markers were analyzed for the vmPFC, VTA, and NAc following systemic administration of METH in rats. Interestingly, there were no differences in IL-1β mRNA although there was a significant upregulation of other proinflammatory markers in the VTA; most notably IL6 mRNA expression was upregulated in the VTA, but not the vmPFC or the NAc. In a follow-up study, (+)-naltrexone suppressed METH-induced IL6 mRNA upregulation, suggesting that this effect is TLR4 dependent. As noted in the discussion (Chapter 4), a role for IL6 associated with METH administration has some support for contributing to other unwanted effects of METH, namely neurotoxicity [248]. This raises the possibility that METH-induced TLR4 signaling is an important element of METH's well-documented neurotoxic effects. How METH-TLR4 signaling differs from cocaine to influence IL6 mRNA and not IL1β, and what implications this has for mediation of the mesolimbic DA pathway remains to be explored. Our finding that TLR4 antagonism both 1) prevents METH-induced increased expression of IL6 mRNA in the VTA and 2) attenuates METH-induced elevations of NAc DA alludes to the possibility that IL6 might mediate some of the effects of TLR4 signaling and how METH influences the mesolimbic DA pathway. However, given that TLR4 antagonism only partially blocks METH-induced DA increases, further investigation is necessary to explore to what extent TLR4 signaling contributes of the rewarding/reinforcing effects of METH and whether or not this has behavioral consequences.

In addition to demonstrating that substances from two different classes of abused drugs have important interactions with TLR4, and exploring a novel role for TLR4 activation and central immune signaling as an underlying component of drug reward and reinforcement, our findings include the characterization of (+)-naloxone and (+)-naltrexone as selective, competitive, TLR4 antagonists. Specifically, we demonstrate that both (+)-isomers bind to MD-2 with *in silico* docking simulations and Bis-ANS displacement assays. These findings are particularly important because prior to the characterization of (+)-naloxone/(+)-naltrexone as TLR4 antagonists, there was no blood-brain-barrier permeable TLR4 antagonist available that was suitable for systemic, *in vivo* administration. Our laboratory has also demonstrated that (+)-naloxone and (+)-naltrexone block of TLR4 signaling through a series of *in vitro* and *in vivo* studies [127, 128, 210, 219]. Specifically relevant to drug reward and reinforcement, here we also demonstrate that (+)-naloxone and/or (+)-naltrexone do not: 1) alter opioid or cocaine access to the brain, 2) alter basal dopamine levels, 3) interfere with TLR4-independent activation of DAergic signaling, 4) induce place preference or aversion, 5) alter food self-administration. Further, neither compound interacts with DAT, or transporters for serotonin or norepinephrine and extensive testing of (+)-naloxone and (+)-naltrexone at a broad range of neuronal targets, including neurotransmitters, steroids, ion channels, second messengers, growth factors, hormones, peptides, and enzymes revealed no off-target interactions.

The selectivity for TLR4 antagonism demonstrated to date by (+)-naloxone and (+)-naltrexone has wide-reaching implications. The first is that not only do our findings provide a novel target for pharmaceutical development that may aid in the treatment of drug abuse, but also a promising compound. The (-)-isomers of naloxone and naltrexone are already approved for

use in humans and as noted in Chapter 1, can be administered in the event of opioid overdose and to prevent opioid and alcohol use[281-283]. It has been shown that (-)-naltrexone reduced cocaine-induced euphoria in humans [284]. It is important to note that both the (+)- and (-)-isomers of naloxone and naltrexone inhibit TLR4 signaling whereas only the (-)-isomer antagonizes μOR [199]. This suggests that we cannot rule out that effects reported in relation to (-)-naloxone/naltrexone administration may also be due to TLR4 antagonism, either in conjunction with or independent of μOR blockade. Interestingly, (-)-naloxone has been reported to diminish cocaine- induced CPP [285, 286] as well as cocaine self-administration [287, 288] and other effects of cocaine, including hyperactivity [286, 289]; there are also similar results with amphetamine-induced CPP[290] and hyperactivity [291]. Further, administration of (-)-naltrexone in the VTA, but not in the NAc, PFC, or other brain regions, attenuated cocaine-self administration[292]. At the time, (-)-naltrexone was thought to be a selective μOR antagonist, so these effects were attributed to a role of endogenous opioids. However, findings with μOR knockout mice are contradictory [293] and the results reported with (-)-naltrexone lack a complete, satisfactory explanation [294]. In light of our recent characterization of (+)-naltrexone as a selective, competitive TLR4 antagonist and with our robust and consistent results demonstrating an important role for TLR4 signaling in psychostimulant reward, it is possible that effects of (-)-naltrexone are due to its TLR4 blocking actions. Altogether, there is compelling evidence that (+)-naloxone/naltrexone are promising in terms of potential pharmacotherapeutics to aid in the treatment of drug abuse.

Importantly, the lack of undesirable, nonspecific, or off-target effects of (+)-naloxone/naltrexone has significant implications for the Xenobiotic Hypothesis. This newly postulated hypothesis proposes that, in serving its immune-surveillance role, TLR4 detects and

identifies drugs of abuse, such as cocaine, morphine, etc. as foreign compounds and initiates proinflammatory immune signaling in response to the perceived threat. Further, we show that this drug-induced proinflammatory immune signaling is a critical mechanism through which abused drugs disrupt mesolimbic dopamine functioning to produce elevations of NAc DA. Our data indicate that opioids, cocaine, and to some extent, METH, rely on their ability to "hijack" mesolimbic DAergic signaling through central immune signaling initiated at TLR4. However, systemic blockade of TLR4 or intra-VTA blockade of TLR4 or IL1β signaling appear to have no effect on basal mesolimbic DA pathway function or alter other "baseline" type behaviors (eg: saline place preference, self-administration). Further, the TLR4-mutant mice self-administered sucrose normally, demonstrating that physiologically relevant appetitive behaviors are not disrupted by a lack of TLR4 signaling. It appears that naturally-rewarding stimuli (non-xenobiotic) are preserved even if TLR4 signaling or glial activation are blocked. As described in Chapter 1, the evolutionary purpose of the mesolimbic DA pathway is to mediate behaviors the promote survival of an organism, such as feeding. In fact, food self administration increases NAc DA concentrations, positively correlated with the palatiability of the food [295]. Ingestion of "normal" food (normal palatability) results in a modest DA increase within the NAc, to approximately 150% of baseline; in contrast to drug administration, which drives NAc DA levels to 250-400% of basal levels. Therefore, that inhibition of TLR4 signaling so potently disrupts drug-induced DA increases in the NAc, but does not interfere with food-self administration behaviors is somewhat remarkable. This highlights that the extreme increases of extracellular DA levels in the NAc, producing enormously disruptive consequences, is a xenobiotic effect. This suggests that innate immune signaling may only be activated in this manner when a foreign compound is detected; given our results emphasizing the importance of proinflammatory TLR4 signaling in the VTA, it might be drug-induced TLR4 signaling in the VTA that drives the

dramatic increase of NAc DA. Otherwise, our data might imply that TLR4 may not be involved in regulating normal or non non-pathological dopaminergic signaling.

TLR4 is thought to be located primarily on microglial cells, although there is evidence that expression of TLR4 can be upregulated on astrocytes when they are activated [188]. It is well documented that microglial TLR4 activation leads to a proinflammatory cascade. Given that systemic opioids and psychostimulants induce upregulation of markers of central immune signaling [147, 210, 246], and that both glial activation inhibitors as well as TLR4 antagonists diminish these proinflammatory reactions, it is likely that it is glial TLR4 mediating these effects. However, there are some instances where TLR4 has been reported on sensory neurons [296] but their functional impact is unknown. Further, there are reports that MD-2 expression is very low in this case [181, 182]. MD-2 is the site where agonists (LPS, opioids, psychostimulants) bind, facilitating heterodimerization of the MD-2 co-factor with TLR4, which then forms a homodimer with another MD2-TLR4 heterodimer to initiate an intracellular cascade that leads to proinflammatory signaling [126, 129, 220, 297]. Therefore, although unlikely, it is still unknown whether TLR4 agonists or antagonists could interact with a neuronal TLR4 lacking MD2 expression. Because it remains to be explored whether or not DAergic neurons in the mesolimbic DA pathway express TLR4s, it is an interesting option to consider. Although it is unknown what specific signaling cascade activation of a dopaminergic MD2-TLR4 complex might trigger, in light of our data demonstrating that TLR4 blockade suppresses increased DA levels and intra-VTA TLR4 activation produces increased DA, it is reasonable to surmise that the result would be a neuroexcitatory signal. Were this to be the case, it would be an intriguing finding; still supportive of TLR4 as a non-traditional drug receptor, but compelling in its implications. Further investigation is needed to test what cell types express TLR4 within the mesolimbic

pathway, and specifically how the resulting signaling cascade influences their functioning.

Here we demonstrate that it is TLR4 signaling within the VTA that has particular influence on the mesolimbic DA pathway. Supporting the xenobiotic hypothesis, we found that LPS microinjected into the VTA indeed produces a significant increase of NAc extracellular DA concentrations. Although, it is important to note that compared to the percent increase from baseline documented in rats receiving systemic opioids or psychostimulants, a modest dose of intra-VTA LPS produces only a partial DA increase. Because LPS has an extremely high affinity for the TLR4 complex, we selected a dose commonly used in CNS-injections that would be low enough to avoid neurotoxic effects, but high enough to induce central immune signaling[298-300]. In order to truly elucidate the effect of intra-VTA TLR4 agonism on NAc DA concentrations, an intra-VTA LPS-dose response study should be conducted. However, even with the limitations of our current data, only examining one dose of LPS, these results allude to glial cell and proinflammatory signaling as being critically important in mediating mesolimbic dopaminergic neuronal responsivity, and may help explain how drugs of abuse act within the VTA to alter DAergic cell firing. However, TLR4 is expressed on glial cells and given that abused drugs are taken systemically, it is possible that TLR4 activation in other brain regions, such as the PFC or the NAc also contributes to mesolimbic DA disruptions. Additionally, the nature of proinflammatory signaling is that it can perpetuate further proinflammatory activation, including the recruitment of astrocytes. As discussed in Chapter 4, there is some evidence that astrocyte activity within the NAc may contribute to the rewarding effects of psychostimulants. Altogether, it appears that in order to "hijack" the mesolimbic DAergic functioning to such an extent that DA levels in the NAc increase two-to-three fold, both disruption of neuronal and glial proinflammatory signaling is required. Because the mesolimbic

DA pathway has the ability to powerfully mediate behavior, it may be that it has more "checks and balances" than other systems. Conversely, it may also be the case that this is the rule rather than the exception for other neuronal systems as well. Glial cells are expressed in varying concentrations throughout the brain, and have been implicated in a number of disorders, both those involving DAerfic systems such as Parkinson's disease [140-142], as well those related to other systems and pathways, such as depression, and anxiety [138, 144, 261, 301] as well as in the regulation of normal behaviors such as learning [302, 303], all of which have overlapping behaviors/disruptions in functioning seen in drug addicts. Interestingly, TLR4 has been specifically implicated in Parkinson's Disease [304], which involves direct disruption of DAergic function.

Drug addicts can display shared characteristics to depressed or anxious patients; yet, related systems are predominately thought to be mediated by serotonin. However, while there is abundant evidence that DA is an important neurotransmitter mediating the rewarding effects of drugs, there is some evidence that the other neurotransmitter systems, including serotonin and norephinephrine, may also contribute to the rewarding/reinforcing effects of drugs. For example, as discussed in Chapters 3 and 4, psychostimulant reward/reinforcement is preserved in DAT KO mice [93, 94, 305]; to achieve a true deficiency in self-administration, a mouse with knock-outs for at least two of the three neurotransmitters transporters (DA, serotonin, or norephinephrine) is required [95, 306]. However, there are also contradictory findings; for example, mutant mice with an insensitive DAT do not demonstrate measures of cocaine reward/reinforcement [97, 307]. Therefore, it may be that in the case of DAT KO mice, other neurotransmitters become involved only as compensatory mechanisms; conversely, it may be that both serotonin and/or norepinephrine also play a role in drug reward. As previously discussed, results with KO mice

can be difficult to interpret; the suggestion that other neurotransmitter systems are involved, or become involved with repeated drug use, is worthy of further investigation. Relevant to the findings we present here, there is little documentation as to whether TLR4 activation influences serotonergic and/or norepinephrine systems. There is some evidence that LPS induces intestinal serotonin release [308, 309], however it is difficult to generalize peripheral signaling to CNS signaling. Conversely, serotonin does not influence LPS-induced activation of hypothalamo-pituitary-adrenal (HPA) axis; indicating in that particular circumstance, serotonin was not required for activation of the HPA axis [310]. Further, in primary astrocyte cultures, serotonin administration *reduced* astrocyte activation markers [311]. Norepinephrine has been shown to enhance expression of glial activation markers in rat primary microglial cells [312]; yet again, there is also evidence that norephinephine inhibits LPS-induced production of proinflammatory mediators[313]. Currently, there is not yet a consensus in the literature as to how other neurotransmitters might either influence or be influenced by TLR4 signaling.

Another related point to consider is that astrocytes have been reported to express transporters for serotonin and to a lesser extent, norepinephrine and DA [314, 315]. Although our findings imply that microglial-TLR4 is likely responsible for mediating proinflammatory drug effects that in turn influence the mesolimbic DA pathway, astrocyte contributions to this effect can not be ignored. (For a detailed discussion as to how astrocytes might influence drug reward, refer to Chapter 3). In brief, mediation of synaptic excitability is a role that astrocytes serve in their basal state; however, astrocyte activity can be closely linked to microglial activity. Hence, microglial-activation could lead to astrocyte-activation. When astrocytes become activated, they decrease their usual roles as synaptic modulators. Glial activation could mean that astrocytes are no longer aiding in the transport of neurotransmitters from the synapse, while

simultaneously, central immune signaling drives increased neurotransmission.

Taken together, well-documented neuronal actions of abused drugs paired with our findings of drug-induced TLR4 activation, lead to our proposal of a xenobiotic hypothesis of drug reward and reinforcement. This hypothesis suggests that drugs such as morphine, cocaine, and methamphetamine: 1) bind to their respective neuronal targets within the mesolimbic DA pathway, 2) activate neuroexcitatory proinflammatory signaling via TLR4 signaling, which may drive increased dopaminergic cell firing, and 3) trigger proinflammatory signaling that recruits other cells such as astrocytes, causing them to abandon their basal synaptic modulatory functions, such as neurotransmitter transport. The result of all these concomitant actions would be a mesolimbic DA pathway that has effectively been "hijacked", with no other way to compensate for dramatic increases of DA concentrations within the NAc.

Although the bulk of our data is oriented towards the early phases of the cycle of drug abuse (discussed in Chapter 1), that glial cells and proinflammatory signaling are important for a wide range of behaviors has important implications for drug addiction as well. Drug addiction is a complex disorder, and involves changes in impulse-control, decision-making[254], as well as personality traits and emotional regulation [156, 316]. So while our investigation thus far has focused on the initial rewarding aspects of abused drugs, it is possible that these substances are also initiating proinflammatory signaling in other brains regions that could contribute to the development of drug addiction.

Altogether, our findings uncover a novel mechanism underlying the rewarding and reinforcing effects of opioids, cocaine and methamphetamine, that likely contributes to their addictive effects and high abuse potential. These results give rise to our newly proposed

xenobiotic hypothesis of drug reward and reinforcement. This hypothesis includes a specific receptor, TLR4, as a promising target for pharmacotherapeutic development. These results demand a fundamental shift of our understanding as to how drugs of abuse exert their reinforcing effects; it is becoming clear that drug abuse and addiction should be conceptualized as issues of neuro*immuno*pharmacology. These implications have the potential to widely impact not only the research community, but also clinicians, the development of pharmacotherapies to treat drug abuse and addiction, and even classroom pharmacology.

References

1. Bosworth, F.H., *Is Cocaine an Enslaving Drug?* Trans Am Climatol Assoc, 1895. **11**: p. 136-40.
2. *National Drug Intelligence Center (2011) "The Economic Impact of Illicit Drug Use on American Society."* Washington D.C., United States Department of Justice. .
3. *National Institute on Drug Abuse,* http://www.drugabuse.gov. 2012.
4. Wills, T.A., et al., *Escalated substance use: a longitudinal grouping analysis from early to middle adolescence.* J Abnorm Psychol, 1996. **105**(2): p. 166-80.
5. Scheier, L.M. and G.J. Botvin, *Effects of early adolescent drug use on cognitive efficacy in early-late adolescence: a developmental structural model.* J Subst Abuse, 1995. **7**(4): p. 379-404.
6. *Drug Abuse and Addiction Research: The Sixth Triennial Report to Congress From the Secretary of Health and Human Services.* National Institutes of Health and National Institute on Drug Abuse 1999.
7. Everitt, B.J. and T.W. Robbins, *Neural systems of reinforcement for drug addiction: from actions to habits to compulsion.* Nat Neurosci, 2005. **8**(11): p. 1481-9.
8. Baik, J.H., *Dopamine signaling in reward-related behaviors.* Front Neural Circuits, 2013. **7**: p. 152.
9. Luo, A.H., et al., *Linking context with reward: a functional circuit from hippocampal CA3 to ventral tegmental area.* Science, 2011. **333**(6040): p. 353-7.
10. Berridge, K.C., *The debate over dopamine's role in reward: the case for incentive salience.* Psychopharmacology (Berl), 2007. **191**(3): p. 391-431.
11. Waelti, P., A. Dickinson, and W. Schultz, *Dopamine responses comply with basic assumptions of formal learning theory.* Nature, 2001. **412**(6842): p. 43-8.
12. Pierce, R.C. and V. Kumaresan, *The mesolimbic dopamine system: the final common pathway for the reinforcing effect of drugs of abuse?* Neurosci Biobehav Rev, 2006. **30**(2): p. 215-38.
13. Wise, R.A., *Neurobiology of addiction.* Curr Opin Neurobiol, 1996. **6**(2): p. 243-51.

14. Wise, R.A., *Dopamine, learning and motivation.* Nat Rev Neurosci, 2004. **5**(6): p. 483-94.
15. Voorn, P., et al., *The dopaminergic innervation of the ventral striatum in the rat: a light- and electron-microscopical study with antibodies against dopamine.* J Comp Neurol, 1986. **251**(1): p. 84-99.
16. Volkow, N.D., et al., *Imaging dopamine's role in drug abuse and addiction.* Neuropharmacology, 2009. **56 Suppl 1**: p. 3-8.
17. Johnson, S.W. and R.A. North, *Two types of neurone in the rat ventral tegmental area and their synaptic inputs.* J Physiol, 1992. **450**: p. 455-68.
18. Yamaguchi, T., W. Sheen, and M. Morales, *Glutamatergic neurons are present in the rat ventral tegmental area.* Eur J Neurosci, 2007. **25**(1): p. 106-18.
19. Omelchenko, N. and S.R. Sesack, *Glutamate synaptic inputs to ventral tegmental area neurons in the rat derive primarily from subcortical sources.* Neuroscience, 2007. **146**(3): p. 1259-74.
20. Grace, A.A., *Phasic versus tonic dopamine release and the modulation of dopamine system responsivity: a hypothesis for the etiology of schizophrenia.* Neuroscience, 1991. **41**(1): p. 1-24.
21. Grace, A.A. and B.S. Bunney, *Paradoxical GABA excitation of nigral dopaminergic cells: indirect mediation through reticulata inhibitory neurons.* Eur J Pharmacol, 1979. **59**(3-4): p. 211-8.
22. Grace, A.A. and S.P. Onn, *Morphology and electrophysiological properties of immunocytochemically identified rat dopamine neurons recorded in vitro.* J Neurosci, 1989. **9**(10): p. 3463-81.
23. Grace, A.A. and B.S. Bunney, *The control of firing pattern in nigral dopamine neurons: burst firing.* J Neurosci, 1984. **4**(11): p. 2877-90.
24. Goto, Y., S. Otani, and A.A. Grace, *The Yin and Yang of dopamine release: a new perspective.* Neuropharmacology, 2007. **53**(5): p. 583-7.
25. Grace, A.A., *The tonic/phasic model of dopamine system regulation: its relevance for understanding how stimulant abuse can alter basal ganglia function.* Drug Alcohol Depend, 1995. **37**(2): p. 111-29.
26. Floresco, S.B., et al., *Afferent modulation of dopamine neuron firing differentially regulates tonic and phasic dopamine transmission.* Nat Neurosci, 2003. **6**(9): p. 968-73.
27. Fabre, M., et al., *Activity of neurons in the ventral tegmental region of the behaving monkey.* Behav Brain Res, 1983. **9**(2): p. 213-35.
28. Kiaytkin, E.A., *Functional properties of presumed dopamine-containing and other ventral tegmental area neurons in conscious rats.* Int J Neurosci, 1988. **42**(1-2): p. 21-43.
29. Miller, J.D., M.K. Sanghera, and D.C. German, *Mesencephalic dopaminergic unit activity in the behaviorally conditioned rat.* Life Sci, 1981. **29**(12): p. 1255-63.
30. Schultz, W., P. Apicella, and T. Ljungberg, *Responses of monkey dopamine neurons to reward and conditioned stimuli during successive steps of learning a delayed response task.* J Neurosci, 1993. **13**(3): p. 900-13.
31. Schultz, W. and R. Romo, *Dopamine neurons of the monkey midbrain: contingencies of responses to stimuli eliciting immediate behavioral reactions.* J Neurophysiol, 1990. **63**(3): p. 607-24.

32. Tsai, H.C., et al., *Phasic firing in dopaminergic neurons is sufficient for behavioral conditioning.* Science, 2009. **324**(5930): p. 1080-4.
33. Wanat, M.J., et al., *Phasic dopamine release in appetitive behaviors and drug addiction.* Curr Drug Abuse Rev, 2009. **2**(2): p. 195-213.
34. Zahm, D.S. and J.S. Brog, *On the significance of subterritories in the "accumbens" part of the rat ventral striatum.* Neuroscience, 1992. **50**(4): p. 751-67.
35. Meredith, G.E., *The synaptic framework for chemical signaling in nucleus accumbens.* Ann N Y Acad Sci, 1999. **877**: p. 140-56.
36. Zahm, D.S. and L. Heimer, *Specificity in the efferent projections of the nucleus accumbens in the rat: comparison of the rostral pole projection patterns with those of the core and shell.* J Comp Neurol, 1993. **327**(2): p. 220-32.
37. Xia, Y., et al., *Nucleus accumbens medium spiny neurons target non-dopaminergic neurons in the ventral tegmental area.* J Neurosci, 2011. **31**(21): p. 7811-6.
38. Nauta, W.J., et al., *Efferent connections and nigral afferents of the nucleus accumbens septi in the rat.* Neuroscience, 1978. **3**(4-5): p. 385-401.
39. Gangarossa, G., et al., *Distribution and compartmental organization of GABAergic medium-sized spiny neurons in the mouse nucleus accumbens.* Front Neural Circuits, 2013. **7**: p. 22.
40. Einhorn, L.C., P.A. Johansen, and F.J. White, *Electrophysiological effects of cocaine in the mesoaccumbens dopamine system: studies in the ventral tegmental area.* J Neurosci, 1988. **8**(1): p. 100-12.
41. Kalivas, P.W., *Neurotransmitter regulation of dopamine neurons in the ventral tegmental area.* Brain Res Brain Res Rev, 1993. **18**(1): p. 75-113.
42. Rahman, S. and W.J. McBride, *Feedback control of mesolimbic somatodendritic dopamine release in rat brain.* J Neurochem, 2000. **74**(2): p. 684-92.
43. Ito, R. and A. Hayen, *Opposing roles of nucleus accumbens core and shell dopamine in the modulation of limbic information processing.* J Neurosci, 2011. **31**(16): p. 6001-7.
44. Di Chiara, G., *Nucleus accumbens shell and core dopamine: differential role in behavior and addiction.* Behav Brain Res, 2002. **137**(1-2): p. 75-114.
45. Cadoni, C. and G. Di Chiara, *Reciprocal changes in dopamine responsiveness in the nucleus accumbens shell and core and in the dorsal caudate-putamen in rats sensitized to morphine.* Neuroscience, 1999. **90**(2): p. 447-55.
46. Cadoni, C., M. Solinas, and G. Di Chiara, *Psychostimulant sensitization: differential changes in accumbal shell and core dopamine.* Eur J Pharmacol, 2000. **388**(1): p. 69-76.
47. Madsen, H.B., R.M. Brown, and A.J. Lawrence, *Neuroplasticity in addiction: cellular and transcriptional perspectives.* Front Mol Neurosci, 2012. **5**: p. 99.
48. Kalivas, P.W. and C. O'Brien, *Drug addiction as a pathology of staged neuroplasticity.* Neuropsychopharmacology, 2008. **33**(1): p. 166-80.
49. Racz, I., *Neuroplastic changes in addiction.* Front Mol Neurosci, 2014. **6**: p. 56.
50. Duncan, J.R., *Current perspectives on the neurobiology of drug addiction: a focus on genetics and factors regulating gene expression.* ISRN Neurol, 2012. **2012**: p. 972607.
51. Luscher, C. and R.C. Malenka, *Drug-evoked synaptic plasticity in addiction: from molecular changes to circuit remodeling.* Neuron, 2011. **69**(4): p. 650-63.
52. Kalivas, P.W., et al., *Glutamate transmission in addiction.* Neuropharmacology, 2009. **56 Suppl 1**: p. 169-73.

53. Robinson, T.E. and B. Kolb, *Persistent structural modifications in nucleus accumbens and prefrontal cortex neurons produced by previous experience with amphetamine.* J Neurosci, 1997. **17**(21): p. 8491-7.
54. Sklair-Tavron, L., et al., *Chronic morphine induces visible changes in the morphology of mesolimbic dopamine neurons.* Proc Natl Acad Sci U S A, 1996. **93**(20): p. 11202-7.
55. Volkow, N.D., et al., *Dopamine in drug abuse and addiction: results of imaging studies and treatment implications.* Arch Neurol, 2007. **64**(11): p. 1575-9.
56. Volkow, N.D., et al., *Dopamine in drug abuse and addiction: results from imaging studies and treatment implications.* Mol Psychiatry, 2004. **9**(6): p. 557-69.
57. *Substance Abuse and Mental Health Services Administration, Results from the 2012 National Survey on Drug Use and Health: Summary of National Findings, NSDUH Series H-46, HHS Publication No. (SMA) 13-4795. Rockville, MD: Substance Abuse and Mental Health Services Administration.* 2013.
58. De Vries, T.J. and T.S. Shippenberg, *Neural systems underlying opiate addiction.* J Neurosci, 2002. **22**(9): p. 3321-5.
59. Self, D.W. and L. Stein, *Receptor subtypes in opioid and stimulant reward.* Pharmacol Toxicol, 1992. **70**(2): p. 87-94.
60. Dilts, R.P. and P.W. Kalivas, *Autoradiographic localization of mu-opioid and neurotensin receptors within the mesolimbic dopamine system.* Brain Res, 1989. **488**(1-2): p. 311-27.
61. Garzon, M. and V.M. Pickel, *Plasmalemmal mu-opioid receptor distribution mainly in nondopaminergic neurons in the rat ventral tegmental area.* Synapse, 2001. **41**(4): p. 311-28.
62. German, D.C., et al., *Opioid receptors in midbrain dopaminergic regions of the rat. I. Mu receptor autoradiography.* J Neural Transm Gen Sect, 1993. **91**(1): p. 39-52.
63. Mansour, A., et al., *Opioid-receptor mRNA expression in the rat CNS: anatomical and functional implications.* Trends Neurosci, 1995. **18**(1): p. 22-9.
64. Mansour, A., et al., *Immunohistochemical localization of the cloned mu opioid receptor in the rat CNS.* J Chem Neuroanat, 1995. **8**(4): p. 283-305.
65. Svingos, A.L., et al., *Mu-opioid receptors in the ventral tegmental area are targeted to presynaptically and directly modulate mesocortical projection neurons.* Synapse, 2001. **41**(3): p. 221-9.
66. Johnson, S.W. and R.A. North, *Opioids excite dopamine neurons by hyperpolarization of local interneurons.* J Neurosci, 1992. **12**(2): p. 483-8.
67. Gysling, K. and R.Y. Wang, *Morphine-induced activation of A10 dopamine neurons in the rat.* Brain Res, 1983. **277**(1): p. 119-27.
68. Spanagel, R. and F. Weiss, *The dopamine hypothesis of reward: past and current status.* Trends Neurosci, 1999. **22**(11): p. 521-7.
69. Matthews, R.T. and D.C. German, *Electrophysiological evidence for excitation of rat ventral tegmental area dopamine neurons by morphine.* Neuroscience, 1984. **11**(3): p. 617-25.
70. Bozarth, M.A. and R.A. Wise, *Intracranial self-administration of morphine into the ventral tegmental area in rats.* Life Sci, 1981. **28**(5): p. 551-5.
71. Devine, D.P. and R.A. Wise, *Self-administration of morphine, DAMGO, and DPDPE into the ventral tegmental area of rats.* J Neurosci, 1994. **14**(4): p. 1978-84.

72. Kiyatkin, E.A. and G.V. Rebec, *Activity of presumed dopamine neurons in the ventral tegmental area during heroin self-administration.* Neuroreport, 1997. **8**(11): p. 2581-5.
73. Kiyatkin, E.A. and G.V. Rebec, *Impulse activity of ventral tegmental area neurons during heroin self-administration in rats.* Neuroscience, 2001. **102**(3): p. 565-80.
74. Wise, R.A., et al., *Fluctuations in nucleus accumbens dopamine concentration during intravenous cocaine self-administration in rats.* Psychopharmacology (Berl), 1995. **120**(1): p. 10-20.
75. Dworkin, S., et al., *Effects of 5,7-dihydroxytryptamine lesions of the nucleus accumbens in rats responding on a concurrent schedule of food, water and intravenous morphine self-administration.* NIDA Res Monogr, 1988. **81**: p. 149-55.
76. Zito, K.A., G. Vickers, and D.C. Roberts, *Disruption of cocaine and heroin self-administration following kainic acid lesions of the nucleus accumbens.* Pharmacol Biochem Behav, 1985. **23**(6): p. 1029-36.
77. Churchill, L., R.P. Dilts, and P.W. Kalivas, *Changes in gamma-aminobutyric acid, mu-opioid and neurotensin receptors in the accumbens-pallidal projection after discrete quinolinic acid lesions in the nucleus accumbens.* Brain Res, 1990. **511**(1): p. 41-54.
78. David, V., T.P. Durkin, and P. Cazala, *Self-administration of the GABAA antagonist bicuculline into the ventral tegmental area in mice: dependence on D2 dopaminergic mechanisms.* Psychopharmacology (Berl), 1997. **130**(2): p. 85-90.
79. Ikemoto, S., J.M. Murphy, and W.J. McBride, *Self-infusion of GABA(A) antagonists directly into the ventral tegmental area and adjacent regions.* Behav Neurosci, 1997. **111**(2): p. 369-80.
80. Olds, M.E., *Reinforcing effects of morphine in the nucleus accumbens.* Brain Res, 1982. **237**(2): p. 429-40.
81. David, V., T.P. Durkin, and P. Cazala, *Differential effects of the dopamine D2/D3 receptor antagonist sulpiride on self-administration of morphine into the ventral tegmental area or the nucleus accumbens.* Psychopharmacology (Berl), 2002. **160**(3): p. 307-17.
82. Ettenberg, A., et al., *Heroin and cocaine intravenous self-administration in rats: mediation by separate neural systems.* Psychopharmacology (Berl), 1982. **78**(3): p. 204-9.
83. Gerber, G.J. and R.A. Wise, *Pharmacological regulation of intravenous cocaine and heroin self-administration in rats: a variable dose paradigm.* Pharmacol Biochem Behav, 1989. **32**(2): p. 527-31.
84. Gerrits, M.A., et al., *Lack of evidence for an involvement of nucleus accumbens dopamine D1 receptors in the initiation of heroin self-administration in the rat.* Psychopharmacology (Berl), 1994. **114**(3): p. 486-94.
85. Compton, W.M. and N.D. Volkow, *Abuse of prescription drugs and the risk of addiction.* Drug Alcohol Depend, 2006. **83 Suppl 1**: p. S4-7.
86. Carboni, E., et al., *Cocaine and amphetamine increase extracellular dopamine in the nucleus accumbens of mice lacking the dopamine transporter gene.* J Neurosci, 2001. **21**(9): p. RC141: 1-4.
87. Volkow, N.D., et al., *Relationship between subjective effects of cocaine and dopamine transporter occupancy.* Nature, 1997. **386**(6627): p. 827-30.

88. Pettit, H.O., et al., *Destruction of dopamine in the nucleus accumbens selectively attenuates cocaine but not heroin self-administration in rats.* Psychopharmacology (Berl), 1984. **84**(2): p. 167-73.
89. Roberts, D.C. and G.F. Koob, *Disruption of cocaine self-administration following 6-hydroxydopamine lesions of the ventral tegmental area in rats.* Pharmacol Biochem Behav, 1982. **17**(5): p. 901-4.
90. Kuhar, M.J., M.C. Ritz, and J.W. Boja, *The dopamine hypothesis of the reinforcing properties of cocaine.* Trends Neurosci, 1991. **14**(7): p. 299-302.
91. Spealman, R.D., B.K. Madras, and J. Bergman, *Effects of cocaine and related drugs in nonhuman primates. II. Stimulant effects on schedule-controlled behavior.* J Pharmacol Exp Ther, 1989. **251**(1): p. 142-9.
92. Giros, B., et al., *Hyperlocomotion and indifference to cocaine and amphetamine in mice lacking the dopamine transporter.* Nature, 1996. **379**(6566): p. 606-12.
93. Rocha, B.A., et al., *Cocaine self-administration in dopamine-transporter knockout mice.* Nat Neurosci, 1998. **1**(2): p. 132-7.
94. Sora, I., et al., *Cocaine reward models: conditioned place preference can be established in dopamine- and in serotonin-transporter knockout mice.* Proc Natl Acad Sci U S A, 1998. **95**(13): p. 7699-704.
95. Sora, I., et al., *Molecular mechanisms of cocaine reward: combined dopamine and serotonin transporter knockouts eliminate cocaine place preference.* Proc Natl Acad Sci U S A, 2001. **98**(9): p. 5300-5.
96. Uhl, G.R., D.J. Vandenbergh, and L.L. Miner, *Knockout mice and dirty drugs. Drug addiction.* Curr Biol, 1996. **6**(8): p. 935-6.
97. Chen, R., et al., *Abolished cocaine reward in mice with a cocaine-insensitive dopamine transporter.* Proc Natl Acad Sci U S A, 2006. **103**(24): p. 9333-8.
98. Ritz, M.C., et al., *Cocaine receptors on dopamine transporters are related to self-administration of cocaine.* Science, 1987. **237**(4819): p. 1219-23.
99. Wilson, M.C. and C.R. Schuster, *Mazindol self-administration in the rhesus monkey.* Pharmacol Biochem Behav, 1976. **4**(2): p. 207-10.
100. Chait, L.D., E.H. Uhlenhuth, and C.E. Johanson, *Reinforcing and subjective effects of several anorectics in normal human volunteers.* J Pharmacol Exp Ther, 1987. **242**(3): p. 777-83.
101. Jones, S.R., et al., *Mechanisms of amphetamine action revealed in mice lacking the dopamine transporter.* J Neurosci, 1998. **18**(6): p. 1979-86.
102. Butcher, S.P., et al., *Amphetamine-induced dopamine release in the rat striatum: an in vivo microdialysis study.* J Neurochem, 1988. **50**(2): p. 346-55.
103. Hurd, Y.L. and U. Ungerstedt, *In vivo neurochemical profile of dopamine uptake inhibitors and releasers in rat caudate-putamen.* Eur J Pharmacol, 1989. **166**(2): p. 251-60.
104. Chu, P.W., et al., *Differential regional effects of methamphetamine on dopamine transport.* Eur J Pharmacol, 2008. **590**(1-3): p. 105-10.
105. Fleckenstein, A.E., et al., *A rapid and reversible change in dopamine transporters induced by methamphetamine.* Eur J Pharmacol, 1997. **323**(2-3): p. R9-10.
106. Fleckenstein, A.E., et al., *Rapid and reversible effects of methamphetamine on dopamine transporters.* J Pharmacol Exp Ther, 1997. **282**(2): p. 834-8.

107. Kokoshka, J.M., et al., *Nature of methamphetamine-induced rapid and reversible changes in dopamine transporters.* Eur J Pharmacol, 1998. **361**(2-3): p. 269-75.
108. Robertson, S.D., H.J. Matthies, and A. Galli, *A closer look at amphetamine-induced reverse transport and trafficking of the dopamine and norepinephrine transporters.* Mol Neurobiol, 2009. **39**(2): p. 73-80.
109. Arnold, E.B., P.B. Molinoff, and C.O. Rutledge, *The release of endogenous norepinephrine and dopamine from cerebral cortex by amphetamine.* J Pharmacol Exp Ther, 1977. **202**(3): p. 544-57.
110. Azzaro, A.J., R.J. Ziance, and C.O. Rutledge, *The importance of neuronal uptake of amines for amphetamine-induced release of 3H-norepinephrine from isolated brain tissue.* J Pharmacol Exp Ther, 1974. **189**(1): p. 110-8.
111. Forrest, L.R., et al., *Mechanism for alternating access in neurotransmitter transporters.* Proc Natl Acad Sci U S A, 2008. **105**(30): p. 10338-43.
112. Erreger, K., et al., *Currents in response to rapid concentration jumps of amphetamine uncover novel aspects of human dopamine transporter function.* J Neurosci, 2008. **28**(4): p. 976-89.
113. Sulzer, D., et al., *Amphetamine redistributes dopamine from synaptic vesicles to the cytosol and promotes reverse transport.* J Neurosci, 1995. **15**(5 Pt 2): p. 4102-8.
114. *Treatment for Stimulant Use Disorders. Treatment Improvement Protocol (TIP) Series, No. 33.* Center for Substance Abuse Treatment. Rockville (MD): Substance Abuse and Mental Health Services Administration (US); Available from: http://www.ncbi.nlm.nih.gov/books/NBK64333/, 1999. .
115. Vollm, B.A., et al., *Methamphetamine activates reward circuitry in drug naive human subjects.* Neuropsychopharmacology, 2004. **29**(9): p. 1715-22.
116. Haydon, P.G., *GLIA: listening and talking to the synapse.* Nat Rev Neurosci, 2001. **2**(3): p. 185-93.
117. Inagaki, N., et al., *Type-2 astrocytes show intracellular Ca2+ elevation in response to various neuroactive substances.* Neurosci Lett, 1991. **128**(2): p. 257-60.
118. Kommers, T., et al., *Regulation of the phosphorylation of glial fibrillary acidic protein (GFAP) by glutamate and calcium ions in slices of immature rat spinal cord: comparison with immature hippocampus.* Neurosci Lett, 1998. **248**(2): p. 141-3.
119. Bruce-Keller, A.J., *Microglial-neuronal interactions in synaptic damage and recovery.* J Neurosci Res, 1999. **58**(1): p. 191-201.
120. Shao, Y. and K.D. McCarthy, *Plasticity of astrocytes.* Glia, 1994. **11**(2): p. 147-55.
121. Watkins, L.R., E.D. Milligan, and S.F. Maier, *Glial activation: a driving force for pathological pain.* Trends Neurosci, 2001. **24**(8): p. 450-5.
122. Watkins, L.R., et al., *"Listening" and "talking" to neurons: implications of immune activation for pain control and increasing the efficacy of opioids.* Brain Res Rev, 2007. **56**(1): p. 148-69.
123. Gehrmann, J., Y. Matsumoto, and G.W. Kreutzberg, *Microglia: intrinsic immuneffector cell of the brain.* Brain Res Brain Res Rev, 1995. **20**(3): p. 269-87.
124. Raivich, G., *Like cops on the beat: the active role of resting microglia.* Trends Neurosci, 2005. **28**(11): p. 571-3.
125. Lee, H., et al., *Toll-like receptors: sensor molecules for detecting damage to the nervous system.* Curr Protein Pept Sci, 2013. **14**(1): p. 33-42.

126. Miyake, K., *Endotoxin recognition molecules, Toll-like receptor 4-MD-2.* Semin Immunol, 2004. **16**(1): p. 11-6.
127. Hutchinson, M.R., et al., *Evidence that opioids may have toll-like receptor 4 and MD-2 effects.* Brain Behav Immun, 2010. **24**(1): p. 83-95.
128. Wang, X., et al., *Morphine activates neuroinflammation in a manner parallel to endotoxin.* Proc Natl Acad Sci U S A, 2012. **109**(16): p. 6325-30.
129. Shimazu, R., et al., *MD-2, a molecule that confers lipopolysaccharide responsiveness on Toll-like receptor 4.* J Exp Med, 1999. **189**(11): p. 1777-82.
130. Fitzgerald, K.A., D.C. Rowe, and D.T. Golenbock, *Endotoxin recognition and signal transduction by the TLR4/MD2-complex.* Microbes Infect, 2004. **6**(15): p. 1361-7.
131. Watkins, L.R., et al., *Norman Cousins Lecture. Glia as the "bad guys": implications for improving clinical pain control and the clinical utility of opioids.* Brain Behav Immun, 2007. **21**(2): p. 131-46.
132. Viviani, B., et al., *Interleukin-1beta enhances NMDA receptor-mediated intracellular calcium increase through activation of the Src family of kinases.* J Neurosci, 2003. **23**(25): p. 8692-700.
133. Stellwagen, D., et al., *Differential regulation of AMPA receptor and GABA receptor trafficking by tumor necrosis factor-alpha.* J Neurosci, 2005. **25**(12): p. 3219-28.
134. Haydon, P.G. and G. Carmignoto, *Astrocyte control of synaptic transmission and neurovascular coupling.* Physiol Rev, 2006. **86**(3): p. 1009-31.
135. Eroglu, C. and B.A. Barres, *Regulation of synaptic connectivity by glia.* Nature, 2010. **468**(7321): p. 223-31.
136. Aldskogius, H. and E.N. Kozlova, *Central neuron-glial and glial-glial interactions following axon injury.* Prog Neurobiol, 1998. **55**(1): p. 1-26.
137. Watkins, L.R., et al., *Glia: novel counter-regulators of opioid analgesia.* Trends Neurosci, 2005. **28**(12): p. 661-9.
138. Dantzer, R., et al., *From inflammation to sickness and depression: when the immune system subjugates the brain.* Nat Rev Neurosci, 2008. **9**(1): p. 46-56.
139. Hutchinson, M.R. and L.R. Watkins, *Why is neuroimmunopharmacology crucial for the future of addiction research?* Neuropharmacology, 2014. **76 Pt B**: p. 218-27.
140. Hirsch, E.C., et al., *Glial cells and inflammation in Parkinson's disease: a role in neurodegeneration?* Ann Neurol, 1998. **44**(3 Suppl 1): p. S115-20.
141. Teismann, P., et al., *Pathogenic role of glial cells in Parkinson's disease.* Mov Disord, 2003. **18**(2): p. 121-9.
142. Vila, M., et al., *The role of glial cells in Parkinson's disease.* Curr Opin Neurol, 2001. **14**(4): p. 483-9.
143. Bauer, J., et al., *The participation of interleukin-6 in the pathogenesis of Alzheimer's disease.* Res Immunol, 1992. **143**(6): p. 650-7.
144. Howren, M.B., D.M. Lamkin, and J. Suls, *Associations of depression with C-reactive protein, IL-1, and IL-6: a meta-analysis.* Psychosom Med, 2009. **71**(2): p. 171-86.
145. Bland, S.T., et al., *The glial activation inhibitor AV411 reduces morphine-induced nucleus accumbens dopamine release.* Brain Behav Immun, 2009. **23**(4): p. 492-7.
146. Hutchinson, M.R., et al., *Minocycline suppresses morphine-induced respiratory depression, suppresses morphine-induced reward, and enhances systemic morphine-induced analgesia.* Brain Behav Immun, 2008. **22**(8): p. 1248-56.

147. Cearley, C.N., et al., *Acute cocaine increases interleukin-1beta mRNA and immunoreactive cells in the cortex and nucleus accumbens.* Neurochem Res, 2011. **36**(4): p. 686-92.
148. Goncalves, J., et al., *Methamphetamine-induced early increase of IL-6 and TNF-alpha mRNA expression in the mouse brain.* Ann N Y Acad Sci, 2008. **1139**: p. 103-11.
149. Sekine, Y., et al., *Methamphetamine causes microglial activation in the brains of human abusers.* J Neurosci, 2008. **28**(22): p. 5756-61.
150. Compton, W.M. and N.D. Volkow, *Abuse of prescription drugs and the risk of addiction.* Drug and alcohol dependence, 2006. **83 Suppl 1**: p. S4-7.
151. Manchikanti, L., *Prescription drug abuse: what is being done to address this new drug epidemic? Testimony before the Subcommittee on Criminal Justice, Drug Policy and Human Resources.* Pain physician, 2006. **9**(4): p. 287-321.
152. Ikemoto, S., *Dopamine reward circuitry: two projection systems from the ventral midbrain to the nucleus accumbens-olfactory tubercle complex.* Brain research reviews, 2007. **56**(1): p. 27-78.
153. Laviolette, S.R., K. Nader, and D. van der Kooy, *Motivational state determines the functional role of the mesolimbic dopamine system in the mediation of opiate reward processes.* Behav Brain Res, 2002. **129**(1-2): p. 17-29.
154. Vargas-Perez, H., et al., *Ventral tegmental area BDNF induces an opiate-dependent-like reward state in naive rats.* Science, 2009. **324**(5935): p. 1732-4.
155. Takagi K, F.H., Watanabe M, Sato M *Studies on antitussives. III (+)-Morphine and its derivatives.* Yakugaku Zasshi, 1960. **80**: p. 1506-1509.
156. Goldstein, R.Z. and N.D. Volkow, *Drug addiction and its underlying neurobiological basis: neuroimaging evidence for the involvement of the frontal cortex.* Am J Psychiatry, 2002. **159**(10): p. 1642-52.
157. Hutchinson, M.R., et al., *Exploring the neuroimmunopharmacology of opioids: an integrative review of mechanisms of central immune signaling and their implications for opioid analgesia.* Pharmacological reviews, 2011. **63**(3): p. 772-810.
158. Matic, M., et al., *Pregnane X receptor: promiscuous regulator of detoxification pathways.* Int J Biochem Cell Biol, 2007. **39**(3): p. 478-83.
159. Buchanan, M.M., et al., *Toll-like receptor 4 in CNS pathologies.* Journal of neurochemistry, 2010. **114**(1): p. 13-27.
160. Yirmiya, R. and I. Goshen, *Immune modulation of learning, memory, neural plasticity and neurogenesis.* Brain, behavior, and immunity, 2011. **25**(2): p. 181-213.
161. Hutchinson, M.R., et al., *Evidence that opioids may have toll-like receptor 4 and MD-2 effects.* Brain, behavior, and immunity, 2010. **24**(1): p. 83-95.
162. Wang, X., et al., *Morphine: the new endotoxin.* Proc. National Acad. Sci., 2012: p. in invited revision.
163. Hiranita, T., et al., *Decreases in cocaine self-administration with dual inhibition of dopamine transporter and sigma receptors.* J. Pharmacol. Exp. Ther., 2011: p. Aug 22 Epub ahead of print.
164. Panlilio, L.V., et al., *Variability of drug self-administration in rats.* Psychopharmacology, 2003. **167**(1): p. 9-19.
165. Bland, S.T., et al., *The glial activation inhibitor AV411 reduces morphine-induced nucleus accumbens dopamine release.* Brain, behavior, and immunity, 2009. **23**(4): p. 492-7.

166. Milligan, E.D., et al., *A method for increasing the viability of the external portion of lumbar catheters placed in the spinal subarachnoid space of rats.* J Neurosci Methods, 1999. **90**(1): p. 81-6.
167. Hutchinson, M.R., et al., *Non-stereoselective reversal of neuropathic pain by naloxone and naltrexone: involvement of toll-like receptor 4 (TLR4).* The European journal of neuroscience, 2008. **28**(1): p. 20-9.
168. Hargreaves, K., et al., *A new and sensitive method for measuring thermal nociception in cutaneous hyperalgesia.* Pain, 1988. **32**(1): p. 77-88.
169. Van Crugten, J.T., et al., *The effect of old age on the disposition and antinociceptive response of morphine and morphine-6 beta-glucuronide in the rat.* Pain, 1997. **71**(2): p. 199-205.
170. Doverty, M., et al., *Methadone maintenance patients are cross-tolerant to the antinociceptive effects of morphine.* Pain, 2001. **93**: p. 155-163.
171. Lakowicz, J.R., *Principles of Fluorescence Spectroscopy*. 2nd ed. 2006, New York: Springer-Verlanger.
172. Resman, N., et al., *Taxanes inhibit human TLR4 signaling by binding to MD-2.* FEBS letters, 2008. **582**(28): p. 3929-34.
173. Hutchinson, M.R., et al., *Minocycline suppresses morphine-induced respiratory depression, suppresses morphine-induced reward, and enhances systemic morphine-induced analgesia.* Brain, behavior, and immunity, 2008. **22**(8): p. 1248-56.
174. Hutchinson, M.R., et al., *Evidence that tricyclic small molecules may possess toll-like receptor and myeloid differentiation protein 2 activity.* Neuroscience, 2010. **168**(2): p. 551-63.
175. Lewis, S.S., et al., *Evidence that intrathecal morphine-3-glucuronide may cause pain enhancement via toll-like receptor 4/MD-2 and interleukin-1beta.* Neuroscience, 2010. **165**(2): p. 569-83.
176. Park, B.S., et al., *The structural basis of lipopolysaccharide recognition by the TLR4-MD-2 complex.* Nature, 2009. **458**(7242): p. 1191-5.
177. Trott, O. and A.J. Olson, *AutoDock Vina: improving the speed and accuracy of docking with a new scoring function, efficient optimization, and multithreading.* Journal of computational chemistry, 2010. **31**(2): p. 455-61.
178. Mancek-Keber, M. and R. Jerala, *Structural similarity between the hydrophobic fluorescent probe and lipid A as a ligand of MD-2.* The FASEB journal : official publication of the Federation of American Societies for Experimental Biology, 2006. **20**(11): p. 1836-42.
179. Diogenes, A., et al., *LPS sensitizes TRPV1 via activation of TLR4 in trigeminal sensory neurons.* Journal of dental research, 2011. **90**(6): p. 759-64.
180. Ferraz, C.C., et al., *Lipopolysaccharide from Porphyromonas gingivalis sensitizes capsaicin-sensitive nociceptors.* Journal of endodontics, 2011. **37**(1): p. 45-8.
181. Divanovic, S., et al., *Inhibition of TLR-4/MD-2 signaling by RP105/MD-1.* J Endotoxin Res, 2005. **11**(6): p. 363-8.
182. Okun, E., K.J. Griffioen, and M.P. Mattson, *Toll-like receptor signaling in neural plasticity and disease.* Trends Neurosci, 2011. **34**(5): p. 269-81.
183. Bsibsi, M., et al., *Broad expression of Toll-like receptors in the human central nervous system.* J Neuropathol Exp Neurol, 2002. **61**(11): p. 1013-21.

184. Fujihara, M., et al., *Molecular mechanisms of macrophage activation and deactivation by lipopolysaccharide: roles of the receptor complex.* Pharmacol Ther, 2003. **100**(2): p. 171-94.
185. Holm, T.H., D. Draeby, and T. Owens, *Microglia are required for astroglial Toll-like receptor 4 response and for optimal TLR2 and TLR3 response.* Glia, 2012. **60**(4): p. 630-8.
186. Zhang, X.Q., et al., *Activation of p38 signaling in the microglia in the nucleus accumbens contributes to the acquisition and maintenance of morphine-induced conditioned place preference.* Brain, behavior, and immunity, 2012. **26**(2): p. 318-25.
187. Coller, J.K. and M.R. Hutchinson, *Implications of central immune signaling caused by drugs of abuse: mechanisms, mediators and new therapeutic approaches for prediction and treatment of drug dependence.* Pharmacol Ther, 2012. **134**(2): p. 219-45.
188. Watkins, L.R., et al., *The "toll" of opioid-induced glial activation: improving the clinical efficacy of opioids by targeting glia.* Trends Pharmacol Sci, 2009. **30**(11): p. 581-91.
189. Wang, Z., et al., *Reduced expression of glutamate transporter EAAT2 and impaired glutamate transport in human primary astrocytes exposed to HIV-1 or gp120.* Virology, 2003. **312**(1): p. 60-73.
190. De, A., J.M. Krueger, and S.M. Simasko, *Tumor necrosis factor alpha increases cytosolic calcium responses to AMPA and KCl in primary cultures of rat hippocampal neurons.* Brain Res, 2003. **981**(1-2): p. 133-42.
191. Youn, D.H., H. Wang, and S.J. Jeong, *Exogenous tumor necrosis factor-alpha rapidly alters synaptic and sensory transmission in the adult rat spinal cord dorsal horn.* J Neurosci Res, 2008. **86**(13): p. 2867-75.
192. Schwarz, J.M., M.R. Hutchinson, and S.D. Bilbo, *Early-life experience decreases drug-induced reinstatement of morphine CPP in adulthood via microglial-specific epigenetic programming of anti-inflammatory IL-10 expression.* The Journal of neuroscience : the official journal of the Society for Neuroscience, 2011. **31**(49): p. 17835-47.
193. Narita, M., et al., *Direct evidence of astrocytic modulation in the development of rewarding effects induced by drugs of abuse.* Neuropsychopharmacology : official publication of the American College of Neuropsychopharmacology, 2006. **31**(11): p. 2476-88.
194. Liu, L., et al., *Association of IL-1B genetic polymorphisms with an increased risk of opioid and alcohol dependence.* Pharmacogenet Genomics, 2009. **19**(11): p. 869-76.
195. Lewis, S.S., et al., *(+)-Naloxone, an opioid-inactive toll-like receptor 4 signaling inhibitor, reverses multiple models of chronic neuropathic pain in rats.* Journal of Pain, 2012: p. invited revision in review.
196. Burns, L.H. and H.Y. Wang, *PTI-609: a novel analgesic that binds filamin A to control opioid signaling.* Recent Pat CNS Drug Discov, 2010. **5**(3): p. 210-20.
197. He, L., et al., *Toll-like receptor 9 is required for opioid-induced microglia apoptosis.* PLoS One, 2011. **6**(4): p. e18190.
198. Zhang, Y., et al., *Essential role of toll-like receptor 2 in morphine-induced microglia activation in mice.* Neurosci Lett, 2011. **489**(1): p. 43-7.
199. Dunwiddie, T.V., et al., *Stereoselectivity of opiate antagonists in rat hippocampus and neocortex: responses to (+) and (-) isomers of naloxone.* Neuroscience, 1982. **7**(7): p. 1691-702.

200. Bowers, M.S. and P.W. Kalivas, *Forebrain astroglial plasticity is induced following withdrawal from repeated cocaine administration.* Eur J Neurosci, 2003. **17**(6): p. 1273-8.
201. He, J. and F.T. Crews, *Increased MCP-1 and microglia in various regions of the human alcoholic brain.* Exp Neurol, 2008. **210**(2): p. 349-58.
202. Thomas, D.M., et al., *Microglial activation is a pharmacologically specific marker for the neurotoxic amphetamines.* Neurosci Lett, 2004. **367**(3): p. 349-54.
203. Thomas, D.M., et al., *Methamphetamine neurotoxicity in dopamine nerve endings of the striatum is associated with microglial activation.* J Pharmacol Exp Ther, 2004. **311**(1): p. 1-7.
204. Beardsley, P.M., et al., *The glial cell modulator and phosphodiesterase inhibitor, AV411 (ibudilast), attenuates prime- and stress-induced methamphetamine relapse.* European journal of pharmacology, 2010. **637**(1-3): p. 102-8.
205. Fujita, Y., et al., *The antibiotic minocycline prevents methamphetamine-induced rewarding effects in mice.* Pharmacology, biochemistry, and behavior, 2012.
206. Sofuoglu, M., et al., *Minocycline attenuates subjective rewarding effects of dextroamphetamine in humans.* Psychopharmacology, 2011. **213**(1): p. 61-8.
207. Agrawal, R.G., et al., *Minocycline reduces ethanol drinking.* Brain, behavior, and immunity, 2011. **25 Suppl 1**: p. S165-9.
208. Pontieri, F.E., G. Tanda, and G. Di Chiara, *Intravenous cocaine, morphine, and amphetamine preferentially increase extracellular dopamine in the "shell" as compared with the "core" of the rat nucleus accumbens.* Proc Natl Acad Sci U S A, 1995. **92**(26): p. 12304-8.
209. Koob, G.F. and F.E. Bloom, *Cellular and molecular mechanisms of drug dependence.* Science, 1988. **242**(4879): p. 715-23.
210. Hutchinson, M.R., et al., *Possible involvement of toll-like receptor 4/myeloid differentiation factor-2 activity of opioid inactive isomers causes spinal proinflammation and related behavioral consequences.* Neuroscience, 2010. **167**(3): p. 880-93.
211. Hutchinson, M.R., et al., *Opioid activation of toll-like receptor 4 contributes to drug reinforcement.* J Neurosci, 2012. **32**(33): p. 11187-200.
212. Livak, K.J. and T.D. Schmittgen, *Analysis of relative gene expression data using real-time quantitative PCR and the 2(-Delta Delta C(T)) Method.* Methods, 2001. **25**(4): p. 402-8.
213. Hiranita, T., et al., *Assessment of reinforcing effects of benztropine analogs and their effects on cocaine self-administration in rats: comparisons with monoamine uptake inhibitors.* J Pharmacol Exp Ther, 2009. **329**(2): p. 677-86.
214. Pomrenze, M.B., et al., *Cocaine self-administration in mice with forebrain knock-down of trpc5 ion channels.* F1000Res, 2013. **2**: p. 53.
215. Cass, W.A. and N.R. Zahniser, *Cocaine levels in striatum and nucleus accumbens: augmentation following challenge injection in rats withdrawn from repeated cocaine administration.* Neurosci Lett, 1993. **152**(1-2): p. 177-80.
216. Lewis, S.S., et al., *(+)-naloxone, an opioid-inactive toll-like receptor 4 signaling inhibitor, reverses multiple models of chronic neuropathic pain in rats.* J Pain, 2012. **13**(5): p. 498-506.

217. Hiranita, T., et al., *Decreases in cocaine self-administration with dual inhibition of the dopamine transporter and sigma receptors.* J Pharmacol Exp Ther, 2011. **339**(2): p. 662-77.
218. Garces-Ramirez, L., et al., *Sigma receptor agonists: receptor binding and effects on mesolimbic dopamine neurotransmission assessed by microdialysis.* Biol Psychiatry, 2011. **69**(3): p. 208-17.
219. Hutchinson, M.R., et al., *Non-stereoselective reversal of neuropathic pain by naloxone and naltrexone: involvement of toll-like receptor 4 (TLR4).* Eur J Neurosci, 2008. **28**(1): p. 20-9.
220. Kawai, T. and S. Akira, *Signaling to NF-kappaB by Toll-like receptors.* Trends Mol Med, 2007. **13**(11): p. 460-9.
221. Laitinen, K., et al., *Neurotensin and cholecystokinin microinjected into the ventral tegmental area modulate microdialysate concentrations of dopamine and metabolites in the posterior nucleus accumbens.* Brain Res, 1990. **523**(2): p. 342-6.
222. Bastos, L.F., et al., *Tetracyclines and pain.* Naunyn Schmiedebergs Arch Pharmacol, 2012. **385**(3): p. 225-41.
223. Theberge, F.R., et al., *Effect of chronic delivery of the Toll-like receptor 4 antagonist (+)-naltrexone on incubation of heroin craving.* Biol Psychiatry, 2013. **73**(8): p. 729-37.
224. Mandolesi, G., et al., *Interleukin-1beta alters glutamate transmission at purkinje cell synapses in a mouse model of multiple sclerosis.* J Neurosci, 2013. **33**(29): p. 12105-21.
225. Pogun, S., M.H. Baumann, and M.J. Kuhar, *Nitric oxide inhibits [3H]dopamine uptake.* Brain Res, 1994. **641**(1): p. 83-91.
226. Ho, A. and M. Blum, *Induction of interleukin-1 associated with compensatory dopaminergic sprouting in the denervated striatum of young mice: model of aging and neurodegenerative disease.* J Neurosci, 1998. **18**(15): p. 5614-29.
227. Long-Smith, C.M., et al., *Interleukin-1beta contributes to dopaminergic neuronal death induced by lipopolysaccharide-stimulated rat glia in vitro.* J Neuroimmunol, 2010. **226**(1-2): p. 20-6.
228. Shintani, F., et al., *Interleukin-1 beta augments release of norepinephrine, dopamine, and serotonin in the rat anterior hypothalamus.* J Neurosci, 1993. **13**(8): p. 3574-81.
229. Narita, M., et al., *Direct evidence of astrocytic modulation in the development of rewarding effects induced by drugs of abuse.* Neuropsychopharmacology, 2006. **31**(11): p. 2476-88.
230. Dong, Y. and E.N. Benveniste, *Immune function of astrocytes.* Glia, 2001. **36**(2): p. 180-90.
231. Bowman, C.C., et al., *Cultured astrocytes express toll-like receptors for bacterial products.* Glia, 2003. **43**(3): p. 281-91.
232. Tanga, F.Y., V. Raghavendra, and J.A. DeLeo, *Quantitative real-time RT-PCR assessment of spinal microglial and astrocytic activation markers in a rat model of neuropathic pain.* Neurochem Int, 2004. **45**(2-3): p. 397-407.
233. Bal-Price, A. and G.C. Brown, *Inflammatory neurodegeneration mediated by nitric oxide from activated glia-inhibiting neuronal respiration, causing glutamate release and excitotoxicity.* J Neurosci, 2001. **21**(17): p. 6480-91.

234. Kalivas, P.W. and X.T. Hu, *Exciting inhibition in psychostimulant addiction.* Trends Neurosci, 2006. **29**(11): p. 610-6.
235. Choi, D.W., M. Maulucci-Gedde, and A.R. Kriegstein, *Glutamate neurotoxicity in cortical cell culture.* J Neurosci, 1987. **7**(2): p. 357-68.
236. Block, M.L., L. Zecca, and J.S. Hong, *Microglia-mediated neurotoxicity: uncovering the molecular mechanisms.* Nat Rev Neurosci, 2007. **8**(1): p. 57-69.
237. Little, K.Y., et al., *Decreased brain dopamine cell numbers in human cocaine users.* Psychiatry Res, 2009. **168**(3): p. 173-80.
238. Bechara, A., et al., *Decision-making deficits, linked to a dysfunctional ventromedial prefrontal cortex, revealed in alcohol and stimulant abusers.* Neuropsychologia, 2001. **39**(4): p. 376-89.
239. Yang, S., et al., *Curcumin protects dopaminergic neuron against LPS induced neurotoxicity in primary rat neuron/glia culture.* Neurochem Res, 2008. **33**(10): p. 2044-53.
240. Watkins, L.R. and S.F. Maier, *The pain of being sick: implications of immune-to-brain communication for understanding pain.* Annu Rev Psychol, 2000. **51**: p. 29-57.
241. Dilger, R.N. and R.W. Johnson, *Aging, microglial cell priming, and the discordant central inflammatory response to signals from the peripheral immune system.* J Leukoc Biol, 2008. **84**(4): p. 932-9.
242. Volkow, N.D., et al., *Association of dopamine transporter reduction with psychomotor impairment in methamphetamine abusers.* Am J Psychiatry, 2001. **158**(3): p. 377-82.
243. Gibb, J.W., L. Bush, and G.R. Hanson, *Exacerbation of methamphetamine-induced neurochemical deficits by melatonin.* J Pharmacol Exp Ther, 1997. **283**(2): p. 630-5.
244. McCann, U.D., et al., *Reduced striatal dopamine transporter density in abstinent methamphetamine and methcathinone users: evidence from positron emission tomography studies with [11C]WIN-35,428.* J Neurosci, 1998. **18**(20): p. 8417-22.
245. Darke, S., et al., *Major physical and psychological harms of methamphetamine use.* Drug Alcohol Rev, 2008. **27**(3): p. 253-62.
246. Northcutt, A.L., et al., *DAT isn't all that: cocaine reward and reinforcement requires Toll Like Receptor 4 signaling.* Molecular Psychiatry 2014. **In Press**.
247. Loftis, J.M., et al., *Methamphetamine causes persistent immune dysregulation: a cross-species, translational report.* Neurotox Res, 2011. **20**(1): p. 59-68.
248. Ladenheim, B., et al., *Methamphetamine-induced neurotoxicity is attenuated in transgenic mice with a null mutation for interleukin-6.* Mol Pharmacol, 2000. **58**(6): p. 1247-56.
249. LaVoie, M.J., J.P. Card, and T.G. Hastings, *Microglial activation precedes dopamine terminal pathology in methamphetamine-induced neurotoxicity.* Exp Neurol, 2004. **187**(1): p. 47-57.
250. Nakajima, A., et al., *Role of tumor necrosis factor-alpha in methamphetamine-induced drug dependence and neurotoxicity.* J Neurosci, 2004. **24**(9): p. 2212-25.
251. Marz, P., U. Otten, and S. Rose-John, *Neural activities of IL-6-type cytokines often depend on soluble cytokine receptors.* Eur J Neurosci, 1999. **11**(9): p. 2995-3004.
252. Fann, M.J. and P.H. Patterson, *Neuropoietic cytokines and activin A differentially regulate the phenotype of cultured sympathetic neurons.* Proc Natl Acad Sci U S A, 1994. **91**(1): p. 43-7.

253. Narita, M., et al., *Long-lasting change in brain dynamics induced by methamphetamine: enhancement of protein kinase C-dependent astrocytic response and behavioral sensitization.* J Neurochem, 2005. **93**(6): p. 1383-92.
254. Bechara, A., *Decision making, impulse control and loss of willpower to resist drugs: a neurocognitive perspective.* Nat Neurosci, 2005. **8**(11): p. 1458-63.
255. Haydon, P.G., et al., *Astrocytic control of synaptic transmission and plasticity: a target for drugs of abuse?* Neuropharmacology, 2009. **56 Suppl 1**: p. 83-90.
256. Wilson, J.M., et al., *Differential changes in neurochemical markers of striatal dopamine nerve terminals in idiopathic Parkinson's disease.* Neurology, 1996. **47**(3): p. 718-26.
257. Wilson, J.M., et al., *Striatal dopamine nerve terminal markers in human, chronic methamphetamine users.* Nat Med, 1996. **2**(6): p. 699-703.
258. O'Callaghan, J.P. and D.B. Miller, *Neurotoxicity profiles of substituted amphetamines in the C57BL/6J mouse.* J Pharmacol Exp Ther, 1994. **270**(2): p. 741-51.
259. Weaver, J.D., et al., *Interleukin-6 and risk of cognitive decline: MacArthur studies of successful aging.* Neurology, 2002. **59**(3): p. 371-8.
260. Ganguli, R., et al., *Serum interleukin-6 concentration in schizophrenia: elevation associated with duration of illness.* Psychiatry Res, 1994. **51**(1): p. 1-10.
261. Maes, M., H.Y. Meltzer, and E. Bosmans, *Psychoimmune investigation in obsessive-compulsive disorder: assays of plasma transferrin, IL-2 and IL-6 receptor, and IL-1 beta and IL-6 concentrations.* Neuropsychobiology, 1994. **30**(2-3): p. 57-60.
262. Pomeroy, C., et al., *Role of interleukin-6 and transforming growth factor-beta in anorexia nervosa.* Biol Psychiatry, 1994. **36**(12): p. 836-9.
263. Takeuchi, H., et al., *Tumor necrosis factor-alpha induces neurotoxicity via glutamate release from hemichannels of activated microglia in an autocrine manner.* J Biol Chem, 2006. **281**(30): p. 21362-8.
264. Muller, T., et al., *Interleukin-6 levels in cerebrospinal fluid inversely correlate to severity of Parkinson's disease.* Acta Neurol Scand, 1998. **98**(2): p. 142-4.
265. Flora, G., et al., *Methamphetamine-induced TNF-alpha gene expression and activation of AP-1 in discrete regions of mouse brain: potential role of reactive oxygen intermediates and lipid peroxidation.* Neuromolecular Med, 2002. **2**(1): p. 71-85.
266. Nomura, A., et al., *Association study of the tumor necrosis factor-alpha gene and its 1A receptor gene with methamphetamine dependence.* Ann N Y Acad Sci, 2006. **1074**: p. 116-24.
267. Gaur, U. and B.B. Aggarwal, *Regulation of proliferation, survival and apoptosis by members of the TNF superfamily.* Biochem Pharmacol, 2003. **66**(8): p. 1403-8.
268. Aggarwal, B.B., *Signalling pathways of the TNF superfamily: a double-edged sword.* Nat Rev Immunol, 2003. **3**(9): p. 745-56.
269. Davidson, C., et al., *Methamphetamine neurotoxicity: necrotic and apoptotic mechanisms and relevance to human abuse and treatment.* Brain Res Brain Res Rev, 2001. **36**(1): p. 1-22.
270. Ritchie, P.K., et al., *Dopamine increases interleukin 6 release and inhibits tumor necrosis factor release from rat adrenal zona glomerulosa cells in vitro.* Eur J Endocrinol, 1996. **134**(5): p. 610-6.
271. Hutchinson, M.R., et al., *Reduction of opioid withdrawal and potentiation of acute opioid analgesia by systemic AV411 (ibudilast).* Brain Behav Immun, 2009. **23**(2): p. 240-50.

272. Hutchinson, M.R., et al., *Opioid-induced glial activation: mechanisms of activation and implications for opioid analgesia, dependence, and reward.* ScientificWorldJournal, 2007. **7**: p. 98-111.
273. Hutchinson, M.R., et al., *Exploring the neuroimmunopharmacology of opioids: an integrative review of mechanisms of central immune signaling and their implications for opioid analgesia.* Pharmacol Rev, 2011. **63**(3): p. 772-810.
274. Hutchinson, M.R., et al., *Proinflammatory cytokines oppose opioid-induced acute and chronic analgesia.* Brain Behav Immun, 2008. **22**(8): p. 1178-89.
275. Crews, F.T., J. Zou, and L. Qin, *Induction of innate immune genes in brain create the neurobiology of addiction.* Brain Behav Immun, 2011. **25 Suppl 1**: p. S4-S12.
276. de Wit, H. and J. Stewart, *Reinstatement of cocaine-reinforced responding in the rat.* Psychopharmacology (Berl), 1981. **75**(2): p. 134-43.
277. Meil, W.M. and R.E. See, *Conditioned cued recovery of responding following prolonged withdrawal from self-administered cocaine in rats: an animal model of relapse.* Behav Pharmacol, 1996. **7**(8): p. 754-763.
278. Gawin, F.H. and H.D. Kleber, *Abstinence symptomatology and psychiatric diagnosis in cocaine abusers. Clinical observations.* Arch Gen Psychiatry, 1986. **43**(2): p. 107-13.
279. O'Brien, C.P., et al., *Conditioning factors in drug abuse: can they explain compulsion?* J Psychopharmacol, 1998. **12**(1): p. 15-22.
280. Childress, A.R., et al., *Limbic activation during cue-induced cocaine craving.* Am J Psychiatry, 1999. **156**(1): p. 11-8.
281. Kunoe, N., et al., *Naltrexone implants after in-patient treatment for opioid dependence: randomised controlled trial.* Br J Psychiatry, 2009. **194**(6): p. 541-6.
282. Pettinati, H.M., et al., *The status of naltrexone in the treatment of alcohol dependence: specific effects on heavy drinking.* J Clin Psychopharmacol, 2006. **26**(6): p. 610-25.
283. Minozzi, S., et al., *Oral naltrexone maintenance treatment for opioid dependence.* Cochrane Database Syst Rev, 2011(4): p. CD001333.
284. Kosten, T., et al., *Intravenous cocaine challenges during naltrexone maintenance: a preliminary study.* Biol Psychiatry, 1992. **32**(6): p. 543-8.
285. Houdi, A.A., M.T. Bardo, and G.R. Van Loon, *Opioid mediation of cocaine-induced hyperactivity and reinforcement.* Brain Res, 1989. **497**(1): p. 195-8.
286. Kim, H.S., et al., *Blockade by naloxone of cocaine-induced hyperactivity, reverse tolerance and conditioned place preference in mice.* Behav Brain Res, 1997. **85**(1): p. 37-46.
287. De Vry, J., I. Donselaar, and J.M. Van Ree, *Food deprivation and acquisition of intravenous cocaine self-administration in rats: effect of naltrexone and haloperidol.* J Pharmacol Exp Ther, 1989. **251**(2): p. 735-40.
288. Mello, N.K. and S.S. Negus, *Preclinical evaluation of pharmacotherapies for treatment of cocaine and opioid abuse using drug self-administration procedures.* Neuropsychopharmacology, 1996. **14**(6): p. 375-424.
289. Chatterjie, N., et al., *Prevention of cocaine-induced hyperactivity by a naloxone isomer with no opiate antagonist activity.* Neurochem Res, 1996. **21**(6): p. 691-3.
290. Trujillo, K.A., J.D. Belluzzi, and L. Stein, *Naloxone blockade of amphetamine place preference conditioning.* Psychopharmacology (Berl), 1991. **104**(2): p. 265-74.
291. Chatterjie, N., et al., *Dextro-naloxone counteracts amphetamine-induced hyperactivity.* Pharmacol Biochem Behav, 1998. **59**(2): p. 271-4.

292. Ramsey, N.F., M.A. Gerrits, and J.M. Van Ree, *Naltrexone affects cocaine self-administration in naive rats through the ventral tegmental area rather than dopaminergic target regions.* Eur Neuropsychopharmacol, 1999. **9**(1-2): p. 93-9.
293. Hall, F.S., et al., *mu-Opioid receptor knockout mice display reduced cocaine conditioned place preference but enhanced sensitization of cocaine-induced locomotion.* Brain Res Mol Brain Res, 2004. **121**(1-2): p. 123-30.
294. Van Ree, J.M., et al., *Endogenous opioids and reward.* Eur J Pharmacol, 2000. **405**(1-3): p. 89-101.
295. Martel, P. and M. Fantino, *Mesolimbic dopaminergic system activity as a function of food reward: a microdialysis study.* Pharmacol Biochem Behav, 1996. **53**(1): p. 221-6.
296. Diogenes, A., et al., *LPS sensitizes TRPV1 via activation of TLR4 in trigeminal sensory neurons.* J Dent Res, 2011. **90**(6): p. 759-64.
297. Miyake, K., *Endotoxin recognition molecules MD-2 and toll-like receptor 4 as potential targets for therapeutic intervention of endotoxin shock.* Curr Drug Targets Inflamm Allergy, 2004. **3**(3): p. 291-7.
298. Lee, J.C., et al., *Accelerated cerebral ischemic injury by activated macrophages/microglia after lipopolysaccharide microinjection into rat corpus callosum.* Glia, 2005. **50**(2): p. 168-81.
299. Matsuoka, Y., et al., *Interferon-gamma plus lipopolysaccharide induction of delayed neuronal apoptosis in rat hippocampus.* Neurochem Int, 1999. **34**(2): p. 91-9.
300. Cho, G.S., et al., *N-Methyl-D-aspartate receptor antagonists memantine and MK-801 attenuate the cerebral infarct accelerated by intracorpus callosum injection of lipopolysaccharides.* Neurosci Lett, 2013. **538**: p. 9-14.
301. Cotter, D.R., C.M. Pariante, and I.P. Everall, *Glial cell abnormalities in major psychiatric disorders: the evidence and implications.* Brain Res Bull, 2001. **55**(5): p. 585-95.
302. Avital, A., et al., *Impaired interleukin-1 signaling is associated with deficits in hippocampal memory processes and neural plasticity.* Hippocampus, 2003. **13**(7): p. 826-34.
303. Matsutani, S. and M. Leon, *Elaboration of glial cell processes in the rat olfactory bulb associated with early learning.* Brain Res, 1993. **613**(2): p. 317-20.
304. Noelker, C., et al., *Toll like receptor 4 mediates cell death in a mouse MPTP model of Parkinson disease.* Sci Rep, 2013. **3**: p. 1393.
305. Medvedev, I.O., et al., *Characterization of conditioned place preference to cocaine in congenic dopamine transporter knockout female mice.* Psychopharmacology (Berl), 2005. **180**(3): p. 408-13.
306. Rocha, B.A., *Stimulant and reinforcing effects of cocaine in monoamine transporter knockout mice.* Eur J Pharmacol, 2003. **479**(1-3): p. 107-15.
307. Thomsen, M., et al., *Lack of cocaine self-administration in mice expressing a cocaine-insensitive dopamine transporter.* J Pharmacol Exp Ther, 2009. **331**(1): p. 204-11.
308. Kidd, M., et al., *IL1beta- and LPS-induced serotonin secretion is increased in EC cells derived from Crohn's disease.* Neurogastroenterol Motil, 2009. **21**(4): p. 439-50.
309. Mendoza, C., et al., *Lipopolysaccharide induces alteration of serotonin transporter in human intestinal epithelial cells.* Innate Immun, 2009. **15**(4): p. 243-50.
310. Conde, G.L., et al., *Serotonin depletion does not alter lipopolysaccharide-induced activation of the rat paraventricular nucleus.* J Endocrinol, 1998. **156**(2): p. 245-51.

311. Le Prince, G., et al., *Neuron-glia interactions: effect of serotonin on the astroglial expression of GFAP and of its encoding message.* Brain Res Dev Brain Res, 1990. **51**(2): p. 295-8.
312. Schlachetzki, J.C., et al., *Norepinephrine enhances the LPS-induced expression of COX-2 and secretion of PGE2 in primary rat microglia.* J Neuroinflammation, 2010. **7**: p. 2.
313. Goyarts, E., et al., *Norepinephrine modulates human dendritic cell activation by altering cytokine release.* Exp Dermatol, 2008. **17**(3): p. 188-96.
314. Inazu, M., et al., *Pharmacological characterization and visualization of the glial serotonin transporter.* Neurochem Int, 2001. **39**(1): p. 39-49.
315. Hosli, E. and L. Hosli, *Receptors for neurotransmitters on astrocytes in the mammalian central nervous system.* Prog Neurobiol, 1993. **40**(4): p. 477-506.
316. Haertzen, C.A. and N.T. Hooks, Jr., *Changes in personality and subjective experience associated with the chronic administration and withdrawal of opiates.* J Nerv Ment Dis, 1969. **148**(6): p. 606-14.